Role of delay differential equations in modelling low level HIV viral load

A Thesis:

submitted in partial fulfilment
of the requirements for the award of
Doctor of Philosophy (Ph.D.)
in the School of Computing,
Faculty of Engineering and Computing,

Dublin City University

Ed McGuinness M.Sc., B.Eng.

Supervisors: Prof. Heather J. Ruskin and Dr. Martin Crane

January 25, 2012

Declaration

I hereby certify that this material, which I now submit for assessment on the programme of study leading to the award of Doctor of Philosophy (Ph.D.) is entirely my own work, that I have exercised reasonable care to ensure that the work is original, and does not to the best of my knowledge breach any law of copyright, and has not been taken from the work of others save and to the extent that such work has been cited and acknowledged within the text of my work.

Ed McGuinness: 55134785

Signed:_____

Date:_____

Role of delay differential equations in modelling low level HIV viral load

Ed McGuinness M.Sc, B.Eng
School of Computing,
Dublin City University

Abstract

Over the past 30 years HIV has infected over 60 million people, with almost half succumbing to AIDS related illnesses. While antiretroviral therapy, used to significantly reduce within-host HIV replication, was available within 10 years of the discovery of HIV/AIDS, it is only within the last 10 years that it has become truly effective and universally accessible. However, there are problems with this therapy, not least that it must be administered indefinitely but is expensive and highly toxic. Furthermore, as therapy reaches more resource limited regions continual access can not be guaranteed, resulting in therapy interruptions. This, coupled with a significant cost reduction by systematically interrupting therapy, means a set of models which can account for both treatment events need to be developed, as numerous models exist for therapy introduction, but those for therapy removal are limited. Thus a set of delayed differential models are designed, which account for previously overlooked important features of intracellular delay and HIV latency. Incorporation of these features requires additional model components, leading to a rapid increase in complexity. To combat this complexity issue dimensional analysis is introduced, as a novel method of identifying key components to model function, thus allowing significant reduction in parameter space. Based on these developed models a number of existing and potential treatment interruption regimes are investigated, with a best practice regime suggested.

Contents

Abstract iii

Acknowledgements vi

List of Tables viii

List of Figures ix

Acronyms xiii

1 Introduction 1
- 1.1 Background . . . 1
- 1.2 Mathematical modelling . . . 3
- 1.3 Thesis structure and scope . . . 4

2 AIDS pandemic and HIV infection progression 5
- 2.1 HIV/AIDS overview . . . 6
  - 2.1.1 Current HIV/AIDS pandemic . . . 6
    - 2.1.1.1 Developed countries . . . 6
    - 2.1.1.2 Developing countries . . . 7
    - 2.1.1.3 HIV therapy . . . 8
    - 2.1.1.4 HIV/AIDS funding . . . 8
  - 2.1.2 Origin of HIV/AIDS . . . 9
  - 2.1.3 HIV progression to AIDS . . . 11
    - 2.1.3.1 Acute phase . . . 11
    - 2.1.3.2 Chronic phase or clinical latency . . . 12
    - 2.1.3.3 AIDS . . . 12
  - 2.1.4 HIV transmission . . . 13
- 2.2 HIV replication . . . 14
  - 2.2.1 Immune system . . . 15
  - 2.2.2 HIV target cells . . . 15
  - 2.2.3 HIV replication in target cells . . . 16
  - 2.2.4 Viral production types . . . 20
  - 2.2.5 Viral mutations . . . 20
- 2.3 Treating HIV/AIDS . . . 21
  - 2.3.1 Therapy monitoring . . . 22

2.3.2 Anti-retroviral therapy . . . 23
2.3.3 Treatment strategies . . . 24
2.4 HIV/AIDS future . . . 25
2.5 Summary . . . 26

3 HIV/AIDS Research **27**
3.1 Overview of HIV/AIDS research . . . 28
3.1.1 *In vivo* analysis . . . 28
3.1.2 *In vitro* analysis . . . 29
3.1.3 *In silico* analysis . . . 29
3.2 Mathematical modelling of HIV/AIDS . . . 29
3.2.1 Epidemiology models . . . 31
3.2.2 Pathogenesis models . . . 31
3.2.3 Estimation of parameters . . . 32
3.2.3.1 Limitations of data . . . 32
3.2.4 Reducing model complexity using dimensional analysis . . . 33
3.3 Deterministic modelling of within-host HIV progression . . . 34
3.3.1 Pre-1995 models . . . 34
3.3.2 Single-target-cell models (STC) . . . 35
3.3.3 Multiple-target-cell models (MTC) . . . 39
3.3.4 Multiple-target-cell model allowing for chronic infection (MTC-CI) 40
3.3.5 Multiple-target-cell model allowing for immune response (MTC-IR) 43
3.4 Summary . . . 47

4 Modelling therapy removal **48**
4.1 Modelling intracellular delay . . . 48
4.1.1 Distributed intracellular delay . . . 49
4.1.2 Discrete intracellular delay . . . 50
4.1.3 Justification for selection of discrete intracellular delay . . . 51
4.2 Quantifying model accuracy . . . 51
4.2.1 Doubling-time and half-life . . . 51
4.3 Incorporating discrete intracellular delay . . . 52
4.3.1 STC model including intracellular delay (STC-ID) . . . 52
4.3.2 MTC-CI model including intracellular delay (MTC-CI-ID) . . . 56
4.3.3 MTC-IR model including intracellular delay (MTC-IR-ID) . . . 56
4.4 Modelling HIV latency . . . 58
4.4.1 STC-ID including a minimum viral load (STC-ID-MVL) . . . 60
4.4.2 MTC-CI-ID including a minimum viral load (MTC-CI-ID-MVL) . 62
4.4.3 MTC-IR-ID including a minimum viral load (MTC-IR-ID-MVL) . 64
4.5 Summary of inclusion of intracellular delay and latency . . . 66
4.5.1 Intracellular delay . . . 66
4.5.2 HIV latency . . . 67
4.5.3 Overall model selection based on viral load doubling-time . . . 67
4.6 Summary . . . 70

5 Dimensional analysis **71**
5.1 Model parameter comparison using dimensional analysis 71
5.1.1 Dimensionless STC-ID-MVL model (STC-ID-MVL-DA) 72
5.1.2 Dimensionless MTC-CI-ID-MVL model (MTC-CI-ID-MVL-DA) . 76
5.1.3 Dimensionless MTC-IR-ID-MVL (MTC-IR-ID-MVL-DA) 79
5.2 Summary of sensitivity analysis 82

6 Modelling treatment interruptions **83**
6.1 Structured treatment interruption 84
6.1.1 Two-week-on two-week-off strategy (14/14) 84
6.1.2 Five-day-on two-day-off strategy (5/2) 86
6.1.3 Impact of length of varying on/off period 88
6.1.4 Overall STI regime comparison 88
6.2 Summary of structured treatment interruptions 91

7 Conclusions and future direction **92**
7.1 Summary of findings 92
7.2 Future direction 94
7.3 Concluding remarks 95

Bibliography **96**

A Variables and parameter values **112**

B Publications / Conferences **114**

C Full dimensional analysis **115**
C.1 STC-ID-L-DA full dimensional analysis 115
C.2 MTC-CI-ID-L-DA full dimensional analysis 118
C.3 MTC-IR-ID-L-DA full dimensional analysis 122

Glossary **127**

Acknowledgements

This journey would not have been possible without the help of a number of people:

This research has its origins in the main project for my Masters in Bioinformatics: based on the initial ideas of my supervisors it has mutated to be the work presented here. Over the years both Prof. Heather Ruskin and Dr. Martin Crane have provided guidance, direction and support; without their efforts this work would not have been possible. Therefore I am forever in their debt.

The dark art of dimensional analysis was illuminated by talks with Dr. Lawrence Crane. Thanks must be expressed to him for making this aspect of work possible, providing important analysis of the models developed here.

Finally, to those outside the confines of the research, without whom a prolonged period of work is impossible. To my parents for providing the environment and encouragement to undertake this immense body of work. To my friends and family for their support, and providing distractions when necessary. Lastly, to Katniss, who provided the impetus for the final push.

List of Tables

3.1 **STC variables:** Dependent variables for STC model 37
3.2 **STC parameters:** Parameters for STC model 39
3.3 **MTC-CI variables:** Dependent variables for MTC-CI model, additional variables are shown in bottom half 42
3.4 **MTC-CI parameters:** Parameters for MTC-CI model, additional parameters are shown in bottom half 42
3.5 **MTC-IR variables:** Dependent variable for MTC-IR model, additional variable shown in bottom part 44
3.6 **MTC-IR parameters:** Parameters for MTC-IR model, additional parameters shown in bottom half 46

4.1 **STC-ID-MVL steady-states:** The natural steady-states for STC-ID-MVL model. These are achieved by allowing the model to run over long periods of time as seen in *Fig. 4.6*. 61
4.2 **MTC-CI-ID-MVL steady-states:** The natural steady-states for MTC-CI-MVL model. These are achieved by allowing the model to run over long periods of time. 62
4.3 **MTC-IR-ID-MVL steady-states:** The natural steady-states for MTC-IR-MVL model. These are achieved by allowing the model to run over long periods of time. 64
4.4 **Model doubling-time:** Comparison of doubling-time for the three models discussed 66
4.5 **Intracellular delay and doubling-time:** The effect of varying intracellular delay on viral doubling-time, selected values from *Fig. 4.10* 67

5.1 **STC-ID-MVL-DA dimensionless values** The values for each of the dimensionless parameters and initial conditions across both therapy events and steady-states. 73
5.2 **STC-ID-MVL-DA parameter variation effect:** Quantification of effect in variation in initial parameter values and initial conditions based on doubling-time and half-life of viral growth. Initial values were varied from 90% to 110% of their initial value, with the resulting change in viral growth shown. 74
5.3 **MTC-CI-ID-MVL-DA parameter variation effect:** Quantification of effect in variation in initial parameter values and initial conditions based on doubling-time and half-life of viral growth. Initial values were varied from 90% to 110% of their initial value, with the resulting change in viral growth shown. 77

5.4 **MTC-IR-ID-MVL-DA parameter variation effect:** Quantification of effect in variation in initial parameter values and initial conditions based on doubling-time and half-life of viral growth. Initial values were varied from 90% to 110% of their initial value, with the resulting change in viral growth shown. 80

6.1 **Comparison of STI regimes** Potential STI regimes compared based on average viral load, peak viral load and cost savings. Highlighted are potential regimes which provide the best trade off between cost and suppression. . . 91

A.1 **All model variables:** Dependent variables for all models discussed 112
A.2 **All parameters:** Parameters for all models discussed 113

C.1 **STC-ID-L-DA dimensionless values** The values for each of the dimensionless parameters and initial conditions across both therapy events and steady states (SS). 116
C.2 **STC-ID-L-DA parameter variation effect:** Quantification of effect in variation in initial parameter values and initial conditions based on doubling time and half life of viral growth. Initial values were varied from 90% to 110% of their initial value, with the resulting change in viral growth shown. 116
C.3 **MTC-CI-ID-L dimensionless values** The values for each of the dimensionless parameters and initial conditions across both therapy events and steady states (SS). 118
C.4 **MTC-CI-ID-L-DA parameter variation effect:** Quantification of effect in variation in initial parameter values and initial conditions based on doubling time and half life of viral growth. Initial values were varied from 90% to 110% of their initial value, with the resulting change in viral growth shown. 119
C.5 **MTC-IR-ID-L dimensionless values** The values for each of the dimensionless parameters and initial conditions across both therapy events and steady states (SS). 123
C.6 **MTC-IR-ID-L-DA parameter variation effect:** Quantification of effect in variation in initial parameter values and initial conditions based on doubling time and half life of viral growth. Initial values were varied from 90% to 110% of their initial value, with the resulting change in viral growth shown. 124

List of Figures

2.1 **New HIV infections USA and Ireland:** Typical break down of new infection for developed countries, USA and Ireland in 2009 and 2010 respectively. Based on data from [1, 2] 7

2.2 **New HIV infections South Africa:** Break down of new infection for a typical developing country, South Africa from 2009. Also shown is the percentage of children orphaned due to AIDS, at least one parent lost due to an AIDS-related illness. Based on data from [3] 7

2.3 **HIV sub-type distribution:** Distribution of HIV sub-types in 2002. (Image obtained from public domain: http://en.wikipedia.org/wiki/File HIV-1_subtype_prevalence_in_2002.png) 10

2.4 **Natural HIV progression:** Natural HIV/AIDS life cycle, from initial infection to AIDS. Note: no therapy is shown, if included this would prolong the Clinical Latency period by reducing the viral load to undetectable levels ($< 50 copies/\mu L$). 13

2.5 **Diagram of HIV virion:** The 120nm virion contains two copies of single-stranded RNA containing vital proteins and enzymes necessary for HIV replication. Also shown are the glycoproteins necessary for binding to target cells. (Image obtained from public domain: http://en.wikipedia.org/wiki/File:HIV_Virion-en.png) 17

2.6 **HIV infection process:** Diagram showing HIV infection process, from binding through replication to budding. (Image obtained from public domain: http://en.wikipedia.org/wiki/File:HIV_gross_cycle_only.png) 19

3.1 **STC flow diagram:** Flow diagram for single-target-cell model 37

3.2 **Therapy events for STC model:** Shown is the effect of therapy introduction and removal to a stable system for STC model. This gives the effect on the key cells, specifically target cells (T_p), infected cells (T_p^*), infectious virus (V_i and non-infectious virus (V_{ni}). Clearly shown is how the viral levels (V_i) drop to unrealistic levels when therapy is introduced, viral levels are thought to maintain a constant low level $\approx 10 virions/mL$ as discussed in Section 4.4. This unrealistic viral load is a severe limitation of these models. Also shown is how non-infectious virus remains low under therapy removal, as this models virus produced by drug intervention alone. 38

3.3 **Therapy events for MTC-CI model:** Shown is the effect of therapy introduction and removal to a stable system for MTC-CI model. The effect on the key cells, specifically target cells (T_p and T_s), productively infected cells (T_p^* and T_s^*), chronically infected cells (C_p^* and C_s^*), and virus (V) is shown. The introduction of secondary target cells (T_s) and to a lesser extent chronic infection (C_p^* and C_s^*) allow viral levels to retain a more realistic values under drug induced viral suppression. This realism overcomes a severe limitation seen in the STC models. 41

3.4 **Therapy events for MTC-IR model:** Shown is the effect of therapy introduction and removal to a stable system for MTC-IR model. Again the effect on the key cells, specifically target cells (T_p and T_s), infected cells (T_p^* and T_s^*), effector cells (E), and virus (V) is shown. The inclusion of secondary target cells (T_s) allows viral levels to remain at more realistic values under drug induced viral suppression. By incorporating effector cells (E), a more detailed immune response is modelled. Thus, viral rebound is reduced, as HIV replication is limited by the immune system. 45

4.1 **Effect of intracellular delay on STC models:** Comparison between STC and STC-ID models. Plot A shows therapy removal, from a fixed viral load of $25 virions/mL$, accounting for intracellular delay, (ID), increases the viral doubling-time, (T_d), from 0.98 to 1.65 days. Plot B shows therapy introduction, with drug efficiency of 0.9, viral half-life, ($T_{1/2}$), remains consistent, 1.30 and 1.24 days for zero delay and 24 hour delay respectively. 54

4.2 **Effect of intracellular delay on viral load for STC models:** Comparison between viral load for STC and STC-ID model. Only therapy removal, from a viral load of $25 virions/mL$, is shown, as it is the main transition affected. The inclusion of intracellular delay, (ID), increases the viral doubling-time, (T_d), from 0.98 to 1.65 days. 55

4.3 **Effect of intracellular delay on MTC-CI models:** Comparison between MTC-CI and MTC-CI-ID models. Only therapy removal, from a viral load of $25 virions/mL$, is shown. The inclusion of the delay increases the viral doubling-time, (T_d), from 1.03 to 1.69 days. 57

4.4 **Effect of intracellular delay on MTC-IR models:** Comparison between MTC-IR and MTC-IR-ID models. Only therapy removal, from a viral load of $25 virions/mL$, is shown. The inclusion of the delay increases the viral doubling-time, (T_d), from 0.96 to 1.67 days. 59

4.5 **Effect of setting a minimum viral load on STC-ID model:** Impact of setting a minimum low viral load of $10 virions/mL$, (STC-ID-MVL), to eliminate unrealistically low levels seen in original models, (STC-ID). Shown is the difference in viral rebound seen when therapy is removed, 0-50 therapy introduction, 50-150 therapy removal. The delay in reaching viral steady-state is highlighted, when viral load is allowed to drop to unrealistic levels. . 60

4.6 **STC-ID-MVL steady-state:** Plot of steady-state for STC-ID-MVL model. 0-200 shows therapy introduction and 200-600 shows therapy removal, values are given in Table 4.1. 61

4.7 **Effect of setting a minimum viral load on MTC-CI-ID model:** Impact of including a minimum viral load, (MTC-CI-ID-MVL), thus allowing for latency. Shown is the difference between models with and without minimum viral load over two treatment events, 0-50 therapy introduction, 50-150 therapy removal. Highlighted is the delay in reaching viral steady-state when viral load is allowed to drop to unrealistic levels. 63
4.8 **Effect of setting a minimum viral load on MTC-IR-ID model:** Impact of including a minimum viral load, (MTC-IR-ID-MVL), thus allowing for latency. Shown is the difference between models with and without minimum viral load over two treatment events, 0-50 therapy introduction, 50-100 therapy removal. Highlighted is the delay in reaching viral steady-state when unrealistically low viral load are allowed. 65
4.9 **Effect of intracellular delay across all models:** Comparison of inclusion of intracellular delay across all models, (STC-ID-MVL, MTC-CI-ID-MVL and MTC-IR-ID-MVL). Plot A shows the effect on viral doubling-time for therapy removal. Specifically shown is the difference in viral doubling-time between zero intracellular delay ($ID = 0hrs$, $T_d = 1.00days$) and an intracellular delay of one day ($ID = 24hrs$, $T_d = 1.67days$). Plot B shows there is little change in viral half-life when intracellular delay is accounted for under therapy introduction, (for $ID = 0hrs$ or $ID = 24hrs$, $T_{1/2} = 1.28days$). 68
4.10 **MTC-IR-ID delay effect:** The effect of inclusion of intracellular delay on viral doubling-time. Plot A shows how doubling-time increases as intracellular delay is varied from 0 to 2 days. Plot B shows this linear relationship between intercellular delay and viral doubling-time, whereby the viral doubling time, (T_d), is given based on intracellular delay. 69

5.1 **STC-ID-MVL-DA parameter variation for therapy introduction:** Effect of varying dimensionless parameters and initial conditions for the STC-ID-MVL-DA model for therapy introduction. The specific values are given in Tables 5.2 and C.2 75
5.2 **MTC-CI-ID-MVL-DA parameter variation for therapy introduction:** Effect of varying dimensionless parameters and initial conditions for the MTC-CI-ID-MVL-DA model for therapy introduction. The specific values are given in Tables 5.3 and C.4 78
5.3 **MTC-IR-ID-MVL-DA parameter variation for therapy introduction:** Effect of varying dimensionless parameters and initial conditions for the MTC-IR-ID-MVL-DA model for therapy introduction. The specific values are given in Tables 5.4 and C.6 81

6.1 **STI using MTC-IR-ID-MVL model with 14d on and 14d off:** This is an example of an equal on/off therapy STI. This shows an average viral load of $8,446virions/mL$ with zero delay and $586virions/mL$ for 24hr delay, compared with $33virions/mL$ for continuous therapy. The peak viral loads are $58,137virions/mL$ and $3,371virions/mL$ respectively. . . 85

6.2 **STI using MTC-IR-ID-MVL model with 5d on and 2d off:** This shorter STI shows an average viral load of $4,951 virions/mL$ with zero delay and $412 virions/mL$ for 24hr delay, compared with $33 virions/mL$ for continuous therapy. Peak viral loads are lower, $10,037 virions/mL$ and $712 virions/mL$ respectively. 87
6.3 **Comparison between 5/2, 20/8 and 26/2 STI using MTC-IR-ID-MVL model:** This give a comparison between a number of potential STI; 5/2, a scaled up 5/2 to give 20d on and 8d off (20/8), and a 26d on and 2d off (26/2). The average viral loads are $437 virions/mL$, $352 virions/mL$ and $68 virions/mL$ respectively. The peak viral loads are $756 virions/mL$, $1,648 virions/mL$ and $141 virions/mL$ respectively. 89
6.4 **Suggested best practice overall STI regime 18/3:** This demonstrated a potential best practice regime of 18 days on and 3 days off. The average viral load is $120 virions/mL$ with a peak of $285 virions/mL$. The potential cost savings are 17%. 90

C.1 **STC-ID-L-DA parameter variation for therapy introduction:** Effect of varying dimensionless parameters and initial conditions for the STC-ID-L-DA model for therapy introduction. The specific values are given in Table C.2 117
C.2 **STC-ID-L-DA parameter variation for therapy removal:** Effect of varying dimensionless parameters and initial conditions for the STC-ID-L-DA model for therapy removal. The specific values are given in Table C.2 117
C.3 **MTC-CI-ID-L-DA parameter variation for therapy introduction:** Effect of varying dimensionless parameters and initial conditions for the STC-ID-L-DA model for therapy introduction. The specific values are given in Table C.4 120
C.4 **MTC-CI-ID-L-DA parameter variation for therapy removal:** Effect of varying dimensionless parameters and initial conditions for the STC-ID-L-DA model for therapy removal. The specific values are given in Table C.4 121
C.5 **MTC-IR-ID-L-DA parameter variation for therapy introduction:** Effect of varying dimensionless parameters and initial conditions for the STC-ID-L-DA model for therapy introduction. The specific values are given in Table C.6 125
C.6 **MTC-IR-ID-L-DA parameter variation for therapy removal:** Effect of varying dimensionless parameters and initial conditions for the STC-ID-L-DA model for therapy removal. The specific values are given in Table C.6 126

Acronyms

AIDS	Acquired immune deficiency syndrome
ART	Antiretroviral therapy
CA	Cellular automata
CI	Chronic infection (model)
CRF	Circulating recombinant form
DA	Dimensional analysis
DDE	Delay differential equation
DNA	Deoxyribonucleic acid
DRM	Drug resistant mutation
HIV	Human immunodeficiency virus
ID	Intracellular delay (model)
IDU	Intravenous drug user
IR	Immune response (model)
LTNP	Long term non-progressors
MSM	Men who have sex with men
MTC	Multiple-target-cell (model)
NNRTI	Non-nucleoside reverse transcriptase inhibitor
NRTI	Nucleoside reverse transcriptase inhibitor
ODE	Ordinary differential equation
OI	Opportunistic infection
PI	Protease inhibitor
RNA	Ribonucleic acid
RTI	Reverse transcriptase inhibitor
STC	Single-target-cell (model)
STI	Structured treatment interruption
TB	Tuberculosis
UN	United nations
WHO	World health organisation

Chapter 1

Introduction

1.1 Background

Acquired immune deficiency syndrome (AIDS) has spread from a handful of cases to a worldwide pandemic in three short decades [4, 5]. Although a reduction of 19% in new human immunodeficiency virus (HIV) infections has been seen in 2010, compared to their peak in 1999, new infections still remain unacceptably high [6, 7]. There are currently 33.3 million people living with HIV/AIDS, of which 2.5 million are children. The majority of these cases are within one region, sub-Saharan Africa which is responsible for 68% of the global total (22.5 million) [8]. As access to therapy increases there has been a corresponding decrease in deaths due to AIDS related illnesses, namely 1.8 million in 2009 compared with 2.1 million in 2004 [6]. Unfortunately, due to the large numbers of HIV positive people the pandemic is expected to continue to grow into the foreseeable future [9].

There is currently no cure or vaccine for HIV/AIDS. However, significant international efforts in treating those infected and controlling the spread of HIV have reduced both new infections and those dying of AIDS related illnesses [5, 10, 11]. Nevertheless, there is a US$10 billion gap between current funding and what is needed to improve access to therapy and preventative measures [9]. Furthermore, due to current fiscal constraints, recent annual funding levels have not risen for the first time in HIV/AIDS history, remaining at 2008 levels of US$15.9 billion [6]. This is despite projected estimates that funding levels will need to rise to US$35 billion annually by 2031 to maintain current treatment levels [9]. This indicates that the funding gap will widen in the future, emphasising that the limited money available will need to be spread more thinly and will motivate the sourcing of cheaper solutions to controlling HIV/AIDS.

Primarily there are two methods of controlling HIV/AIDS; (i) reducing the number of new infections and (ii) treating those infected with HIV, thus delaying the onset of AIDS or AIDS-related illness, e.g. opportunistic infections (OIs). Reduction in the number of new infections requires significant behavioural changes, which take time. However, increased education and wider access to condoms have been observed to produce positive results. This is shown by the fact that in sub-Saharan Africa, with 22% of annual AIDS spending on HIV prevention in recent years, new infection rates have dropped by more than 25% over the last 10 years [6, 7]. Furthermore, by increasing access to therapy, to 5.2 million, (a 30% increase from 2008), AIDS-related deaths have decreased in sub-Saharan Africa by 20% from 2004 [8]. It is estimated that, since the introduction of antiretroviral therapy (ART) in 1996, approximately 14.4 million life-years have been added to those living with HIV/AIDS [11]. Some places, like Brazil, where access to therapy is greater, report an estimated 1.2 million life-years gained. As a result part of the United Nations (UN) Millennium Development Goals is providing access to therapy for all who need it, currently estimated at 15 million people, [12, 6].

The drive for universal access to ART has highlighted the problems associated with maintaining successful regimes for this therapy. This treatment controls but does not provide a cure for HIV [13, 14]. As such it must be administered indefinitely, but this is difficult to maintain due to complex pill regimes and build up in toxicity levels due to continual use. This poor adherence to treatment regimes can result in therapy failure, primarily due to development of drug-resistant mutations (DRMs) [15]. These mutant viruses can evade specifically-targeted drug types and replicate unchecked, thus making whole drug types ineffective and requiring changes to therapy regimes [16]. If enough different DRMs develop, thus blocking numerous drug types, then effective therapy becomes difficult to devise and there is little that can be offered to the patient. This is extremely important in developing countries where only primary therapy, (based on an initial drug combination), may be available [17]. Thus, accurate understanding of viral replication, during drug-induced viral suppression, is needed, which can be used to indicate why therapy fails and under what circumstances it can be stopped/resumed. This research develops new mathematical models which can be used to answer these questions.

1.2 Mathematical modelling

Since the early days of HIV/AIDS a number of methods have been used to increase our understanding of the way in which infection progresses. Mathematical modelling has played a vital role in this process and a subset of these models are utilised here to identify what happens when therapy stops or fails. These models use ordinary differential equations (ODEs) to track changes in the levels of key cells associated with HIV infection, i.e. target cells, infected cells and virus level. However, to achieve an accurate representation of drug-induced viral suppression, seen under successful ART, existing ODE models need to be modified, specifically to include the time between a cell becoming infected and producing virions, (intracellular delay). This delay plays a crucial role in delaying viral rebound seen upon removal of therapy and has not being fully investigated to date. Thus current ODE models are modified to include intracellular delay, resulting in a set of delay differential equation (DDE) models. These adapted models can then be used to investigate viral growth from low viral loads, thus allowing modelling of therapy failure or removal, and gives important insight to when therapy may be stopped/resumed and under what circumstances. Furthermore, this allows detailed investigation of structured treatment interruptions (STIs) analysing why these have failed in the past and what needs to change for future success. Successful STIs can reduce the time on ART, thus providing health and cost benefits.

Developing any model involves a trade-off between complexity and available data. Within the context of the DDE models developed here, data are limited to treatment transitions, which generally occur infrequently. Furthermore, the transition necessary to fully validate the developed models is therapy removal, which is not part of current treatment regimes. As such the approach taken here is to investigate the impact of intracellular delay on models and parameters already published, which are then validated using viral half-life and doubling time. Also a slightly different perspective of dimensional analysis (DA) is introduced as a method of limiting the number of parameters to be estimated. The objective is to focus on key parameters, which determine model function. This produces a model which is both as simple and accurate as possible, which can be used for both treatment events, allowing STI regimes to be evaluated, at least in theory. This also allows potential STI regimes to be designed for resource-limited regions, where continuous access to therapy can not be guaranteed, and treatment interruption is inevitable. Furthermore, there is a cost saving associated with interrupting therapy, which will become increasingly more important as need continues to outstrip HIV funding.

1.3 Thesis structure and scope

This thesis is split into a number of chapters, each chapter building on the previous, to provide the set of DDE models which are capable of modelling treatment events, thus allowing investigation of STI and therapy failure. The chapters are summarised as follows:

Chapter 2 gives a general background to HIV/AIDS, including the global cost, both human and financial, of the HIV/AIDS pandemic to date. It also covers HIV transmission and how this can be controlled. Finally, the biological background necessary to develop the mathematical models is given, including how HIV progresses within-host, how ART blocks replication and the treatment strategies used to delay progression to AIDS.

Chapter 3 covers HIV/AIDS research, starting out with a general overview and then focusing on mathematical modelling of HIV/AIDS, with the modelling of within-host HIV progression discussed in detail. The deterministic ODE models used as the basis for the remainder of the research are then introduced and their limitations detailed.

Chapter 4 is the start of original research and addresses the limitations of the ODE models discussed in the previous chapter, by adapting these to include intracellular delay and HIV latency. As these are newly developed models, the rationale for these updates is discussed and evaluated. These DDE models form the basis for the treatment event analysis discussed in chapter 6.

Chapter 5 continues the novel material by using dimensional analysis to develop a dimensionless representation of the DDE models developed in chapter 4, such that the key parameters can be identified. The relative importance of each dimensionless parameter is determined by varying each separately and determining the effect this has on model function. The biological meaning behind these key parameters is then discussed, determining why they are important to model function.

Chapter 6 concludes the new work by using the models developed in the previous chapters to analyse treatment events, determining why STIs have failed in the past and what is necessary for future success. These DDE models are then used to design potential STI regimes for future testing.

Chapter 7 provides an overall summary and discussion of the impact that these new DDE models have on HIV/AIDS understanding. Future work is then identified. Finally an overall conclusion of the research is given.

Chapter 2

AIDS pandemic and HIV infection progression

HIV/AIDS has spread from a mere handful of cases in the early 1980's to the present day where over 60 million cases have been reported worldwide, of which over 25 million have died due to AIDS related illnesses [6]. While this pandemic[1] is thought to have peaked in the late 1990's there is a large number of people living with HIV, meaning the pandemic will continue into the foreseeable future. Although the spread has been exceedingly rapid it has not been uniform with some regions carrying the main burden. Sub-Saharan Africa, for example, accounts for approximately 60% of overall infection but only accounts for 10% of world population [8, 6]. Even within regions some groups are at greater risk than others; for example, within the USA over half new infections are within the 'men who have sex with men' (MSM) group.

This chapter gives the main mechanisms responsible for the transmission of HIV, how it progresses to AIDS and what can be done to reduce the pandemic. This information is set in context by giving an overview of the scale of the pandemic and the efforts to control current and new infections. The biology of target cell infection is also covered, indicating how disruption of each replication steps occurs, as this forms the basis for a large part of the work in this thesis. This disruption delays the onset of AIDS by reducing HIV replication, and thus the amount of virus present in an individual. The therapeutic strategies for delaying onset of AIDS are then discussed.

[1] **Pandemic:** wide spread of an infectious disease within a human population across multiple countries or, as in the case of HIV, worldwide.

2.1 HIV/AIDS overview

Currently the HIV/AIDS pandemic is estimated at more than 33 million people living with HIV/AIDS with more than 25 million lives lost due to AIDS related illnesses [6]. In the process this has created over 16 million AIDS orphans, children who have lost one or more parents to AIDS. With 2.5 million children living with HIV/AIDS the number of HIV/AIDS infected people is expected to remain unacceptably high for the foreseeable future. Although there have been significant progresses in treatment and prevention over the last decades there is still a need for new strategies to target the reduction of pandemic size [4, 9].

2.1.1 Current HIV/AIDS pandemic

Over the last thirty years HIV/AIDS has moved from a single reported infection cluster [18] to the current world wide pandemic [6]. While new infection levels are thought to have peaked at 3.2 million in 1997 they still remain extremely high, at 2.6 million just over ten years later, a 19% reduction [6]. The increase in the total infected population is set to continue, as new infections are added to the 33.3 million already infected. With nobody cured, and an estimated 1.8 million dying due to AIDS related illness, 0.8 million are added to the total infected annually. This increase is bolstered by a population increasing globally. However, the transmission rate of HIV/AID is not universal, and can be geographically split in developed and developing countries:

2.1.1.1 Developed countries

The original cases, of what would be later known as AIDS, were first identified in a specific group in the USA [18]. The majority of early diagnosed cases were confined to this initial group, defined as MSM [19]. This group still makes up over 50% of new infections in the USA [1, 20, 21]. The other primary group to initially report high incidence were IDU (intravenous drug users)[19], and this group also still makes up a significant portion of the overall infection in the USA [1, 20], as can be seen in *Fig. 2.1*. Given the relatively small number of individuals in each of these respective groups, compared to the population at large, infection incidence is disproportionately large, creating 'at-risk' groups. This trend is followed in most other developed countries, e.g. in 2010 Ireland's 331 new HIV infection were 37.2% heterosexual, 40.5% MSM, 6.6% IDU, 11.2% unknown [2], *Fig. 2.1*. The trend can be generalised across the developed world, where a small number of 'at-risk' groups make up a disproportionate amount of new HIV infections [6].

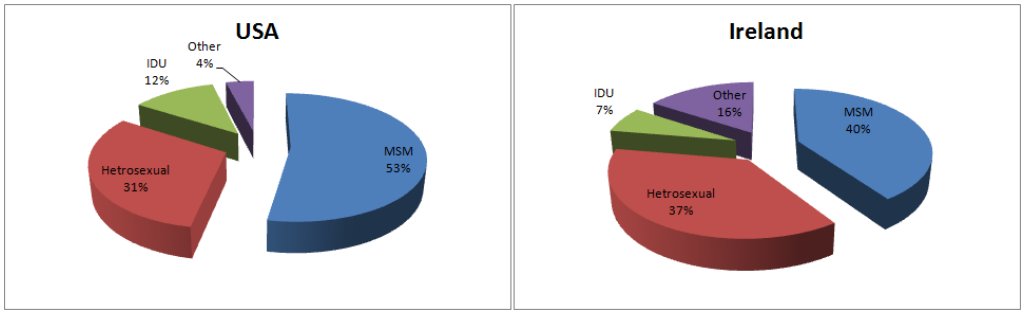

Figure 2.1: New HIV infections USA and Ireland: Typical break down of new infection for developed countries, USA and Ireland in 2009 and 2010 respectively. Based on data from [1, 2]

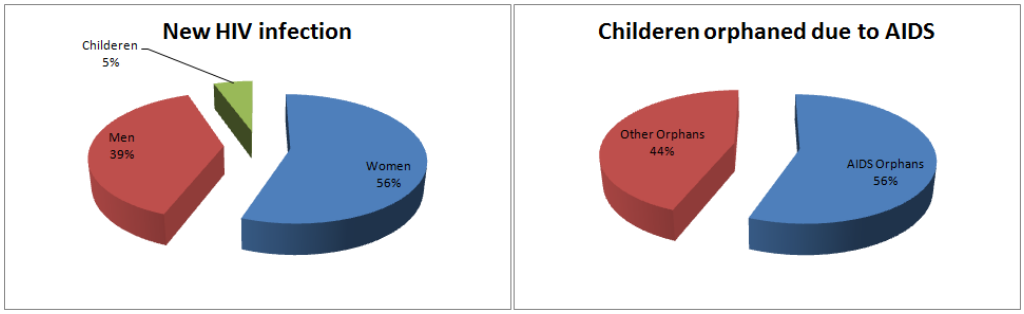

Figure 2.2: New HIV infections South Africa: Break down of new infection for a typical developing country, South Africa from 2009. Also shown is the percentage of children orphaned due to AIDS, at least one parent lost due to an AIDS-related illness. Based on data from [3]

2.1.1.2 Developing countries

In parallel with the first cases being reported across the developed world, in the early 1980's, a new disease, known locally as 'slim disease' was also seen in parts of Africa [22]. This disease resembled the AIDS seen in developed countries closely, but had different transmission patterns, being predominately transmitted by heterosexual sexual intercourse. This pattern is still true for most developing countries, where transmission is mainly among the heterosexual population. Furthermore, the majority of new HIV infection is in the developing world, for example sub-Saharan Africa accounts for 68% (22.5 million) of all people living with HIV/AIDS and 72% (1.3 million) of those who died from an AIDS related illness [6]. New infection distribution for a typical developing country, South Africa, is shown in *Fig. 2.2*. This figure also highlights the large proportion of children orphaned due to AIDS, (at leat one parent lost due to AIDS-related illness), compared with the general orphaned population.

2.1.1.3 HIV therapy

There is currently no cure for HIV; the accepted strategy is to delay progression to full-blown AIDS or AIDS related illness by therapeutic means. Therapy comes in the form of anti-retroviral therapy (ART), which blocks within-host HIV replication and lowers the amount of virus in the body. It is thought that high viral levels continually stimulate the immune system, slowly damaging key immune components, eventually leading to AIDS [14]. While ART has been widely available in the developed world, since the mid 1990's, it is only now reaching the wider global population, specifically in developing countries, with the World Health Organisation (WHO) objective being access to all in need by 2015 [23]. Although major strides have been made in this direction, with access to treatment in developing countries increasing by 30% between 2008 and 2009 [6]; it is still significantly less than required. Across the world only 35% of those eligible for treatment have access. However, a recent change in the WHO therapy guidelines, advocating earlier initiation of therapy in the HIV life cycle, has increased the number eligible for therapy by 4.5 million [23].

2.1.1.4 HIV/AIDS funding

There is a significant cost associated with therapy: for example in the developed world the monthly cost for ART is in the region of US$\$1,000$. This is a cost which current global HIV/AIDS funding levels can not match. The 2009 global HIV/AIDS budget of US$\$15.9$ billion is only 60% of what is required, leaving a funding gap of US$\$10$ billion [9]. Furthermore, the increase in ART eligibility has significantly added to the funding shortfall seen in developing countries [23]. In the future this gap is expected to grow, due to contraction of the world economy, the projected additional demand for therapy and increasing world population. Based on this, and future shortfalls, there is a need to allocate the limited funds more efficiently, by developing more cost effective solutions for treating HIV infection. This is seen in the drive for generic drugs and simpler combination therapy which are continually reducing costs [17]. Furthermore, given the different demographics in transmission, a universal treatment strategy is not possible and must be tailored to each situation, thus increasing the expenditure [17, 13, 24].

While delaying the onset of AIDS decreases the mortality and morbidity observed, it can not reduce the overall pandemic alone. Approximately 20% of the annual budget to fight HIV/AIDS is spent on increasing awareness and promoting less risky sexual practices [6]. While having an impact on future HIV infection numbers, through increasing public knowledge of HIV and how it is transmitted, a significant behavioural change is required, and this is something which happens slowly. While some positive results have been seen, there have also been significant setbacks, e.g. infection levels are actually rising in USA among MSM [20, 1, 21].

2.1.2 Origin of HIV/AIDS

The first reports of AIDS were in the early 1980's when 5 cases of *pneumocystis pneumonia* (PCP) were reported in the Los Angeles region of the USA between October 1980 and May 1981 [18]. These cases stood out because PCP normally only affected severely immuno-suppressed patients, and these were relatively healthy young homosexual men. Shortly after this *Kaposis sarcoma* was used as primary indication of what was subsequently described as AIDS [25]. HIV was then identified as the underlying cause of AIDS, in the mid 1980s [26, 27, 28, 29].

It is widely accepted that HIV originated in Africa and had been present for a number of years before identification of AIDS [30]. There are two distinct viral strains of HIV known today:

HIV-1 is the prevalent strain throughout the world and also the most virulent. Most cases progress to AIDS, and death due to AIDS-related illnesses, within ten years, if untreated. HIV-1 has been shown to have originated in sub-Saharan regions of Africa around the 1930's [31] with the earliest HIV-1 sequence coming from the Democratic Republic of Congo in 1959, (then Belgian Congo), [32]. As HIV-1 accounts for virtually all HIV infection, it is the focus of most research and drug trials. As such HIV-1 is the subject of the mathematical models discussed in this research.

HIV-2 is confined to West Africa and is less virulent than HIV-1 [33]. Most infected individuals show few symptoms and generally do not progress to full-blown AIDS as fast [34, 35]. As it only infects a small number of people, compared to HIV-1, it does not form the basis of much HIV/AIDS research. The exception is comparison of differences with HIV-1 and what can be learned about its slower progression to AIDS.

These types are further split into a number of groups. For HIV-1 there are 4 primary groups (M,N,O and P) [36]. As more than 90% of HIV-1 infection is confined to group M this is again the primary focus of research. HIV-1 group M is subdivided into subtypes (or

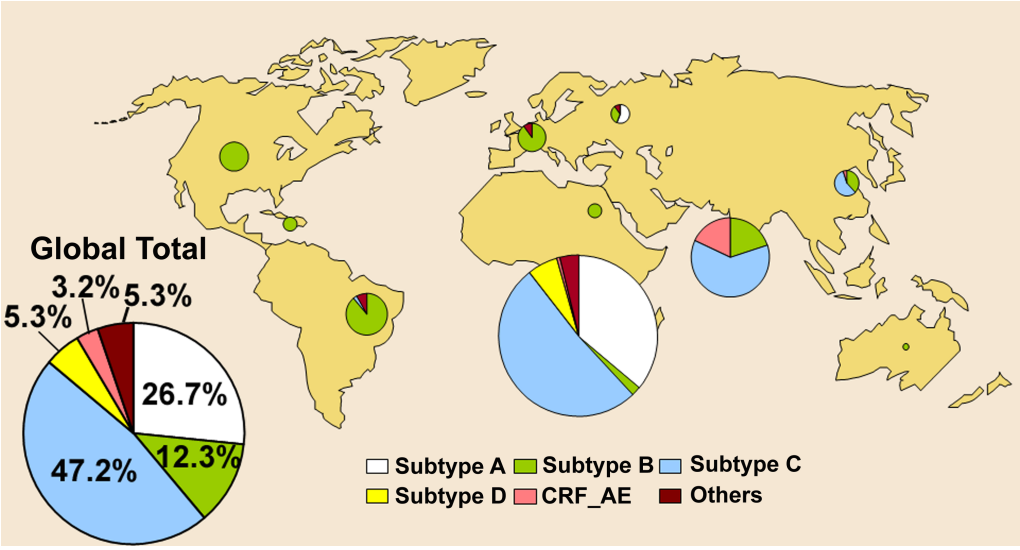

Figure 2.3: HIV sub-type distribution: Distribution of HIV sub-types in 2002. (Image obtained from public domain: http://en.wikipedia.org/wiki/File HIV-1_subtype_prevalence_in_2002.png)

clades): A, B, C, D, F, G, H, J and K. As each subtype is generally confined to a geographical location, as shown in *Fig. 2.3*, therapy can be tailored to individual subtypes. However, there is a risk of cross-subtype infection, which can produce new hybrid virus [15]. If these survive they are called CRFs (circulating recombinant forms), the most prominent being CRF_AE. The presence of CRFs significantly increase the difficulty in treating HIV, as some of these CRFs can produce a viral strain which is resistant to particular therapy regimes [37]. This means that, for effective therapy to be administered, knowledge of the potential HIV viral strain, or strains, involved in infection of an individual is required. As individual testing is not economically viable in the developing world, knowledge of the geographical location of the above subtypes becomes very useful.

HIV has been shown to have developed from primates [38, 30]. In particular, an example is provided by the Sooty Managabey monkeys (*Cercocebus atys*), prevalent in sub-Saharan Africa, where a similar virus SIV (Simian Immunodeficiency Virus) has been identified [30, 39]. SIV is present in more than 20 African Primate species, but each has their own built-in viral immunity and the virus does not appear to universally progress to AIDS, as it does for humans. However, when different SIV viral strains are introduced, this specific immunity is lost, and the virus, yet again, is likely to prove fatal [40]. The possible reason for this specific immunity is that it is built up over a number of years by survival of the fittest i.e. only those able to fight the virus survive [30], an observation which obviously can not be accepted for humans.

2.1.3 HIV progression to AIDS

HIV is an infection which, with the help of co-infections[2], depletes a key part of the immune system, leading to AIDS, and possible death due to AIDS-related illnesses [14, 41, 42]. How this depletion occurs is still not fully understood, but is widely accepted to involve a number of factors that combine to disrupt natural immune system function [43, 44, 45]. One important factor is the continual activation of the immune system, suggesting exhaustion over a long period of time. This is consistent with other research, e.g. investigation into severe cold on the immune system [46]. Currently the only way to delay progression to AIDS is to significantly reduce HIV replication, thus allowing the normal immune function to return.

The natural progression from HIV to AIDS, (i.e. without therapeutic intervention), takes approximately ten years from initial infection to the terminal stage of death, due to AIDS-related illnesses [47]. However, this progression can be much shorter, depending on how infection was transmitted, the presence of co-infections, individual age and access to palliative care in treatment of opportunistic infections. On the other hand, advances in therapeutic intervention, to reduce virus levels, can delay the time between infection and terminal stages significantly [13]. In consequence, HIV is now considered a chronic illness, given access to therapy, whereby death may occur from non-HIV related cause [48].

HIV is a very complex infection undergoing a number of stages before it eventually culminates in AIDS. Thus is only possible to give an overview of progression here, for a fuller description the reader is referred to [14, 49], also HIV replication is covered in detail in Section 2.2. The natural progression of HIV infection, shown in *Fig. 2.4*, follows the three stages described below:

2.1.3.1 Acute phase

After primary infection, when HIV first enters the body, the immune system initiates a response to fight against the new invader. As HIV has a very high replication rate, producing about $10^{10} - 10^{12}$ new virions (complete viral particles) per day, the viral load (amount of virus in the body) grows faster than the immune system can respond [14, 49]. This period, which last a number of weeks, shows a peak in viral load before the immune system recovers and starts to reduce and control the amount of virus present. Thus the immune response is reasonably successful at controlling the initial virus attack. However, key components of the immune system, namely the CD4^+T cells which orchestrate immune response, are significantly diminished. A healthy person can expect to have about $1,000$ CD4^+T $cells/\mu L$

[2]**Co-infection:** Simultaneous infection with more than one virus, bacterium, or other micro-organism at a given time, which may increase the severity and duration of one or both. Significant HIV co-infections include: tuberculosis (TB) and hepatitis B and C

of plasma and these drop by about 50%, to around $500 cells/\mu L$. Common symptoms of acute infection are fever, nausea and malaise [42].

2.1.3.2 Chronic phase or clinical latency

After the initial immune response a viral load 'set-point' is reached, with HIV replicating at a relatively constant level [14, 49]. This period can last a number of years, and while not immediately harmful, the number of $CD4^+$T cells are slowly depleted, generally without any outwardly-observable change to patient health. As a result many patients present in the final stages of AIDS, without knowing they are infected. This asymptotic period led original researchers to identify HIV as a *latent virus*, laying dormant and waiting to be reactivated, similar to other viruses, e.g. *herpes simplex virus* [50, 51]. However, as knowledge of HIV and AIDS increased, it was shown that a large amount of free virus was continuously replicating with the immune system barely keeping it in check [52, 53]. This stage is now also described as the 'clinical latency' period, referring back to the original identification of HIV.

The introduction of therapy, in the form of ART blocking HIV replication, means viral load can be reduced significantly [13]. Under continual administration of therapy, viral load drops below detectable levels, and the progression towards AIDS is halted [13]. Nevertheless, there is still some virus present, as HIV does have true latent reserves in other cells which therapy can not reach, e.g. in the brain and lymphatic nodes [54, 55]. If therapy is removed, or fails, the viral load rebounds quickly, re-stimulating disease progression towards AIDS [56]. However, if the therapy regime can be maintained indefinitely, then HIV becomes a chronic infection, never progressing to AIDS [48]. Current ART can be administered indefinitely and, with the escalation of access to therapy, it is hoped to make HIV/AIDS a universal chronic infection. Furthermore, while on successful therapy, viral load drops significantly, thus reducing transmission rates [57, 58].

2.1.3.3 AIDS

This equilibrium situation, of viral replication being kept in check by the immune system, can be sustained for a number of years, (approximately 10 years), without therapeutic intervention [14]. Eventually the numbers of $CD4^+$T helper cells are depleted and the immune system can no longer even orchestrate a token response to opportunistic infections, (OIs) [59]. OIs are a number of infections associated with AIDS, such as PCP (*pneumocystis pneumonia*), TB, *candidiasis*, *herpes zoster* and many others [51, 42]. It is the presence of these OIs that give an indication that a patient has progressed to the AIDS stage. The inability to fight off an OI is the general cause of AIDS-related death, not the actual HIV infection itself. It is because of one of these OIs that HIV/AIDS first came to light [18].

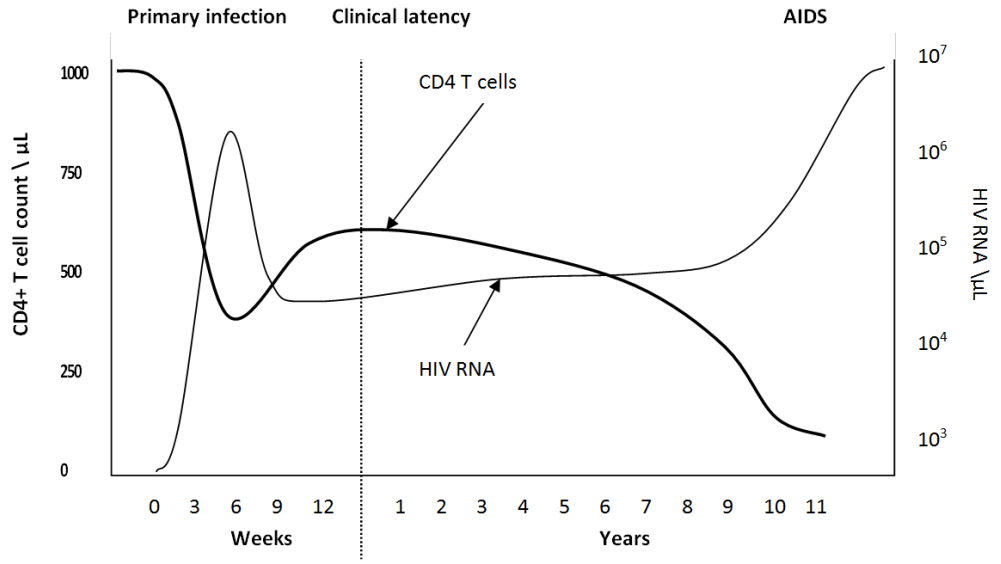

Figure 2.4: Natural HIV progression: Natural HIV/AIDS life cycle, from initial infection to AIDS. Note: no therapy is shown, if included this would prolong the Clinical Latency period by reducing the viral load to undetectable levels ($< 50 copies/\mu L$).

2.1.4 HIV transmission

HIV exists outside of host cells, which it needs to replicate, as tiny roughly spherical particles (virions) about $120nm$ in size. These virions can not survive outside the body, meaning the passage from individual to individual must take place through bodily fluids i.e. direct contact between a mucous membrane or the bloodstream and blood, semen, preseminal fluid, vaginal fluid or breast milk. Furthermore, HIV has a relatively low transmission rate[3] ($1:1000$ to $1:100$), which is $1/10$ that of hepatitis C and $1/100$ that of hepatitis B [42]. The primary transmission routes are:

Sexual Intercourse Passage of bodily fluids through unprotected sexual intercourse is the main method of HIV infection and accounts for the majority of new infections [60]. The probability of infection depends on the type of intercourse, with receptive anal intercourse (0.82%) significantly greater than vaginal intercourse (0.05%) [42, 61, 38].

Intravenous Drug Users The use of unsterilised injection equipment by intravenous drug users (IDU) puts them at great risk of contracting HIV. If this equipment has previously used by an infected person the chance of infection is 20%, compared with 0.5% for accidental needle pricks from contaminated needles [42, 62].

[3]**Transmission rate:** The rate at which an infectious agent is spread between individuals

Mother to Child (vertical) Vertical transmission, either during pregnancy, during birth or via breast feeding, has a 25% probability of HIV infection. However, this can be reduced to less than 1% by introducing ART to lower the mother's viral load [42]. Much research has been done in this area resulting in a significant reduction in transmission rates [63, 64].

Blood Products Exposure to contaminated blood products is one of the fastest ways in which progression of infection occurs, because of the relatively large amount of the virus introduced to the body, coupled with a naturally active immune system response. However, virtually all blood products are routinely screened for HIV and other diseases, with reduced screening levels in developing countries.

2.2 HIV replication

After primary infection HIV must locate and enter target cells to replicate [65]. Depending on the initial amount of virus that enters, an infection may or may not establish itself, as the immune system utilises a number of tools to fight any infection [14]. However, once the infection is established the immune system alone can not clear it. HIV uses CD4 receptors to bind to target cells and while, in general, the virus itself does not directly kill these cells, it does have adverse affects on the immune system [14]. The primary targets for HIV replication are $CD4^+$T helper cells [66]. Further, it is the depletion of these cells that results in AIDS, although the exact depletion process is not yet fully understood [38].

Generally, after initial infection the target cells migrate to the regional lymphoid tissue within 3 to 5 days. The increased activation of $CD4^+$T cells results in a large increase in viral replication within the first 2 weeks, as locally induced inflammatory responses actually facilitate replication. In $40 - 90\%$ of cases this response may result in flu-like symptoms, which may last as long as two weeks, but some infections may not show any symptoms within the first few years [38, 42]. At this stage the immune system is mounting only a relatively inefficient response, thus allowing the virus to replicate unchecked. Patients are *highly infectious* at this stage, but the common HIV test does not produce a positive result, as it based on presence of HIV antibodies and there are none to detect. This lack of a definite result, coupled with laboratory abnormalities that may alter infection status, make it necessary to carry out several tests over time, after a suspected infection event, to get an accurate result [38, 42]. Furthermore, the possibility of cross-reaction with other infections, along with the expense of testing multiple times, means HIV testing in developing countries is not as frequent as desired [6].

2.2.1 Immune system

The immune system play a vital role in HIV replication, both fighting infection and providing the necessary target cells needed for HIV replication. The immune system can be split into two broad response types:

Innate immune response is a non-specific immune response which is the first line of defence against infection [49].

Adaptive immune response is a pathogen and antigen-specific response which develops in response to an infection. This is a slower but more specific response which also retains memory of specific infections allowing for faster activation upon reinfection. It is by this process that vaccination is possible, e.g. by exposure to an attenuated vaccine which triggers an adaptive immune response but not actual infection. Unfortunately, vaccination is not possible for HIV infection at the moment.

Both responses are triggered by HIV infection and, as described above, provide some control of HIV replication leading to the chronic phase. Furthermore, the responses are reduced with successful therapy, as the amount of virus in the system is greatly reduced, but are stimulated if therapy stops or fails.

2.2.2 HIV target cells

HIV targets cells presenting CD4 receptors, which are used to bind the virion to the target cell. There are a number of cells presenting this receptor:

T helper cells are a sub-group of lymphocytes, a type of white blood cell, which help establish and control an immune response [67]. They do not kill infected cells but direct other immune system cells to do so.

Regulatory T cells help suppress the immune response, thus preventing an excessive immune response [68].

Monocytes move to sites of infection and differentiate into macrophages and dendritic cells to elicit an immune response [66].

Macrophages are white blood cells produced by the differentiation of monocytes in tissues [69]. Their role is to engulf and then digest cellular debris and pathogens. They can also stimulate other immune cells.

Dendritic cells are antigen-presenting cells processing antigen material and presenting it on the surface to other cells of the immune system [70, 66].

The population, and accessibility, vary with each cell type but T helper cells are the primary target for HIV replication. The slow depletion of these leads to AIDS, as already stated, because they control immune responses. Furthermore, these target cells produce virus at different rates and react differently to ART, meaning that they have to be incorporated separately in models, as discussed in detail in Chapter 3.

2.2.3 HIV replication in target cells

HIV, as shown in *Fig. 2.5*, is a retrovirus and must use a host cell to produce new virus. A retrovirus is single-stranded chain of nucleotides, ribonucleic acid (RNA). These nucleotides are the building blocks of nucleic acids used as a blueprint for all life. This single stranded RNA must be converted to deoxyribonucleic acid (DNA), using a host cell's built in replication processes, to allow HIV to replicate. As a retrovirus must first enter a cell before replication, target cells are chosen based on an affinity for particular receptors. For example, human T-lymphocytes virus type I, (HTVL-I), targets T and B cells as it has an affinity for the glycoprotein 46 (gp46). However, HIV has the most specific targeting system of this type [71]. HIV specifically targets cells presenting CD4 receptors because HIV contains the glycoprotein 120, (gp120), which has a strong affinity for CD4 receptors. HIV's main targets are $CD4^{+}$T helper cells, due to their relative abundance, but other cells like Lymphocytes in plasma and Glial cells in the brain are also targeted [42]. Each stage of the replication process is a potential therapeutic target, by blocking the interactions. The stages, as shown in *Fig. 2.6*, are:

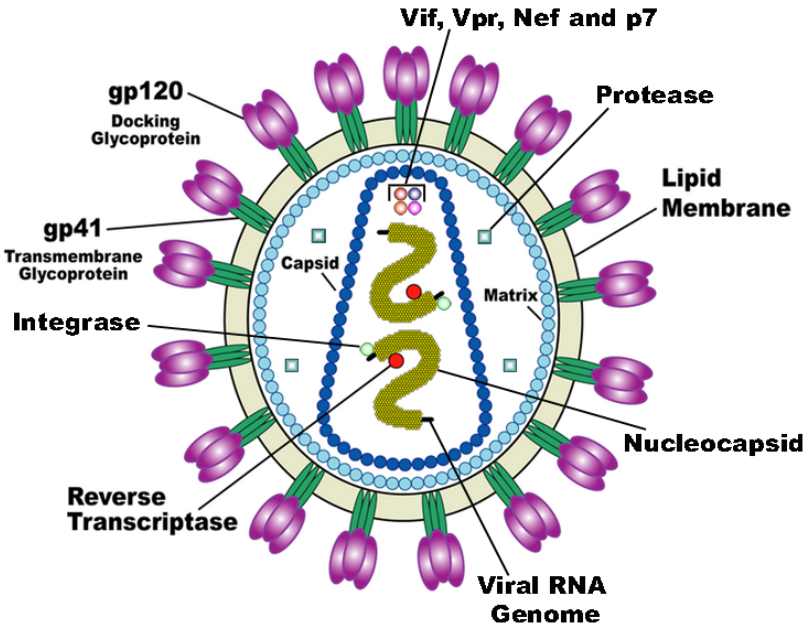

Figure 2.5: Diagram of HIV virion: The 120nm virion contains two copies of single-stranded RNA containing vital proteins and enzymes necessary for HIV replication. Also shown are the glycoproteins necessary for binding to target cells. (Image obtained from public domain: http://en.wikipedia.org/wiki/File:HIV_Virion-en.png)

Binding To facilitate entry the gp120 of the virion binds to the CD4 receptors on the target cell surface. While CD4 is the main receptor other receptors may be utilised but to a much lesser extent. As a result HIV can bind to any cell presenting the CD4 receptor, but the majority are $CD4^+$T helper cells. In addition to using CD4 to bind to the target cell a number of co-receptors are required before it is possible to enter the cell. While there are potentially over 200 co-receptors the most common are CXCR4 and CCR5, named after the natural chemokines that bind to them [42].

Entry After binding HIV RNA is injected into the cell where it will use the cell's own chemistry for replication.

Integration The single stranded RNA genome is converted to a DNA molecule using RT (reverse transcriptase), an enzyme that transcribes single-stranded RNA into double-stranded DNA. This DNA molecule is then transported into the cell nucleus where it is integrated into the host cell's genome by another viral enzyme called integrase. This integration creates a provirus, i.e. a virus genome that is integrated into the DNA of a host cell. Once integrated, this provirus may remain dormant, awaiting cell activation, or immediately start replicating.

Transcription Viral replication happens by transcribing the integrated provirus into mRNA (messenger RNA), which is a RNA molecule with the blueprint for proteins. This mRNA is spliced into smaller parts and exported from the nucleus to where they are translated into proteins and packaged into new virus particles.

Budding HIV protease then cleaves the new virus particles into individual functional HIV proteins and enzymes. These proteins are then assembled to produce a mature HIV virion which slowly buds from the host cell. However, sometimes the cell dies releasing a number of virions at once (lysis). The budded virions are then able to infect another cell.

It is estimated that this replication cycle takes in the region of 24 hours from cell infection until it starts producing virions [72, 73, 74, 75, 76, 77, 78]. However, only active cells produce virions, which allow HIV to remain hidden in inactive cells. These inactive cells may eventually become active and start producing virions, creating latency [54, 79, 80, 55]. Each of the above steps is a potential target for invasive therapy, described in detail in Section 2.3.2.

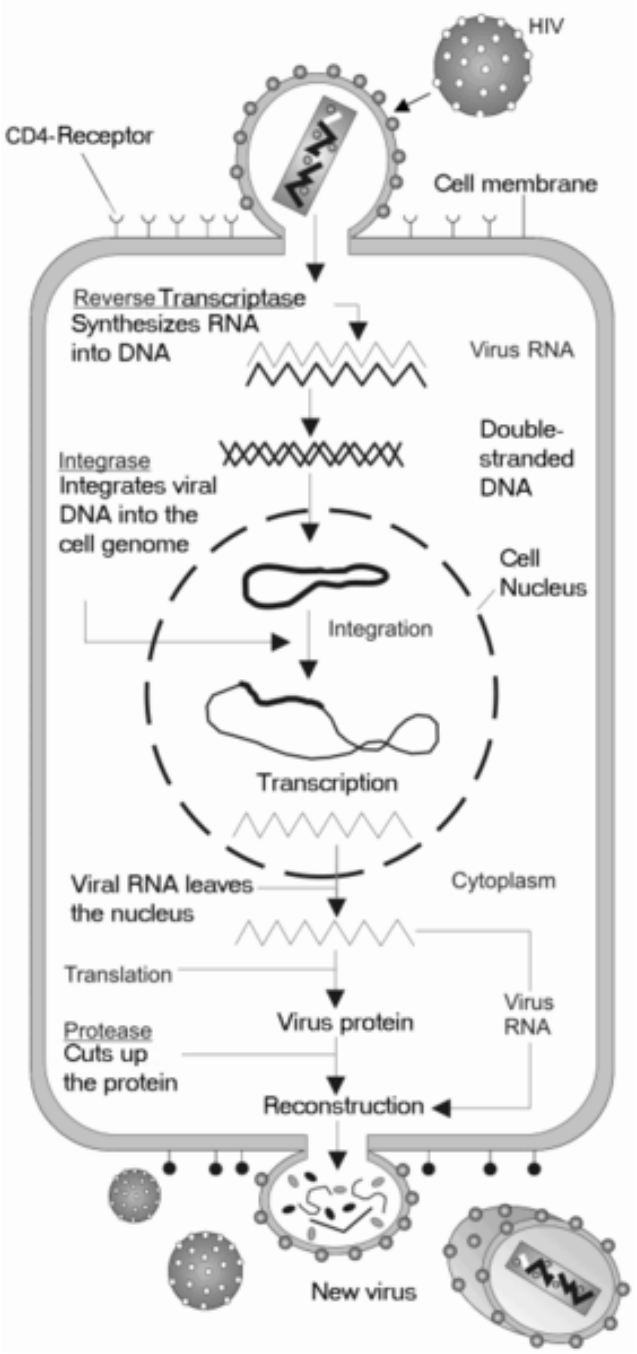

Figure 2.6: HIV infection process: Diagram showing HIV infection process, from binding through replication to budding. (Image obtained from public domain: http://en.wikipedia.org/wiki/File:HIV_gross_cycle_only.png)

2.2.4 Viral production types

The rates at which virions are produced depend on the cell type and its activity. This rate is an important aspect which needs to be incorporated accurately into mathematical models. There are three main rates at which virions are produced:

Acute infection is generally how most virus is produced. These are infected active cells that start producing virions immediately, after the infection process has finished, and at a high rate, e.g. via lysis. As these infected cells are short-lived the introduction of therapy, to stop new infections, rapidly reduces the number of these cells. This creates the first phase seen in the bi-phasic drop in viral load after introduction of therapy.

Chronic infection occurs in active cells, which are infected, but not over-stimulated and hence produce a lower level of virus over a longer period of time than acute infection. Upon therapy introduction the second phase of viral load drop is seen as these cells die naturally, reducing the total infection produced by this pool.

Latent infection is due to cells, which have the provirus fully integrated but not activated. These cells remain infected but do not produce virus unless activated. Furthermore, these cells can reproduce, allowing the provirus to live indefinitely. Effectively this means HIV can not be eradicated from an infected individual unless these cells can be eliminated. This group is primarily responsible for viral rebound when ART is removed after long periods of viral suppression.

The introduction of ART reduces both productive and chronic infected cells but can not truly access latently infected cells. When therapy was first introduced it was hoped that HIV could be eliminated as an individual's the viral levels dropped very fast. However, even after years of undetectable viral load some latent virus remains to re-stimulate viral growth if therapy is removed. It is because of this latency that therapy must be administered indefinitely.

2.2.5 Viral mutations

HIV is unique among infectious diseases because of its extremely high rate of viral mutation. As HIV is a retrovirus it needs to reverse the normal genetic flow when replicating. Thus replication, using RT to convert RNA to DNA, allows a significant number of errors to be produced in the copied DNA, as the RT enzyme does not possess any in-built correction mechanism. As a result ≈ 0.2 errors per genome per replication cycle are produced [30]. This high mutation rate is compounded by the high replication rate of HIV, about $\approx 10^{10}$

replications per day [81]. The combination means that many variants of the virus are produced each day, some of which may be more virulent or able to escape specific therapy. Furthermore, when an individual is infected with more than one sub-type, these can combine to produce recombinant forms, which can be more difficult to treat [16, 82]. As a result these mutations can prove a significant problem in maintaining successful therapy regimes. Also, the selective pressure applied by sub-optimal therapy means drug resistant mutations can develop [15, 16]. These drug resistant mutations generally occur when a therapy regime is not fully adhered to, allowing some virus to replicate. In general these drug resistant viral stains can develop:

Within-host: mutations which evade specific therapy types and develop under the selective pressure of a sub-optimal therapy regimes, where a significant amount of virus is produced despite the presence of ART.

Between-host (super-infection): when a drug resistant viral strain is passed from one individual to another by re-infection through the standard transmission mechanisms [83, 84].

Whatever the source of mutation, the result is the same; whole classes of drugs can become ineffective, as will be seen in Section 2.3.2 which consider individual drugs. Furthermore, it was thought that if the selective pressure of sub-optimal therapy was removed, HIV would revert to its original 'wild type' form. Unfortunately this has been shown not to be the case as drug-resistant mutations are only masked by the large amount of wild type virus. When therapy is reintroduced, these drug-resistant viruses re-emerge and evade suppression.

2.3 Treating HIV/AIDS

Prolonging the life of a HIV infected individual involves combating the reduction of $CD4^{+}T$ cells and fighting the opportunistic infections, if and when these occur. Since the introduction of ART, AIDS survival has increased dramatically [11]. Before ART, survival was measured in weeks to months, now, with multi-drug regimes widely available, this is measured in years [4]. Introduction of 'salvage therapies' for treatment-experienced individuals, with no therapy options left, produced 'Lazarus' like results [85, 42]. As a result of new treatment options opportunistic infections are now rare [13]. Overall, already mentioned, it is estimated that 14.4 million life-years have been gained because of ART [11]. This section focuses on ART, constituent drugs types, and how these are combined to create treatment strategies.

Controlling HIV replication using ART is complicated, as it is necessary to decide when to start, stop and/or change drug combinations. This is achieved by measuring the level of a number of key cells, specifically the $CD4^+$T cells and virus present. Furthermore, there is no universal consensus as to the stage at which infection therapy should be initiated; this varies by individual case. However, it is the general consensus that once therapy is started it should not be stopped and should be monitored closely for failure [86]. 'Failure' status is based on viral load and a number of other clinical indicators, but once viral load increases dramatically drug combinations should be changed quickly, before drug resistant mutations can develop and eliminate future therapy options. A primary cause of therapy failure is a reduction in adherence to a therapy regime, leading to virus not being fully suppressed. Also some patients are known to take 'drug holidays', without clinical supervision, which can quickly lead to development of resistant strains. However, ART drugs are highly toxic and it may be necessary to stop therapy due to a build up of toxicity [15, 42]. The need for such interruptions is being gradually brought under control, due to new drugs and drug combinations, and can be performed under clinical supervision.

2.3.1 Therapy monitoring

To determine therapy strategies it is necessary to monitor HIV progression. Currently there are two main systems of identifying the stages of HIV progression:

CDC Classification System The CDC (U.S.A. Centers for Disease Control and Prevention) system is primarily based on $CD4^+$T cell levels, in combination with viral load and previously diagnosed HIV related conditions. This is primarily used in the developed world and was last revised in 2008 [87]

WHO clinical staging of HIV/AIDS This is used in developing countries where resources are limited and key cell levels may not be readily available. Devised for resource limited countries it was last revised in 2007 and is primarily based on clinical observations [88].

Knowing the stage of infection, regardless of staging system, allows a more appropriate treatment regime to be developed.

2.3.2 Anti-retroviral therapy

ART began in 1987 with the introduction of mono-therapy, a single drug to block HIV replication. Since then, over 25 drugs have been licensed, across 5 different drug classes, with new or refurbished drugs coming on the market all the time [24]. The replication steps targeted by the five main classes of drugs, which are combined to make up a multi-drug cocktail to diminish the development of drug resistant mutations, are:

Integrase inhibitors block entry of virion into target cell. To enter a target cell HIV must bind to the CD4 receptor, attach a co-receptor and then fuse with the cell [89]. Entry of HIV in a target cell can be blocked by interfering with either the binding or fusion process. Based on this there is potential for three classes of drug; attachment inhibitors, co-receptor antagonists and fusion inhibitors. While, in theory, each step is a target, only one drug has been licensed so far, T-20 [89, 24], which blocks the fusion process.

Reverse transcriptase inhibitors, (RTIs), block transcription of viral genome. Transcription of the viral genome is blocked by inserting false nucleotides to abort DNA synthesis [90]. The drug first used in mono-therapy, AZT, is of this type and is still in use today. RTIs have major problems with cross-resistance and severe long-term side effects but do not interact with other drugs and have a relatively low pill burden, (1 per day). There are two classes of nucleoside analogues, (NRTIs or 'nukes') [91], and non-nucleoside reverse transcriptase inhibitors, (NNRTIs) [92]. There is a very high risk of cross-reaction, as a single point mutation can eliminate this entire drug class, making NNRTI regimes very vulnerable. These drugs are relatively easy to take and have few side effects, thus they are an important part of therapy regimes.

Protease inhibitors, (PIs), block cleaving of viral genome to create non-functional virions. These drugs compromise the protease enzyme, which builds the functional virions, thus effectively producing non-infectious virions [93]. These have a high pill burden (6 per day), severe long term side effects and a high chance of cross-resistance, but are still crucial to many ART regimes, especially for treatment-experienced patients.

Refurbished old drugs: With the rapid increase in providing therapy across the developing world old drugs are being combined into easier-to-administer regimes [15, 24]. This helps reduce the pill burden and increases adherence to therapy, which is essential for success. Furthermore, some drugs are being manufactured under license, which reduces the cost significantly.

2.3.3 Treatment strategies

Over the years they have been a number of treatment strategies designed to control HIV replication. From the initial single drug therapies late 1980's [94], treatment strategies have evolved, as newer drugs and better understanding has being gained [5, 10, 48]. The current strategies can be split into:

Mono-therapy is still used in developing countries to reduce vertical transmission, (mother to child), where other options are not available [95]. Not recommended for long term use due to rapid development of resistance, as seen in the late 1980's and early 1990's when it was the only option [96, 97, 94].

Highly active ART (HAART) generally involves at least 3 drugs from two classes. These were introduced in the mid 1990's and produced the first effective way of delaying progression to AIDS [98, 99]. This is still the main therapy in use today, especially for treatment-naive individuals. Newly developed drugs allow pill burden to be reduced significantly, along with reduced long term toxicity. Successful HAART can be maintained for years, possibly even decades.

Mega-HAART sometimes known as giga-HAART [100]. This generally involves five or more drugs from a number of classes. Used in treatment-experienced individuals, who have few remaining therapy options.

Salvage therapy defined here as involving nine or more drugs. This is used to salvage an individual who has become resistant to most of the current drug combinations, making conventional therapy ineffective. Combining a number of drug classes, with newly developed drugs, allows numerous DRM to be suppressed.

Treatment interruptions will always occur, due to limited availability of therapy, potential benefits to therapy strategies, development of toxicity, or requests for 'drug holidays'. However, the case of elite controllers, and specifically the 'Berlin patient' leading to structured treatment interruption, with the aim of bolstering the immune system to a level, where it can control HIV replication alone [101]. However, despite numerous studies this approach has yet to be substantially argued [56]. There is potential for a significant cost reduction to be achieved if therapy was required for only a portion of the time, after full suppression.

These therapies are the main method of controlling HIV replication, but given the associated difficulties it has become increasingly apparent that a further alternative is required. Investigating these strategies, using a mathematical model of low level viral replication,

forms a large part of this research. Specifically investigated is the case for structured treatment interruptions, which is still controversial as, in the majority of cases when therapy is removed, viral load rebounds almost instantaneously.

2.4 HIV/AIDS future

A number of ways exist of reducing the number of new HIV infections. The simplistic view of the HIV/AIDS pandemic suggests that the key to reversing the spread of HIV is to reduce the rate at which it spreads. In a general viral epidemic, vaccination, (i.e. building immunity to a particular infection so individuals are no longer susceptible), is the main method of preventing infection. Equally simplistically, if people do become infected they either recover or die. However, no vaccine exists for HIV/AIDS, as yet, and reducing the spread of infection involves changing the culture of those susceptible, a non-trivial behavioural impact. The majority of the annual 2.6 million new infections could be prevented by significant changes in people behaviour and circumstances. While only gradual behavioural changes are taking place these have seen the number of new infections drop 19% in ten years [6]. Furthermore, there are a number of other strategies currently available, even in the absence of a cure or vaccine, which can reduce new infections further:

Increase knowledge of HIV infection: A reduction in the transmission rate can be achieved by seeking out, and testing, those who are at risk of HIV infection more often. Currently the majority of infection is transmitted by individuals who do not know that they are infectious. Testing also makes people more aware of the risks involved.

Cure a proportion of infected: While a true cure, i.e. complete eradication of all infection, for HIV is beyond current capabilities, suppression of viral replication below detection levels can be achieved for long periods, thus reducing the chance of passing on infection.

Prevent new HIV infection: The wider use of preventative measures can reduce the risk of a new infection greatly.

All of these are interdependent on each other; e.g. knowledge of HIV status will allow informed choices about HIV prevention and therapy if necessary. Furthermore, the amount of virus present while on successful ART is significantly lower (reduced from $64,000$ to less than $50 copies/\mu L$). As a result the chance of spreading infection greatly deceases. Another significant achievement has been the reduction in vertical transmission, whereby a mother passes HIV to her baby. Without therapy the infection rate is 25% but this is reduced significantly using therapy. As a result the number of vertical transmissions have greatly reduced in the developing countries where this is a major issue.

Currently access to ART is widely available in developed countries and is increasing in developing countries, with a drive to get as many people on ART as become newly infected. As access to ART increases this will help decrease the numbers of new infections, which will help decrease the overall pandemic of HIV/AIDS. Current strategies allow therapy to be administered over very long periods, (decades). As a result there is increased chance of drug resistance developing, as adherence levels can drop in the light of no virus for long periods of time. In consequence, there is a great need for developing new therapy options and understanding how infection levels are affected. Furthermore, the cost of ART makes it difficult for developing countries to meet universal access, but generic drugs allow more people to start therapy for a fraction of the cost. This coupled with the drive from the WHO and other world organisations mean soon the numbers starting therapy will exceed those becoming infected, the first step in combating this pandemic.

2.5 Summary

This chapter gave an overview to the HIV/AIDS pandemic and how this can be managed in the future. Also given is the biology of HIV replication and how drugs can be used to interfere with its replication. The next chapter demonstrates how this biology is used to develop models of within-host HIV progression. These models then form the basis of the research which follows, developing a model capable of accurately predicting treatment interruption regimes.

Chapter 3

HIV/AIDS Research

Over the past 30 years our understanding of HIV/AIDS has progressed faster than for any other new infection, almost keeping pace with the spread of HIV/AIDS itself [4, 5]. Within only a few years of its initial discovery, in early 1980's, a diagnosis of AIDS and HIV as the underlying infection was reported [26, 102, 103]. In less than 10 years an initial treatment was provided, using mono-therapy to block HIV replication, albeit with limited success [96, 97, 94]. Over the next 5 years this treatment became more potent and changed the course of HIV infection, delaying the onset of AIDS significantly [98, 99]. Before 20 years had passed the number of new infections were dropping and the pandemic levelling out, with HIV regarded as a chronic infection [6]. Despite this unprecedentedly rapid knowledge scale-up and drive to control HIV/AIDS, the number of those living with HIV/AIDS is now over 30 million, with the pandemic expected to continue for many years to come [11].

While Chapter 2 gave an overview of the biology and global effects of HIV/AIDS, this chapter gives an overview of the tools used to produce such significant advances in HIV/AIDS research, with those employed for this research focused upon in much greater detail. The three broad categories, *in vivo*[1], *in vitro*[2] and *in silico*[3] analysis, are introduced to give the research context [104]. The area of *in silico* analysis is expanded upon and distinctions drawn between mathematical model functions. A subset of these models, which are the focus of this research, is then discussed in greater detail. These are specifically top-down deterministic differential equation models of within-host HIV progression. Modifications and analyses are included in the following chapters.

[1] **In vivo** (Latin: within the living) experimental biology using the original organism in its own environment. This is generally the final stage of experimentation used to determine a concept's accuracy

[2] **In vitro** (Latin: within glass) experiments performed using part of the organism, isolated and performed under controlled conditions, e.g. within a lab environment. These generally provide specific biological information not available *in vivo*.

[3] **In silico** (Pseudo Latin) generally accepted to mean by simulation, which is generally performed using mathematical and or numerical models analysed using a computer.

3.1 Overview of HIV/AIDS research

The rate at which HIV/AIDS research has advanced has been extremely fast, with focus of new research continually shifting. Originally research focused on identifying the underlying cause of AIDS [26, 28, 29] . With HIV identified as its cause the emphasis shifted to HIV, its cause, spread and progression to AIDS [105, 106, 107, 108, 109, 110, 111].

To identify, develop and test new ideas a general process can be to perform simulations, *in silico*, as a proof of concept. This concept is then tested under controlled conditions, *in vitro*, to access safety and verify *in silico* results. Finally, if the previous two steps prove safe and true, the concept can be tested in the real environment, *in vivo*. Each step is discussed in detail below.

3.1.1 *In vivo* analysis

Ideally, the best method of analysis is to observe, and/or test, the subject involved in its own environment. This generally takes the form of clinical trials, where as many external influences are known and, if possible, controlled. In the case of HIV/AIDS the use of clinical trials are strictly controlled, due to the ethics involved in dealing with human subjects. The strict conditions imposed, which are closely monitored, e.g. against control groups, can lead to premature ending of trials, due to adverse effects. For example, some treatment interruption trials were stopped early, as the trial either showed no benefit or was worse than the control group [112, 113]. There have been a number of successful trials, e.g. male circumcision in significantly reducing the probability of HIV transmission [114, 115, 116].

The use of animals, as substitutes for the actual subject being investigated, is also possible. As HIV is a lentivirus[4] a number of other animals are susceptible to similar infections. This is especially useful in those other animals that exhibit similar disease manifestation or share species characteristics. As a result these animals can be used to act as human substitutes and progression of their version of HIV closely monitored. For example, SIV-infected *macaque monkeys* allows analysis of an adequate numbers of hosts, which has been especially useful in HIV vaccine research [117, 118]. However, the problem with using animals as substitutes for humans is that while HIV and SIV are similar, they are still different viruses, so everything must be verified using clinical trials, as mentioned above. This problem has been somewhat overcome by using *chimeric mice*[5], which can support human cells and thus be infected with HIV, to mimic the complex human immune system [119]. These mice are extremely important as they can be bred in the large quantities necessary for sta-

[4] **Lentivirus:** a family of retrovirus that can infect across species. The HIV family has been shown to infect a number of different primates, along with other animals, cats having a similar progress time scale to AIDS as humans

[5] **Chimeric mice:** mice that are composed of different populations of genetically distinct cells, i.e. they can contain human cells which can be used for HIV infection

tistically meaningful results. A similar infection, FIV (feline immunodeficiency) exhibits progression to an 'AIDS-like illness' which takes 6-8 years, similar to HIV progression [120]. However, this slow infection progression also means lengthy delays in obtaining results. Studies of chimpanzees (infected with HIV) are both costly and of limited value, given that disease complications differ from those of humans [121, 122].

3.1.2 *In vitro* analysis

This is the technique of performing a given procedure under a controlled environment outside of a living organism, but they fail to replicate the precise cellular conditions of the given organism [123]. Thus, results based on *in vitro* analysis alone, though more readily reproducible, are intrinsically less accurate than those based on *in vivo* or a combination of both. This low cost molecular biology technique has caused a shift away from *in vivo* research, which is more idiosyncratic and expensive. The identification of HIV was based largely on *in vitro* research [26] and all new drugs are first developed *in vitro* before being tested *in vivo*.

3.1.3 *In silico* analysis

In 1989, Miramontes defined *in silico* as biological experiments carried out using only a computer. As mathematical models form the basis of most computer simulations, it is *in silico* analysis that makes up the remainder of this research. To develop these *in silico* models it is necessary to observe *in vivo* or *in vitro* interactions, which provide the overall model function. Thus *in silico* models are only as accurate as their *in vivo* and *in vitro* studies allow. Furthermore, they should ideally be verifiable using both *in vivo* and *in vitro* analysis. Although all models need verification, there is a time and cost saving by developing models, which can be altered quickly to increase accuracy, which can form the basis for downstream *in vivo* and *in vitro* analysis.

3.2 Mathematical modelling of HIV/AIDS

Mathematical modelling of complex systems can be used to understand many diverse systems, from natural science though engineering to economics [124, 125]. If a mathematical model can be accurately defined for a complex system, then detailed analysis can be performed. This is especially useful if the system can not be easily subjected to physical tests or experimented upon. The approach to developing these models can be either [126, 127]:

Top-down essentially breaks down a system into smaller component parts. Each of these components is then defined in more detail until the required level of system detail can be described. Models of this type aim at representing the overall system as simplistically as accuracy allows. Examples include the differential equation models, which this research is based on [128, 129, 62].

Bottom-up builds up the overall system from detailed knowledge of its most basic components which are then combined together with their interactions. Examples include agent based systems and neural networks [130, 131].

Furthermore, these two modelling frameworks can be combined to produce a hybrid approach. Broad model classes are:

Deterministic models are generally used for top-down frameworks, where models have an output that is a direct result of the input. These are built up of a number of modelled components, which also have a direct input-output relationship, and as such they producing an exact closed form result, through analytical, numerical or semi-analytical techniques. These tend to be very static methods of modelling physical systems, which inherently include variation, as they produce snapshot results, whereby, given a set of initial conditions and parameters, the simulation gives the same end result. In general, solutions are rapidly obtainable and are readily scalable.

Stochastic models are best suited for bottom-up frameworks and are ideally suited to representing biological systems, as they inherently include the stochastic interaction between cells. Computer simulations are typically run over a number of iterations, to produce a convergent result. With faster processing and increased computing power, larger scale models are now routinely feasible, though representation of fully-detailed system elements is non-trivial.

In hybrid form, stochastic elements are added to deterministic models, with both basic model types and hybrids been utilised in HIV/AIDS modelling [132]. Initial modelling aims focused on HIV/AIDS epidemiology, but emphasis has also shifted to HIV pathogenesis, to understand the spread of HIV within the host. Although both epidemiological and pathogenetic models are discussed below, it is pathogenetic models, specifically top-down deterministic models, which make up the core of this research.

3.2.1 Epidemiology models

Epidemiological studies are predominantly concerned with the distribution and spread of disease, or other health-related problems, with an aim to control and further understand the spread of disease [133, 134]. Within this, *descriptive epidemiology* characterises the disease spread, while *analytic epidemiology* focuses on the underlying cause of disease. In the context of HIV/AIDS, initial models were formulated in the early 1980's and focused on the then 'at risk' groups of MSM and IDU [135]. These were based on limited information on AIDS spread, but subsequently model focus has diversified to include heterosexual populations and vertical transmission [136, 137, 138]. Both model frameworks are currently used to describe the HIV/AIDS pandemic, using such methods as deterministic differential equations [139, 138], and stochastic network techniques [140]). Also, large health organisations have purpose-developed software to predict the spread of infection, particularly in the developing world [141, 142]. Formulating a realistic model to a given set of conditions is, nevertheless, complicated by the slow progression to AIDS, delayed even further by introduction of therapy. Such epidemiological models are used to predict future spread of HIV/AIDS and assess the success of current efforts to control this.

3.2.2 Pathogenesis models

As detailed in Chapter 2 the pathogenesis of HIV is extremely complex. After 30 years of research it is still not known exactly how or why $CD4^+$T cells are depleted slowly over time and why this leads to AIDS [14, 49]. Similar to the epidemiological case, these pathogenesis models can be split into two groups:

Bottom-up pathogenesis models focus on cell interactions, modelling how the immune system interacts with the invading virus. These models are inherently suited to construction using stochastic processes, as cell interactions are random. There are a number of key cells that must be modelled ($CD4^+$T cells, B cells, macrophages etc.), while other cell types can be included to improve biological realism. These models are generally based on a matrix of interactions between each cell using a cellular automata (CA) approach [143, 144, 145, 146, 147, 148, 149, 150, 151]. As the size of the matrix of cells increases the required amount of computing power also increases so scalability can become an issue. Furthermore, each simulation must be run over a number of iterations, to obtain statistically viable results.

Top-down pathogenesis models focus on modelling aspects that can be directly measured within the body, e.g. $CD4^+$T cell counts or viral levels [62, 129, 128]. The primary cells involved are those closely associated with HIV infection, $CD4^+$T cells and viral particles, but other cells can also be included to increase biological realism. As these

models operate on a 'cell count' level they are generally deterministic, lacking the low level biological detail of the stochastic models above. However, they are more scalable and produce a single solution, given a set of initial conditions and parameters.

Depending on the system aspect under investigation a particular model type may be more appropriate. For example, to investigate why HIV slowly depletes $CD4^+$T cells, thus leading to AIDS, bottom-up pathogenesis models are generally used. As these models operate on a cell level they have the necessary resolution to model individual immune cells interactions. However, this research focuses on therapy events, as such a higher level modelling approach is more appropriate. Thus, top-down deterministic models of within-host HIV progression are selected. These models, (specifically differential equation models), are better suited to modelling therapy events, as they are based on cell counts rather than individual cell interactions. As a result only this subset of HIV models, (Section 3.3), are discussed in detail, in what follows.

3.2.3 Estimation of parameters

Regardless of model framework, or type, the information base is crucial, with every model requiring some knowledge of data key for estimation of parameters, establishing initial conditions, and assessing overall form. Data for bottom-up models are limited due to the difficulty in obtaining low level, (cell to cell interactions), detail. In our case, top-down models require specific information, which is seldom or, at best, partially available, due to the small number of treatment transitions actually measured for individual patients, as therapy is generally continuous once initiated.

3.2.3.1 Limitations of data

Top-down models are based on changes in $CD4^+$T cell count and viral loads over time. With the course of HIV infection taking years, or tens of years with successful therapy, considerable data per patient is collected, as these cell counts and viral loads are routinely measured at every 3 month check-up. However, much of this data is similar, with these counts remaining static for long periods of time, (e.g. during the 'clinical latency' period already discussed in Section 2.1.3). As a result, data from these periods, although both accurate and detailed, do not add much to model development. If therapy is introduced, or removed, the $CD4^+$T cell count and viral load change significantly [152, 81, 52]. It is during these 'therapy event' periods that most usable data can be extracted for model design. Over the course of infection these changes occur infrequently, as therapy is typically continuous once initiated, unless drug resistant mutations develop [86, 15, 42]. This produces only one therapy event over the whole course of infection, making data very limited. There are

cases when therapy is stopped, e.g. due to build up of toxicity or other side effects, but these are also infrequent [15, 42]. Structured treatment interruptions, (STIs), where therapy is removed and reintroduced, also produce therapy events, and give the largest source of relevant data, but these are restricted to trials evaluating their useability, (Section 2.3.3). Therapy can also fail, but this is generally recorded after the event and does not record exact transition data [86, 15, 42]. Thus, while overall HIV cell count data and viral load data are widely available, a limited subset only is useful in designing and testing the models discussed in the next section (Section 3.3).

3.2.4 Reducing model complexity using dimensional analysis

There is always a trade-off between model complexity and its overall function, whereby the simplest form of a model that describes function accurately is preferable, the well known Occam's razor[6]. Thus increasing biological realism, achieved by inclusion of extra parameters, may not increase overall model usefulness, and is ideally validated by available data. Consequently, focusing on estimation of parameters, which are key to overall model function, ensures that limited data are best utilised. To achieve this, the sensitivity of a model to each parameter must be identified, e.g. through *semi-relative sensitivity analysis* [128]. Dimensional analysis (DA) offers another method of highlighting the key parameters and is pursued here, (Chapter 5).

DA is described in detail in a seminal work by Bridgman [153]. It has been utilised frequently, with examples taken from the ancient Greeks to Einstein to the present day, for a review see [154]. However, in the context of HIV analysis is use is new and provides a novel aspect of this thesis, (Chapter 5). Put simply, DA aims to scale models such that their parameters can be clearly compared, with their significance to overall model operation clearly shown. To allow for accurate comparison each parameter is made 'dimensionless' (i.e. each scales to unity), in terms of the dimensional variables for mass, length and time. By removing parameters that are insignificant, (based on their dimensionless values), a complex model can be simplified, resulting in less complex analysis. Furthermore, as model complexity can grow, with further aspects of HIV progression being identified and included, DA offers a way of retaining model tractability, by systematic simplification of new developments. Additional data needs for new parameter estimation are also controlled. The use of DA also allows a model to be adapted more readily to individuals, requiring knowledge of fewer parameters. The approach is elaborated by example in Chapter 5.

[6]**Occam's razor:** implies that, all things being equal, simpler explanations are generally preferable to more complex ones

3.3 Deterministic modelling of within-host HIV progression

From the initial discovery of HIV as the underlying cause of AIDS, the modelling of its progression has produced significant advances in our understanding and has helped develop future strategies. The differential equation models introduced in this section are top-down deterministic models, which build systematically to include further biological detail or adding necessary overall model function. The models have progressed from pre-1995 models, when HIV was thought to be latent with zero viral replication, to single-target-cell linear models of continually replicating virus [62, 52, 53, 81, 155, 156], to multi-target-cell non-linear models including chronic infection [129] or detailed immune response [128]. Thus, as understanding of HIV progression has advanced, limitations in previous model forms have become increasingly more apparent.

All the models discussed below follow the classic SIR model framework, whereby the population is split up into susceptible, infected and removed individuals. Specifically, the differential equation models that follow have one, (or more), susceptible population, which can be infected. There is not, however, a separate removed population as cell death and clearance are included within the susceptible and infected populations. Thus each population, or compartment, has a source, an infected and removed term which combines to represent the change in that compartment. As will be seen, each compartment is inter-reliant on each other to produce the system which predicts cell levels.

3.3.1 Pre-1995 models

The initial assumption of HIV latency, (little viral activity expected to take place in a 10 year period), was consistent with known biology at the time [157, 158, 159]. Other viruses showing this dormant phase include herpes, which normally resides in the nerve ganglia and only becomes active for brief periods. Consequently a number of models were developed based on this assumption.

Very early differential equation (DE) models focused on the immune system's interaction with HIV. Reibnegger et al. developed a model based on infected $CD4^+T$ cells presenting a target for the immune system [160]. These infected cells were taken to be killed systematically thus leading to their depletion and eventually to AIDS.

Perelson et al. developed a compartmental DE model involving various $CD4^+T$ cells, (*virgin*, *active* and *memory*), which were interacting with the HIV virus [161, 162]. These models assumed that only active cells reproduced the virus but memory cells could become active if stimulated. Although based on low replication rates, this is similar to what is expected today during therapy, with a small number of latent cells able to renew an infection when therapy is stopped.

Work by Nowak et al. used high mutation rates as a basis for a threshold in antigenic diversity, below which the immune system was able to control the infection [163, 164, 165, 166, 167, 168, 169]. When this threshold was breached it led to viral strains that the immune system could not control, (escape mutants), leading ultimately to the onset of AIDS. This was contrary to the idea that antigenic diversity was a symptom not a cause of AIDS. The underlying assumption was that the *earlier* treatment was started the more beneficial it would be, as it would reduce the potential of these mutant viral strains developing [164].

While all early DE models were reasonably consistent with available data, these data were not detailed enough for adequate validation of conjectured theory. As accurate measurement of viral load became possible, the model focus changed drastically [170, 171, 159], in particular when HIV was shown not to exhibit latency but to be continuously replicating [170, 53, 52]. This focused mathematical modelling attention on incorporating this feature. The initial goal was to accurately evaluate key parameters, like viral production and clearance rates. The work of Perelson et al. (1993) formed the basis for the models which followed, (discussed below).

The Nowak models [163, 164, 165, 166, 167, 168, 169], which initially focused on a high replication error as the source of mutations, were also updated to include continuous replication [172]. It was now this high replication rate that was expected to be the driving force behind the escape mutants, and not merely the replication error [173, 174, 156, 175, 176, 177, 178]. This signified that for *long term modelling* the parameters, (rates of clearance, infection, and death etc.), must change over time as the virus adapts. However, for *short term models* these could be taken to have a fixed value.

3.3.2 Single-target-cell models (STC)

The development of new protease inhibitor (PI) drugs in the mid 1990's, administered in combination with existing drugs, achieved effective halting of viral replication. This allowed the decay rate of virus to be accurately measured for the first time. In 1995 Wei et al. and Ho et al. showed that the virus was continuously replicating at extremely high rates, higher than previously expected [53, 52]. Minimum estimates, based on 100% efficient drugs, set viral production at $\approx 10^8$ new virions produced per day, and infected cell life span of approximately 2 days [53]. While these established minimum estimate bounds only, they could be used as the basis for more detailed models. This high production rate also explained the rapid resistance to mono-therapy which was seen at the time, since wild-type virus was being replaced with drug-resistant virus in only two weeks [53].

This new information led to modelling focusing on the short-term dynamics of infection. An early short-term model, developed by Perelson et al., [81], built on their earlier compartmental models [161]. A more general version of this basic model is described here (Eqn. 3.1), in order to explain the model function and underlying assumptions

[81, 125, 155, 62]. The specific aim of this model is to describe introduction of therapy to a stable system. As such the assumption is that pre-treatment viral levels are constant, i.e. a 'clinical latency' period is expected, and that these models are accurate only for the short periods of time while viral load drops, (days to weeks) [128, 129, 156, 179]. The STC model is composed of compartments, used to describing the 'rate of change' of four key cells or viral loads as described below:

STC: single-target-cell model

$$\frac{dT_p(t)}{dt} = \lambda_p - \delta_p T_p(t) - (1-\epsilon_{rt}) k_p V_i(t) T_p(t) \tag{3.1a}$$

$$\frac{dT_p^*(t)}{dt} = (1-\epsilon_{rt}) k_p V_i(t) T_p(t) - \delta T_p^*(t) \tag{3.1b}$$

$$\frac{dV_i(t)}{dt} = (1-\epsilon_p) N_T \delta T_p^*(t) - c V_i(t) \tag{3.1c}$$

$$\frac{dV_{ni}(t)}{dt} = \epsilon_p N_T \delta T_p^*(t) - c V_{ni}(t) \tag{3.1d}$$

This, (identified here as the STC model, Eqn. 3.1), a top-down deterministic model. As can be seen from the flow diagram in *Fig. 3.1* it can be explained, based on each compartment, as follows:

Uninfected CD4^+T cells: The change in the number of uninfected CD4^+T cells (T_p) with time is equal to the rate at which they are produced (λ_p) less the amount that die naturally, at rate δ_p, less those that are lost to infection. This allows for recovery of CD4^+T cells, as seen during treatment, but does not include the proliferation term seen in similar models [62].

Infected CD4^+T cells: The change in the number of infected CD4^+T cells (T_p^*) is based on those that encounter infectious virus (V_i) at rate k_p less those that die at rate δ. A reverse transcriptase inhibitor (RTI), with effectiveness ϵ_{rt}, reduces the amount of infected CD4^+T cells. The delay between a CD4^+T cell becoming infected and producing virions, (intracellular delay), is not included here but is a vital element of this research, see Section 4.1 for details.

Infectious virus: The rate of change of infectious virus (V_i) is the number of actively-infected CD4^+T (T_p^*) producing virus, at rate N_T, less those that die naturally, at rate c.

Non-infectious virus: The production of infectious virus is reduced by the use of PI, with effectiveness ϵ_p, thus producing non-infectious virus (V_{ni}). The non-infectious virus death rate is the same as that for infectious virus. Non-infectious virus, as the name suggest, can not infect target cells.

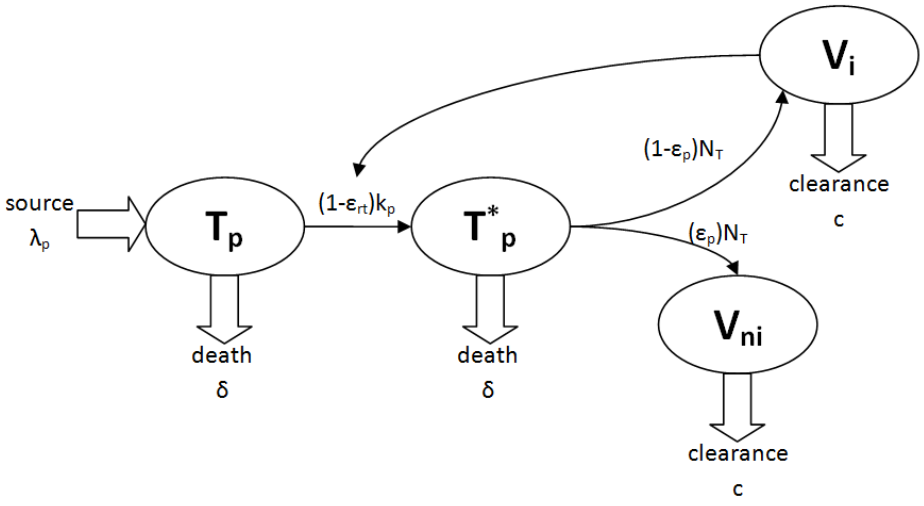

Figure 3.1: STC flow diagram: Flow diagram for single-target-cell model

It is important to note that this is a *linear* approximation to a *non-linear* system and has short-term applications, 2-3 weeks only. Also this model is very dependent on drug treatment efficiency, as demonstrated by Callaway et al. [129]. The required dependent variables (Table 3.1) and parameters (Table 3.2) are also given. These are based on values taken from literature and modified as necessary. *Fig. 3.2* shows the effect of therapy introduction and removal on the key cell types.

A slightly simpler version of this model, based only on PI, led to predictions that 2-3 years of HAART, using 100% effective treatment, would eliminate HIV [155]. This was clearly unrealistic, as no drug is 100% effective, and no account was taken of latently-infected cells, which can re-stimulate an infection even after years of successful viral suppression. Latency requires a longer-term model and is not analysed suitably by these specifically short horizon model forms. This aspect is discussed later in Section 4.4.

Variable	Units	Description
T_p	$\frac{cells}{mL}$	Primary target cells (i.e. CD4$^+$T cells)
T_p^*	$\frac{cells}{mL}$	Primary target acutely infected cells
V_i	$\frac{virions}{mL}$	Infectious virus concentration
V_{ni}	$\frac{virions}{mL}$	Non-infectious virus concentration

Table 3.1: STC variables: Dependent variables for STC model

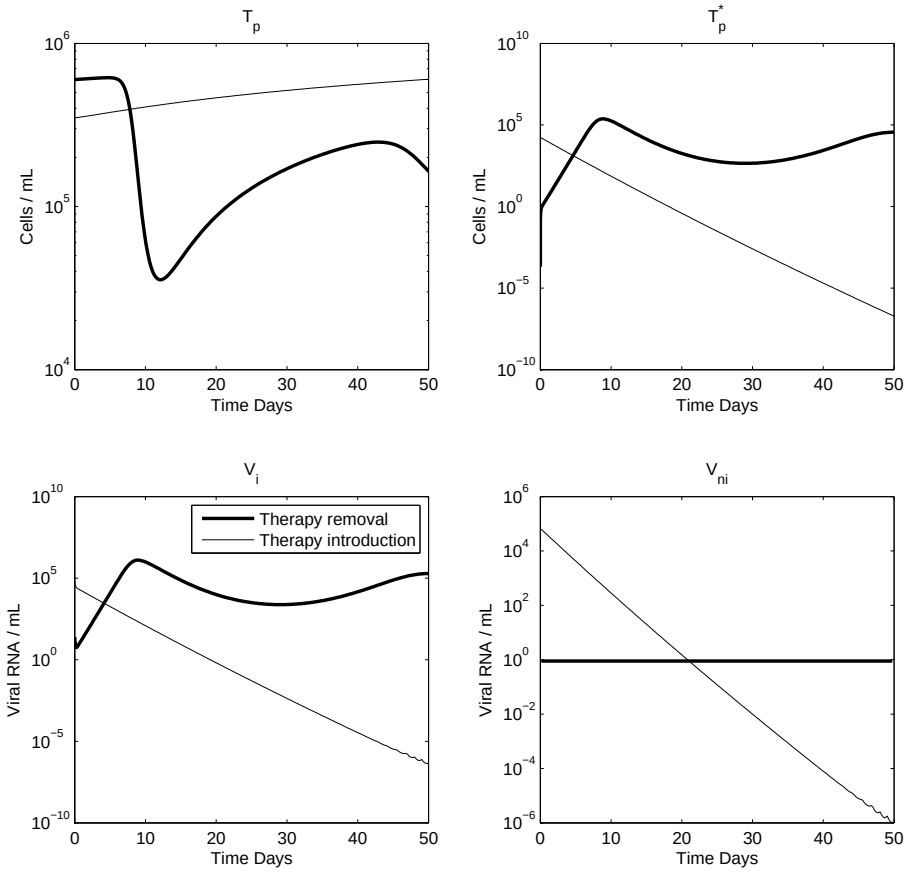

Figure 3.2: Therapy events for STC model: Shown is the effect of therapy introduction and removal to a stable system for STC model. This gives the effect on the key cells, specifically target cells (T_p), infected cells (T_p^*), infectious virus (V_i and non-infectious virus (V_{ni}). Clearly shown is how the viral levels (V_i) drop to unrealistic levels when therapy is introduced, viral levels are thought to maintain a constant low level $\approx 10 virions/mL$ as discussed in Section 4.4. This unrealistic viral load is a severe limitation of these models. Also shown is how non-infectious virus remains low under therapy removal, as this models virus produced by drug intervention alone.

Parameter	Units	Value	Description
λ_p	$\frac{cells}{mL\ day}$	$10,000$	Production source of primary target cells
δ_p	$\frac{1}{day}$	0.01	Death rate of primary target cells
ϵ_{rt}	$-$	$0.8 \in [0,1]$	Efficiency of RTI in primary target population
ϵ_p	$-$	$0.8 \in [0,1]$	Efficiency of PI in primary target population
k_p	$\frac{mL}{virions\ day}$	8×10^{-7}	Infection rate for primary population
N_T	$\frac{virions}{cell}$	100	No. of virions produced per infected cell
c	$\frac{1}{day}$	13	Clearance rate of virions
δ	$\frac{1}{day}$	0.7	Clearance rate of infected cells

Table 3.2: STC parameters: Parameters for STC model

3.3.3 Multiple-target-cell models (MTC)

With the development of more successful therapy regimes, whereby viral load could be suppressed for terms ranging from months to years, model adaptation to describe long-term features was required. The above STC short-term single-target-cell models provided the basis for more advanced models which incorporate more accurate dynamics of T-cells [180], introduction of new drugs [181] and more detailed aspects of the immune system [128, 182]. While these are still compartmental models, the complexity has greatly increased to include such features and thus the accurate determination of parameters becomes more difficult. Also, as time has progressed, the focus of models has shifted to treatment issues, including, (i) when to start therapy, (ii) what type of ART to use, and (iii) when or if therapy needs be altered or stopped. The short-term dynamics of STC models can not fully answer these points.

The increased complexity of the multiple-cell-models comes from; increasing the number of target cells to allow secondary target cell infection, allowing different viral production rates, taking into account chronic infection, and increasing detail on the immune system, and allowing for reduction in viral production rates due to the immune response. Also the modelling of non-zero viral load is essential to longer-term dynamics, which can be modelled using multiple-target-cells models by permitting different reactions to drug therapy in the target cells. The dependency on 'drug efficiency' is also diminished, which is a major limitation of STC models [62]. The desired function of each model dictates which extra compartment terms are included; two such models are discussed in detail here.

3.3.4 Multiple-target-cell model allowing for chronic infection (MTC-CI)

Even very early papers on HIV modelling identified the issue of a relatively small number of residual infected cells enabling re-stimulation of high viral replication [53, 155]. The inability of single-target-cell models to handle this feature, as demonstrated in *Fig. 3.2*, motivated development of models with longer-term dynamics [129]. An appropriate model form is discussed below:

MTC-CI: multiple-target-cell chronic-infection model

$$\frac{dT_p}{dt} = \lambda_p - \delta_p T_p - (1-\epsilon) k_p V T_p \tag{3.2a}$$

$$\frac{dT_s}{dt} = \lambda_s - \delta_s T_s - (1-f\epsilon) k_s V T_s \tag{3.2b}$$

$$\frac{dT_p^*}{dt} = (1-\alpha)(1-\epsilon) k_p V T_p - \delta T_p^* \tag{3.2c}$$

$$\frac{dT_s^*}{dt} = (1-\alpha)(1-f\epsilon) k_s V T_s - \delta T_s^* \tag{3.2d}$$

$$\frac{dC_p^*}{dt} = \alpha(1-\epsilon) k_p V T_p - \mu C_p^* \tag{3.2e}$$

$$\frac{dC_s^*}{dt} = \alpha(1-f\epsilon) k_s V T_s - \mu C_s^* \tag{3.2f}$$

$$\frac{dV}{dt} = N_T \delta (T_p^* + T_s^*) + N_C \mu (C_p^* + C_s^*) - cV \tag{3.2g}$$

This model, (identified as MTC-CI here, Eqn. 3.2), is similar to the previous STC model but allows for inclusion of secondary target cells, defined by subscript 's', (T_s, T_s^* and C_s^*). Furthermore, viral production is either productively infected, producing a larger amount of virus over short periods of time, (T_p^* and T_s^*), or chronically infected, producing lower amounts of virus over longer periods of time, (C_p^* and C_s^*), (Section 2.2.4). Also PI are not modelled, to remain constant with published models, there is no V_{ni} term. Thus this, and subsequent models include only one drug type (RTI), (ϵ), and only one type of virus, (V). The inclusion of PI is possible using the techniques used for the STC models, (Eqn. 3.1)).

The inclusion, of multiple target cells and chronic infection, allow for non-zero virus levels even after long periods (years) of successful therapy. This time scale is more realistically associated with HIV progression in general, and is not represented by the shorter periods relating to specific therapy events, i.e. addition or removal of therapy. The additional variables and parameters necessary are given in Table 3.3 and Table 3.4 respectively. As before the effect of therapy introduction and removal on the key cell types is shown in *Fig. 3.3*.

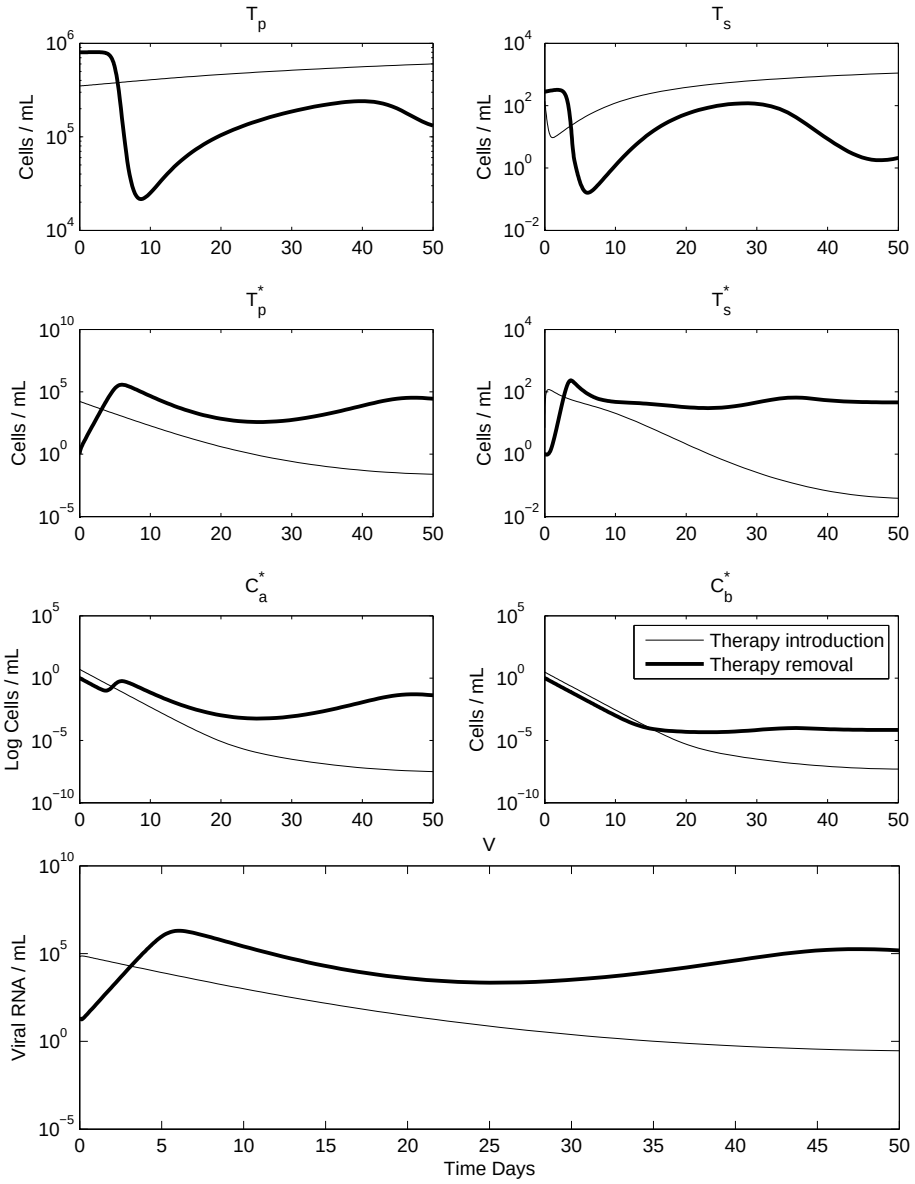

Figure 3.3: Therapy events for MTC-CI model: Shown is the effect of therapy introduction and removal to a stable system for MTC-CI model. The effect on the key cells, specifically target cells (T_p and T_s), productively infected cells (T_p^* and T_s^*), chronically infected cells (C_p^* and C_s^*), and virus (V) is shown. The introduction of secondary target cells (T_s) and to a lesser extent chronic infection (C_p^* and C_s^*) allow viral levels to retain a more realistic values under drug induced viral suppression. This realism overcomes a severe limitation seen in the STC models.

Variable	Units	Description
T_p	$\frac{cells}{mL}$	Primary target cells (i.e. CD4$^+$T cells)
T_p^*	$\frac{cells}{mL}$	Primary target infected cells
V	$\frac{virions}{mL}$	Infectious virus concentration
T_s	$\frac{cells}{mL}$	Secondary target cells (e.g. macrophages)
T_s^*	$\frac{cells}{mL}$	Secondary target acutely infected cells
C_p^*	$\frac{cells}{mL}$	Primary target chronically infected cells
C_s^*	$\frac{cells}{mL}$	Secondary target chronically infected cells

Table 3.3: MTC-CI variables: Dependent variables for MTC-CI model, additional variables are shown in bottom half

Par.	Units	Value	Description
λ_p	$\frac{cells}{mL\ day}$	$10,000$	Production source of primary target cells
δ_p	$\frac{1}{day}$	0.01	Death rate of primary target cells
ϵ	$-$	$0.8 \in [0,1]$	Efficiency of RTI in primary target population
k_p	$\frac{mL}{virions\ day}$	8×10^{-7}	Infection rate for primary population
N_T	$\frac{virions}{cell}$	100	No. of virions produced per infected cell
c	$\frac{1}{day}$	13	Clearance rate of virions
δ	$\frac{1}{day}$	0.7	Clearance rate of infected cells
λ_s	$\frac{cells}{mL\ day}$	32	Production source of secondary target cells
δ_s	$\frac{1}{day}$	0.01	Death rate of secondary target cells
f	-	$0.34 \in [0,1]$	Reduction in efficiency of treatment in secondary population
k_s	$\frac{mL}{virions\ day}$	8×10^{-7}	Infection rate for secondary population
N_c	$\frac{virions}{cell}$	4.11	No. of virions produced per chronically infected cell
α	$\frac{virions}{cell}$	0.195	Ratio of productive to chronic cells
m	$\frac{1}{day}$	0.7	Clearance rate of chronically infected cells

Table 3.4: MTC-CI parameters: Parameters for MTC-CI model, additional parameters are shown in bottom half

3.3.5 Multiple-target-cell model allowing for immune response (MTC-IR)

The above model (MTC-CI) focuses on long-term HIV progression, but a more detailed short-term model was also needed to replace the initial STC models. This multiple-target-cell model (MTC-IR) includes refinements of the immune system or immune response (IR), to allow for a more accurate analysis of therapy removal [128]. The inclusion of more detailed immune system characteristics allows investigation of viral rebound dynamics, when therapy is removed, which is not possible in either the STC or MTC-CI models described above. Viral rebound implies that virus replicates virtually uncontrolled manner, allowing large quantities of virus to be produced. The incorporation of the immune response in one such model is discussed below:

MTC-IR: multiple-target-cell immune-response model

$$\frac{dT_p}{dt} = \lambda_p - \delta_p T_p - (1-\epsilon)k_p V T_p \tag{3.3a}$$

$$\frac{dT_s}{dt} = \lambda_s - \delta_s T_s - (1-f\epsilon)k_s V T_s \tag{3.3b}$$

$$\frac{dT_p^*}{dt} = (1-\epsilon)k_p V T_p - \delta T_p^* - m_p E T_p^* \tag{3.3c}$$

$$\frac{dT_s^*}{dt} = (1-f\epsilon)k_s V T_s - \delta T_s^* - m_s E T_s^* \tag{3.3d}$$

$$\frac{dV}{dt} = N_T \delta (T_p^* + T_s^*) - \left[(1-\epsilon)p_p k_p T_p + (1-f\epsilon)p_s k_s T_s\right] V - cV \tag{3.3e}$$

$$\frac{dE}{dt} = \lambda_E + \frac{b_E (T_p^* + T_s^*)}{(T_p^* + T_s^*) + K_b} E - \frac{d_E (T_p^* + T_s^*)}{(T_p^* + T_s^*) + K_d} E - \delta_E E \tag{3.3f}$$

This is a multi-compartment model very similar to the MTC-CI discussed before. Again it is based on two cells types susceptible to HIV infection (T_p and T_s), typically CD4$^+$T cells and macrophages respectively. Although this model uses only two types of target cell, extra cell types can be included, by increasing the number of compartments used. The dynamics of these cells are similar to that of MTC-CI but do not include the chronic production compartment, (C_p^* and C_s^* seen in Eqn. 3.2 above). The key to this model, however, is detail on immune system components, specifically the removal of infected cells, ($m_p E T_p^*$ and $m_s E T_s^*$ terms), due to effector cells[7] (E), and additional clearance of virus, ($\left[(1-\epsilon)p_p k_p T_p + (1-f\epsilon)p_s k_s T_s\right]$ term), due to the immune system.

[7] **Effector cells: Immune component capable of removing infected cells, thus limiting HIV infection**

Variable	Units	Description
T_p	$\frac{cells}{mL}$	Primary target cells (i.e. CD4$^+$T cells)
T_p^*	$\frac{cells}{mL}$	Primary target infected cells
V	$\frac{virions}{mL}$	Infectious virus concentration
T_s	$\frac{cells}{mL}$	Secondary target cells (e.g. macrophages)
T_s^*	$\frac{cells}{mL}$	Secondary target productively infected cells
E	$\frac{cells}{mL}$	Effector cells

Table 3.5: MTC-IR variables: Dependent variable for MTC-IR model, additional variable shown in bottom part

A primary use of this type of model (MTC-IR) is to determine viral growth after removal of therapy. This allows investigation of STIs, which were hoped to allow the immune system to develop resistance to HIV, and even the possibility of self vaccination. The specific problem with implementing STIs is the speed of viral rebound, which has the possibility of allowing drug resistant strains to increase. Again additional variables and parameters are given in Table 3.5 and Table 3.6, with the effect of therapy introduction and removal shown in *Fig. 3.4*.

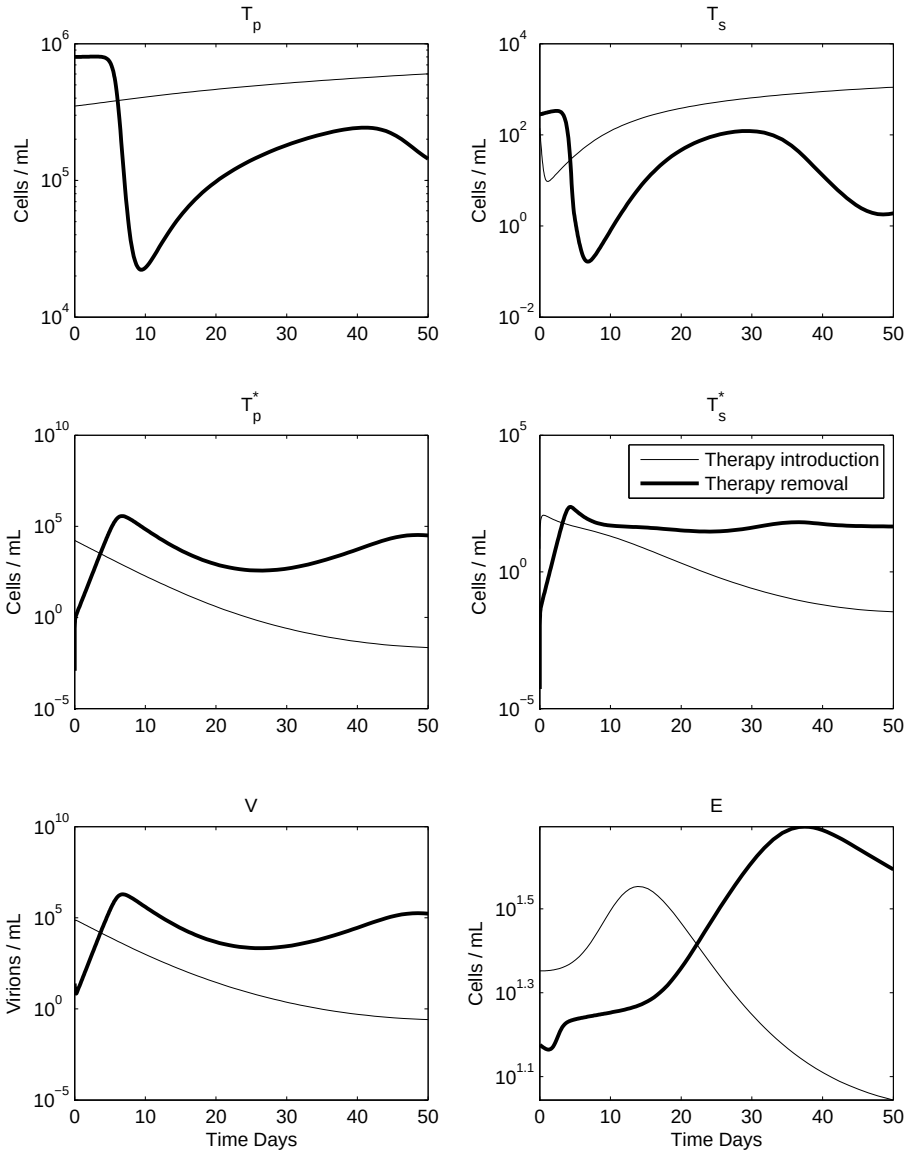

Figure 3.4: Therapy events for MTC-IR model: Shown is the effect of therapy introduction and removal to a stable system for MTC-IR model. Again the effect on the key cells, specifically target cells (T_p and T_s), infected cells (T_p^* and T_s^*), effector cells (E), and virus (V) is shown. The inclusion of secondary target cells (T_s) allows viral levels to remain at more realistic values under drug induced viral suppression. By incorporating effector cells (E), a more detailed immune response is modelled. Thus, viral rebound is reduced, as HIV replication is limited by the immune system.

Par.	Units	Value	Description
λ_p	$\frac{cells}{mL\ day}$	$10,000$	Production source of primary target cells
δ_p	$\frac{1}{day}$	0.01	Death rate of primary target cells
ϵ	–	$0.8 \in [0,1]$	Efficiency of RTI in primary target population
k_p	$\frac{mL}{virions\ day}$	8×10^{-7}	Infection rate for primary population
N_T	$\frac{virions}{cell}$	100	No. of virions produced per infected cell
c	$\frac{1}{day}$	13	Clearance rate of virions
δ	$\frac{1}{day}$	0.7	Clearance rate of infected cells
λ_s	$\frac{cells}{mL\ day}$	32	Production source of secondary target cells
δ_s	$\frac{1}{day}$	0.01	Death rate of secondary target cells
f	-	$0.34 \in [0,1]$	Reduction in efficiency of treatment in secondary population
k_s	$\frac{mL}{virions\ day}$	8×10^{-7}	Infection rate for secondary population
m_p	$\frac{mL}{cells\ day}$	1×10^{-5}	Immune induced clearance rate in primary target
m_s	$\frac{mL}{cells\ day}$	1×10^{-5}	Immune induced clearance rate in secondary target
p_p	$\frac{virions}{cell}$	1	Average number of virions produced per primary target infection
p_s	$\frac{virions}{cell}$	1	Average number of virions produced per secondary target infection
λ_E	$\frac{cells}{mL\ day}$	1	Production rate of immune effectors
b_E	$\frac{1}{day}$	0.3	Max. birth rate of immune effectors
K_b	$\frac{cells}{ml}$	100	Saturation birth for immune effector
d_E	$\frac{1}{day}$	0.25	Max. death rate for immune effectors
K_d	$\frac{cells}{mL}$	500	Saturation death for immune effectors
δ_E	$\frac{1}{day}$	0.1	Natural death rate for immune effectors

Table 3.6: MTC-IR parameters: Parameters for MTC-IR model, additional parameters shown in bottom half

3.4 Summary

This chapter focuses on the three broad areas of *in vivo*, *in vitro* and *in silico* research from a modelling prospective. *In silico* models, specifically top-down deterministic models of within-host HIV progression, have been discussed in detail. The development of these models, from initial single-target-cell forms (STC), to more advanced multiple-target-cell forms (MTC-CI and MTC-IR), is traced. However, even the most advanced of these models has limitations, specifically relevant here is the lack of adequate inclusion of intracellular delay, i.e. the time between a cell becoming infected and producing infectious virus. The proposition of this research is that inclusion of the immune response slows viral rebound significantly, as was seen with the MTC-IR model, while intracellular delay should slow this rebound further. In the next section these STC, MTC-CI and MTC-IR models are thus adapted to include intracellular delay.

Chapter 4

Modelling therapy removal

This chapter uses the previously summarised ideas to develop new models, specifically focused on therapy removal, one of the novel aspects of this work. Models developed here focus on viral load rebound, examining the effect of therapy interruption. This rebound is expected to be inhibited when the time between a cell becoming infected and producing virus is explicitly accounted for. Incorporation of this *intracellular delay*, (ID), is thus a first step in modifying existing models. The next step is to include a minimum viral load, as current models allow virus levels to drop to unrealistic levels, after therapy is introduced. This minimum viral load accounts for *latently infected* cells which can not be eliminated by conventional therapy and provide the viral pool necessary to initiate viral rebound then therapy stops or fails.

The models discussed in the previous chapter (STC, MTC-CI and MTC-IR) primarily focused on therapy introduction, but now both therapy events, (initiation and removal), are considered. As such, it is essential to incorporate intracellular delay, as this has a significant impact by increasing doubling-time, thus delaying the time need for virus to rebound from low viral levels. Intracellular delay, while stochastic in nature, is modelled using a *fixed delay*, justified in Section 4.1.3. A simple model of HIV latency is also introduced, achieved by setting a fixed minimum level viral load during therapy.

4.1 Modelling intracellular delay

For HIV to replicate it must first bind to a target cell and then enter it so that it can use the cell's own chemistry for replication. This biological process takes time, at minimum $\approx 24hrs$ [72, 73, 74, 75, 76, 77, 78], but can take much longer, as seen in latently infected cells which will not actually produce virus until activated [54, 79, 80, 55].

From a modelling perspective, incorporating intracellular delay has different impacts on model function, depending on what aspect of therapy is under investigation. Intracellular delay has no impact on steady-state levels, as the number of infected cells and viral load remain relatively constant. Again there is little impact when therapy is introduced, as viral replication virtually stops. The main pool of virus is from those cells infected before the introduction of therapy, so the viral load drops exponentially based on pre-treatment viral levels. However, when therapy is removed, intracellular delay becomes very important, as viral rebound is significantly reduced due to the fact that each infected cell must wait at least 24 hours before it can produce virus. Thus intracellular delay is masked for therapy introduction models, (such as those discussed in Chapter 3), as it has little impact on this therapeutic event. However, for our research, based on both therapy events, intracellular delay must be included. Before intracellular delay is incorporated possible modelling approaches are considered. In the past single-target-cells have been used, to model this delay for therapy introduction, and these form the basis for what follows [74, 75, 76, 77, 78].

Intracellular delay can be modelled in a number of ways, again either deterministically or stochastically. For a deterministic approach, a discrete delay, the average time taken for a cell to start producing virus after becoming infected, is incorporated. However, as with most biological processes, a mean delay is not necessarily a realistic measure, particularly where variation in initial viral production time is known to occur. Consequently a stochastic approach, using a distributed delay, provides better realism. Specifically this distribution needs to be in a skewed form, as there is a known minimum viral production time but, effectively, no maximum. However, incorporating a distributed delay function involves convolution[1], between the delay function and cell function, thus increasing model complexity, but also its potential to mimic the real dynamics. The merits of a discrete or distributed delay are discussed below.

4.1.1 Distributed intracellular delay

To incorporate a distributed delay, it is necessary to select the most appropriate distribution, which is accurate and can be estimated from data. Based on work by Mittler et al., [76], a bell shaped curve is adopted, centred on the mean=nb with variance=nb^2 and peak=$(n-1)b$ with n and b chosen to give the desired delay function [62, 72]. This modifies our target cell infection equations, for example:

$$\frac{dT_p^*(t)}{dt} = (1-\epsilon)k_p T_p(t) V(t) D(t) - \delta T_p^*(t) \tag{4.1}$$

[1] **Convolution** is basically one function integrated over the time period of the other function.

where $D(t)$ is represented by:

$$D(t) = D_{nb}(t) = \frac{t^{(n-1)}}{(n-1)!b^n} e^{\frac{-t}{b}} \tag{4.2}$$

Based on an average delay of one day, values for n and b were shown to be $n = 8$ and $b = 0.125$ [76]. However, the original Mittler et al. model held the number of target cells, (T_p), constant, i.e. the original model was:

$$\frac{dT_p^*(t)}{dt} = (1-\epsilon)k_p T_p V(t) * D(t) - \delta T_p^*(t) \tag{4.3}$$

Where (T_p) is a constant, and $*$ represents the convolution between the viral function, $(V(t))$, and delay function, $(D(t))$. This turned a relatively simple set of ordinary differential equations into a set of integro-differential equations, which are much more complex to solve and analyse. This increased complexity can be combated by converting the model to the frequency domain, using the Laplace transform, where convolution becomes simple addition. It was investigations in frequency domain usage which formed initial research basis, following on from the author's work during his Masters in Bioinformatics. However investigation into a fixed delay was adopted, as the method of reducing complexity. Furthermore, there is a sound application reasons, discussed below, to use a fixed delay, though some loss in biological realism is inevitable.

4.1.2 Discrete intracellular delay

A discrete delay, based on the average time before viral production modifies our target cell infection equation [75], for example:

$$\frac{dT_p^*(t)}{dt} = (1-\epsilon)k_p V(t-\tau) T_p(t-\tau) e^{-m\tau} - \delta T_p^*(t) \tag{4.4}$$

Where incorporation of intracellular delay is achieved by delaying, by a fixed time τ, the infectious virus, (V), that target cells, (T_p), encounter. This allows for the average time taken between a cell becoming infected, (T_p^*), and producing virus. Furthermore, as some target cells die before producing virus, total infected cells are reduced, at rate $e^{-m\tau}$. The inclusion of this delay changes the original ordinary differential equation models, from Chapter 3, into *delay differential equation*, (DDE), models.

4.1.3 Justification for selection of discrete intracellular delay

To fully model the delay, between cell infection and viral production, it would be necessary to allow for productive, chronic and latent viral production, with each requiring their own specific delay function to be incorporated. However, the models discussed here have separate compartments for each production type and only require the delay between infection and initial production to be accounted for. As such a discrete delay maximises model function with minimum complexity overhead, for investigation of the viral rebound feature. Furthermore, indications are that there is little real difference in introducing either discrete or distributed delays [77, 72]. However, it should be noted these results were obtained from therapy introduction models, where intracellular delay has little impact, so it may be necessary to revisit intracellular delay modelling in the future.

4.2 Quantifying model accuracy

This chapter aims to develop three new models, by modifying standard models of within-host HIV progression, to include intracellular delay. However, while this will improve biological accuracy, and although the base models used, (STC, MTC-CI and MTC-IR), have already been validated, see [62, 129, 183, 128], it is necessary to quantify the benefit of including intracellular delay. Possibly one of the simplest, but most powerful evaluation methods is to compare viral doubling-time and half-life with those seen *in vivo*, as discussed below.

4.2.1 Doubling-time and half-life

The definition of viral doubling-time, (in the context of this work), is the time necessary for a population to double in size, as seen when therapy is stopped of fails. It is calculated using the following formula:

$$T_d \quad = (t_2 - t_1)\frac{ln(2)}{ln(q_2/q_1)} \tag{4.5}$$

Where T_d is the doubling-time, t_1 and t_2 are the time periods over which the growth (q_1, q_2) is measured. As the growth rate is based on exponential growth, $ln(2)$ gives the time necessary for the system to double in size. While exponential growth clearly does not describe the whole HIV cycle, due to limited supply of target cells, it is applicable for the initial stages.

The opposite of doubling-time is half-life, seen when the system decreases in size over time. This is seen when therapy is introduced and has a similar form as for doubling-time and can be calculated as:

$$T_{1/2} \quad = (t_2 - t_1)\frac{ln(2)}{ln(q_1/q_2)} \tag{4.6}$$

With the parameters as before (Eqn. 4.5) but with the ratio of q_2/q_1 inverted to allow for system size decrease.

The doubling-time and half-life can easily be determined from data and are used to describe some of the most basic aspects of the system being measured. It is these measures that are used to determine the impact of inclusion of intracellular delay for the models developed here, using both therapy events.

4.3 Incorporating discrete intracellular delay

Intracellular delay has been incorporated into a number of single-target-cell models but it has not been incorporated into multiple-target-cell models to our knowledge. Including this element in the models discussed in Chapter 3, specifically those including immune response, (Eqn. 3.3), is crucial to modelling treatment interruptions, as will be discussed in Chapter 6.

The delay models discussed here are thus based on the models discussed in Section 3.3, (STC, MTC-CI and MTC-IR). As such they focus on the variation in levels of a number of key cells, which can be either directly measured or indirectly calculated. Incorporating intracellular delay produces three new model variants, (STC-ID, MTC-CI-ID and MTC-IR-ID), as described below.

4.3.1 STC model including intracellular delay (STC-ID)

The single-target-cell ODE model, (STC), discussed in Section 3.3.2 is one of a number of variations on single-target-cell models that have been developed over a period of years [62, 52, 53, 81, 155, 156]. As a result, and to be consistent, a simple illustrative mono-therapy model is discussed here, [77]. The original, non-delayed, form is achieved by setting the delay, (τ), to zero. The delayed form is:

STC-ID: single-target-cell intracellular-delay model

$$\frac{dT_p(t)}{dt} = \lambda_p - (1-\epsilon)k_p V(t) T_p(t) - \delta_p T_p(t) \tag{4.7a}$$

$$\frac{dT_p^*(t)}{dt} = (1-\epsilon)k_p V(t-\tau) T_p(t-\tau) e^{-\delta\tau} - \delta T_p^*(t) \tag{4.7b}$$

$$\frac{dV(t)}{dt} = N_T \delta T_p^*(t) - cV(t) \tag{4.7c}$$

This model, (STC-ID, Eqn.(4.7)), has the same characteristic as the STC model discussed in the previous chapter, (Section 3.3.2). It is based on variation over time in the key cell types, described in the previous chapter, and has similar structure to the multi-cell models that follow. Uninfected cells, (T_p), are produced, at constant rate λ_p, less the proportion that die, at constant rate δ_p, and those that are lost to infection. Cells become infected, (T_p^*), by encountering virus, (V), at a constant rate k_p, less those that die, at constant rate δ. Infectious virus, (V), is produced from these infected cells, (T_p^*), at constant rate N_T, less infected cells that die, at constant rate δ, and the virus that is cleared, at constant rate c. The introduction of therapy, in the form of a reverse transcriptase inhibitor, (RTI), blocks replication and reduces infection rate, with effectiveness ϵ.

As in the discrete delay model above, (Eqn.(4.4)), intracellular delay is allowed for by delaying the virus, (V), which target cells, (T_p), encounter, by a fixed time τ. It is assumed that all infected target cells die at the same rate, allowing cells to die prior to viral production, at rate $e^{-\delta\tau}$.

While only RTIs are modelled here PIs can easily be incorporated, by adding a component for non-infectious virus, as seen in the original STC model, (Section 3.3.2), and detailed in various studies [62, 78].

A graphical comparison of including intracellular delay into these models, compared with the STC model from the previous chapter, (Eqn.(3.1)), is shown in *Fig. 4.1*. The value of the variables, Table A.1, and parameters, Table A.2, for this, and the following models, are given in the appendix. This representation is achieved by numerically solving the above equations, (Eqn.(3.1) and Eqn.(4.7)), using Matlab's built in ODE and DDE solvers, (ODE45, [184], and DDE23, [185]). As both therapy events are shown it is clear that therapy removal, (*Fig. 4.1.A*), is markedly more dependent on accurate intracellular delay modelling than therapy introduction, (*Fig. 4.1.B*). Specifically, while half-life remains consistent for therapy introduction, (1.30 - 1.24 days), therapy removal shows a 60% increase in doubling-time, (0.98 - 1.65 days). Furthermore, the viral load for therapy removal, as shown in *Fig. 4.2*, takes a much longer time to reach viral set-point, from an initial viral load of $25 virions/ml$, when intracellular delay is accounted for. This increase in viral doubling-time is due a reduction in the replication rate due to intracellular delay. Thus, when analysing treatment interruption, as detailed in Chapter 6, it is essential that

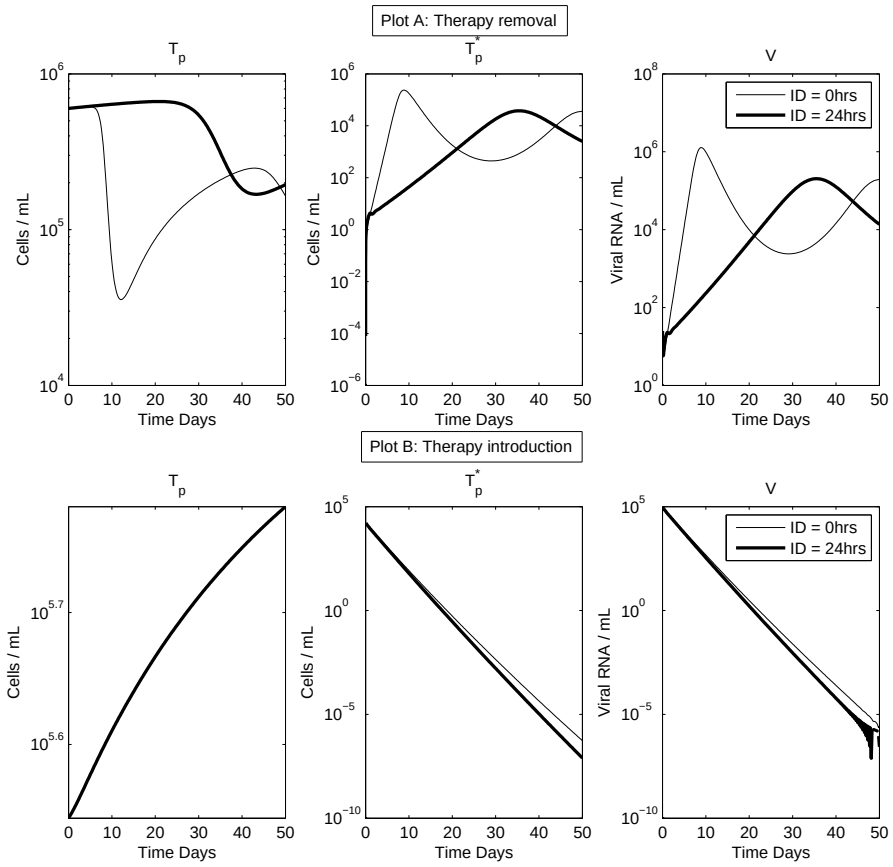

Figure 4.1: Effect of intracellular delay on STC models: Comparison between STC and STC-ID models. Plot A shows therapy removal, from a fixed viral load of $25 virions/mL$, accounting for intracellular delay, (ID), increases the viral doubling-time, (T_d), from 0.98 to 1.65 days. Plot B shows therapy introduction, with drug efficiency of 0.9, viral half-life, ($T_{1/2}$), remains consistent, 1.30 and 1.24 days for zero delay and 24 hour delay respectively.

intracellular delay be accounted for.

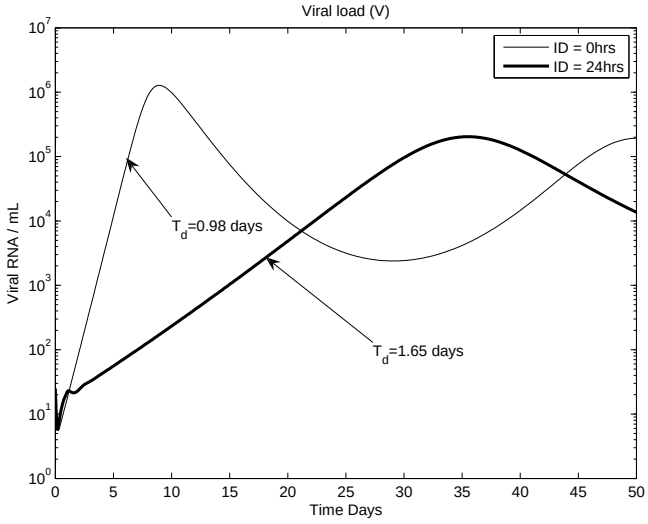

Figure 4.2: Effect of intracellular delay on viral load for STC models: Comparison between viral load for STC and STC-ID model. Only therapy removal, from a viral load of $25 virions/mL$, is shown, as it is the main transition affected. The inclusion of intracellular delay, (ID), increases the viral doubling-time, (T_d), from 0.98 to 1.65 days.

4.3.2 MTC-CI model including intracellular delay (MTC-CI-ID)

As noted, (Section 3.3.3), single-target-cell models are only useful for short term dynamics of HIV infection, whereas multi-target-cell models are required for longer time scales. A delayed version of the long-term chronic infection model, (MTC-CI), from the previous chapter, (Eqn.(3.2)), can be written as:

MTC-CI-ID: multiple-target-cell chronic-infection intracellular-delay model

$$\frac{dT_p(t)}{dt} = \lambda_p - \delta_p T_p(t) - (1-\epsilon)k_p V(t) T_p(t) \tag{4.8a}$$

$$\frac{dT_s(t)}{dt} = \lambda_s - \delta_s T_s(t) - (1-f\epsilon)k_s V(t) T_s(t) \tag{4.8b}$$

$$\frac{dT_p^*(t)}{dt} = (1-\alpha)(1-\epsilon)k_p V(t-\tau) T_p(t-\tau) e^{-\delta\tau} - \delta T_p^*(t) \tag{4.8c}$$

$$\frac{dT_s^*(t)}{dt} = (1-\alpha)(1-f\epsilon)k_s V(t-\tau) T_s(t-\tau) e^{-\delta\tau} - \delta T_s^*(t) \tag{4.8d}$$

$$\frac{dC_p^*(t)}{dt} = \alpha(1-\epsilon)k_p V(t-\tau) T_p(t-\tau) e^{-\mu\tau} - \mu C_p^*(t) \tag{4.8e}$$

$$\frac{dC_s^*(t)}{dt} = \alpha(1-f\epsilon)k_s V(t-\tau) T_s(t-\tau) e^{-\mu\tau} - \mu C_s^*(t) \tag{4.8f}$$

$$\frac{dV(t)}{dt} = N_T \delta (T_p^*(t) + T_s^*(t)) + N_C \mu (C_p^*(t) + C_s^*(t)) - cV(t) \tag{4.8g}$$

Again this has a similar structure to the single-target-cell models, (STC and STC-ID), discussed before. It is made up two susceptible cell types, (T_p and T_s), which can be either acutely infected, (T_p^* and T_s^*), or chronically infected, (C_p^*, C_s^*). As before, the incorporation of intracellular delay is achieved by delaying the virus, (V), which each target cell encounters. Target cells allowed to die before producing virus, at rate $e^{-\delta\tau}$ for acute infection and $e^{-\mu\tau}$ for chronic infection, relating to their respective death rates.

As with the STC models above a significant increase in doubling-time is seen, from 1.03 to 1.69 days, for therapy removal when intracellular delay is incorporated, as shown in *Fig. 4.3*. Correspondingly this slows viral rebound and increases the time to reach viral set-point. As before viral half-life for therapy introduction remains consistent and is not shown.

4.3.3 MTC-IR model including intracellular delay (MTC-IR-ID)

While the previous models, STC and MTC-IC, are accurate for therapy introduction, a more detailed immune system specification is needed when modelling therapy removal, as viral growth is reduced by immune effects. The model discussed here is a delayed version of the MTC-IR models discussed in Section 3.3.5:

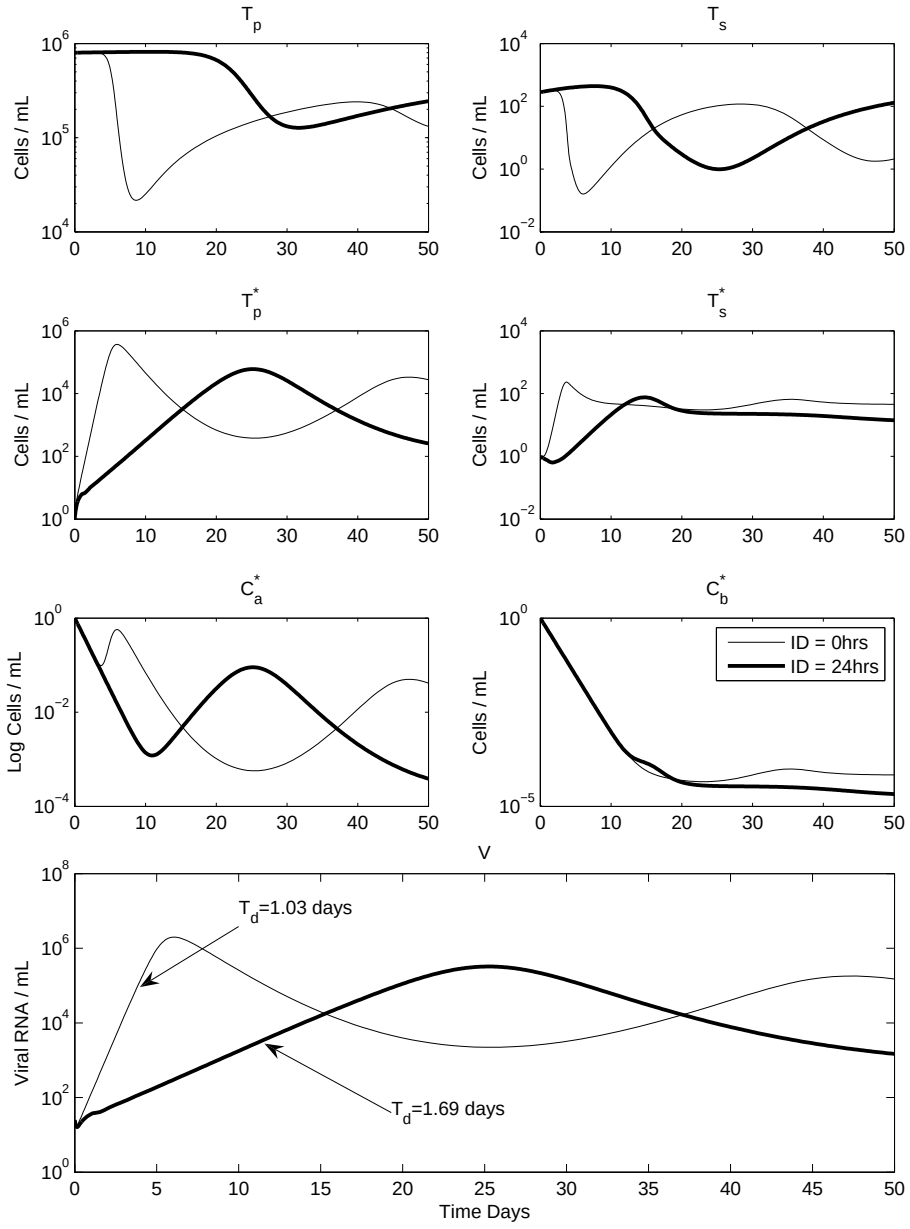

Figure 4.3: Effect of intracellular delay on MTC-CI models: Comparison between MTC-CI and MTC-CI-ID models. Only therapy removal, from a viral load of $25 virions/mL$, is shown. The inclusion of the delay increases the viral doubling-time, (T_d), from 1.03 to 1.69 days.

MTC-IR-ID: multiple-target-cell immune-response intracellular-delay model

$$\frac{dT_p(t)}{dt} = \lambda_p - \delta_p T_p(t) - (1-\epsilon) k_p V(t) T_p(t) \tag{4.9a}$$

$$\frac{dT_s(t)}{dt} = \lambda_s - \delta_s T_s(t) - (1-f\epsilon) k_s V(t) T_s(t) \tag{4.9b}$$

$$\frac{dT_p^*(t)}{dt} = (1-\epsilon) k_p V(t-\tau) T_p(t-\tau) e^{-\delta\tau} - \delta T_p^*(t) - m_p E(t) T_p^*(t) \tag{4.9c}$$

$$\frac{dT_s^*(t)}{dt} = (1-f\epsilon) k_s V(t-\tau) T_s(t-\tau) e^{-\delta\tau} - \delta T_s^*(t) - m_s E(t) T_s^*(t) \tag{4.9d}$$

$$\frac{dV(t)}{dt} = N_T \delta (T_p^*(t) + T_s^*(t)) - \tag{4.9e}$$

$$\left[(1-\epsilon) p_p k_p T_p(t) + (1-f\epsilon) p_s k_s T_s(t)\right] V(t) - cV(t) \tag{4.9f}$$

$$\frac{dE(t)}{dt} = \lambda_E + \frac{b_E (T_p^*(t) + T_s^*(t))}{(T_p^*(t) + T_s^*(t)) + K_b} E(t) - \tag{4.9g}$$

$$\frac{d_E (T_p^*(t) + T_s^*(t))}{(T_p^*(t) + T_s^*(t)) + K_d} E(t) - \delta_E E(t) \tag{4.9h}$$

Again this has similar structure to that of the MTC-IC-ID model discussed above, but does not include chronic cell production, as it focuses on reactions *immediately after* the therapy event. The immune system response, the effector cells, (E), is specifically modelled, with rates of production and death of cells modelled as in the MTC-IR model, Section 3.3.4. Furthermore, the strength of response is dependent on the amount of virus in the system.

As with the previous models there is a significant increase in viral doubling-time, from 0.96 to 1.67 days. Again this delays the time to reach viral set-point. The viral half-life due to therapy introduction remains consistent and is not shown.

4.4 Modelling HIV latency

As seen previously treatment may need to be interrupted at different stages over the course of infection. However, due to inherent latency HIV will rebound once therapy is removed. While intracellular delay, discussed above, plays a role, a finite residual viral load from which this rebound can take place is necessary. This section considers true HIV latency [186, 187]. While a number of models of HIV latency have been developed [188, 189, 190], a simplistic form is used here. A small constant minimum viral load is included to account for sources of viral production, which can not be eliminated during therapy.

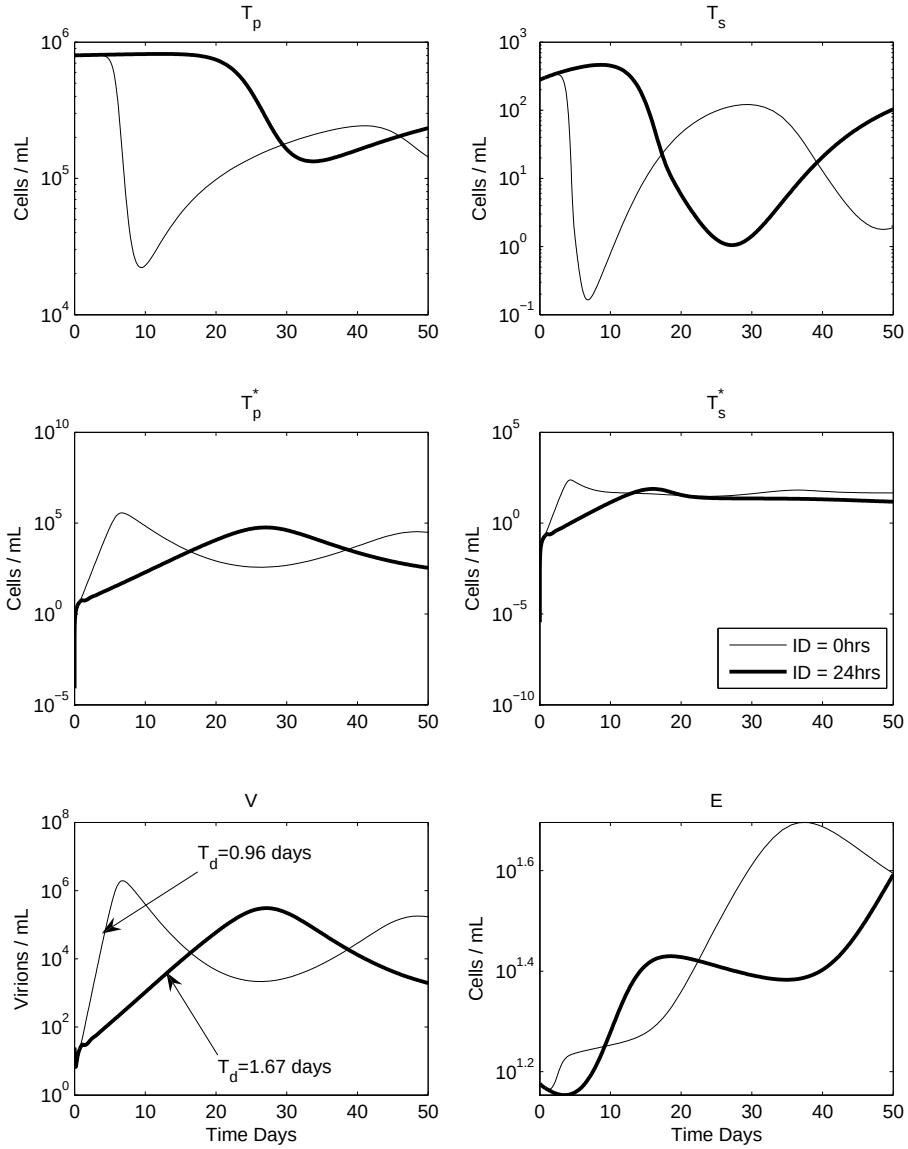

Figure 4.4: Effect of intracellular delay on MTC-IR models: Comparison between MTC-IR and MTC-IR-ID models. Only therapy removal, from a viral load of $25 virions/mL$, is shown. The inclusion of the delay increases the viral doubling-time, (T_d), from 0.96 to 1.67 days.

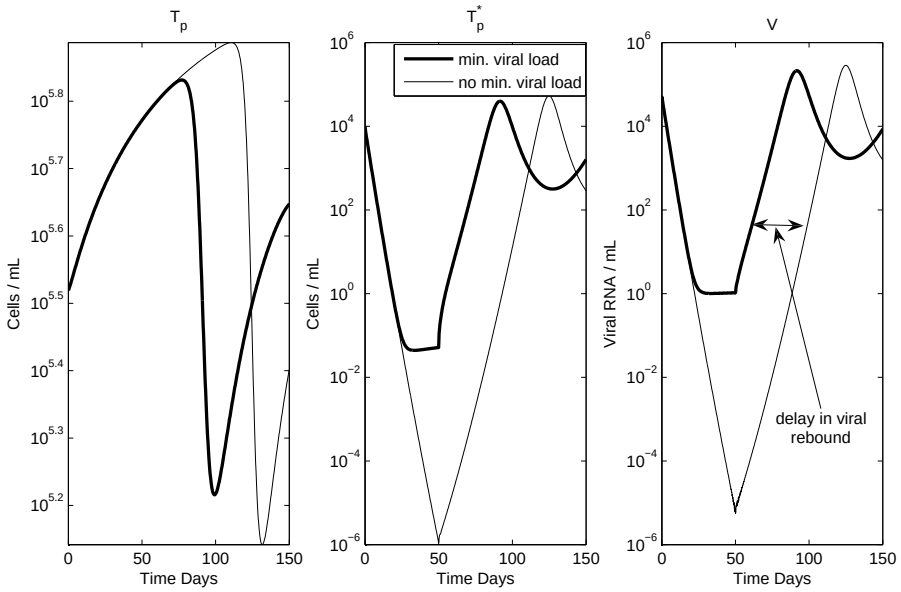

Figure 4.5: Effect of setting a minimum viral load on STC-ID model: Impact of setting a minimum low viral load of $10 virions/mL$, (STC-ID-MVL), to eliminate unrealistically low levels seen in original models, (STC-ID). Shown is the difference in viral rebound seen when therapy is removed, 0-50 therapy introduction, 50-150 therapy removal. The delay in reaching viral steady-state is highlighted, when viral load is allowed to drop to unrealistic levels.

4.4.1 STC-ID including a minimum viral load (STC-ID-MVL)

The inclusion of a fixed minimum viral load to represent viral pools, which are inaccessible to current therapy, gives the following model (STC-ID-MVL):

STC-ID-MVL: single-target-cell intracellular-delay minimum-viral-load model

$$\frac{dT_p(t)}{dt} = \lambda_p - (1-\epsilon)k_p V(t) T_p(t) - \delta_p T_p(t) \tag{4.10a}$$

$$\frac{dT_p^*(t)}{dt} = (1-\epsilon)k_p V(t-\tau) T_p(t-\tau) e^{-\delta\tau} - \delta T_p^*(t) \tag{4.10b}$$

$$\frac{dV(t)}{dt} = N_T \delta T_p^*(t) - cV(t) + V_{mvl} \tag{4.10c}$$

This included a fixed viral term, ($V_{mvl} = 10 virions/mL$), which maintains a residual viral load, preventing the effect of treatment reducing viral load to unrealistic levels, as seen in previous STC models. Clearly, as illustrated, the lower the viral load falls, the longer it takes for virus to rebound to the initial set-point level, (*Fig. 4.5*). While the viral rebound time is increased the viral doubling-time nevertheless remains constant, producing the parallel lines with a corresponding delay in reaching viral set-point.

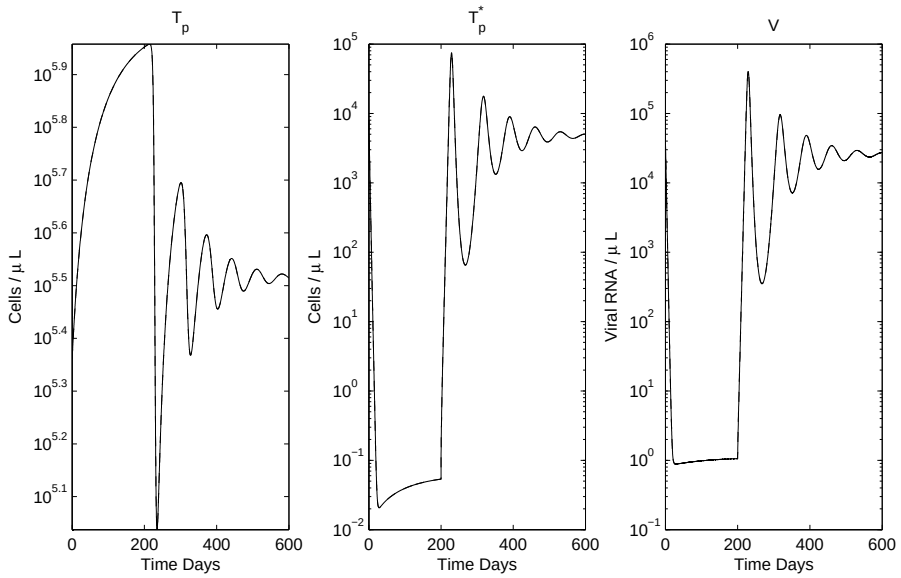

Figure 4.6: STC-ID-MVL steady-state: Plot of steady-state for STC-ID-MVL model. 0-200 shows therapy introduction and 200-600 shows therapy removal, values are given in Table 4.1.

Steady-state	$T_p(t)$ $cells/mL$	$T_p^*(t)$ $cells/mL$	$V(t)$ $HIVRNA/mL$
On-treatment	994,794	0	1
Off-treatment	327,227	4,773	25,700

Table 4.1: STC-ID-MVL steady-states: The natural steady-states for STC-ID-MVL model. These are achieved by allowing the model to run over long periods of time as seen in *Fig. 4.6*.

Another important aspect of these models is their natural steady-states, as detailed in Table 4.1 and shown *Fig. 4.6*, where both 'on treatment' and 'off treatment' periods are shown. These steady-states are measured by allowing the models to run over a long enough period of time such that their level remain constant, between 500 and 1000 days in this case. While the viral load on therapy introduction reaches a high percentage of its final level relatively fast, (in approximately four weeks), the number of target cells takes longer to reach steady-state. Furthermore, when therapy is removed, it takes longer still for the overall model to reach steady-state, due to inclusion of intracellular delay producing oscillations in viral load. The levels of these oscillations reduce exponentially over time and converge to the steady-state level.

Steady-state	$T_p(t)$	$T_s(t)$	$T_p^*(t)$	$T_s^*(t)$	$C_p^*(t)$	$C_s^*(t)$	$V(t)$
On treatment	994,746	3,034	0	1	0	0	8
Off treatment	400,360	17	3,424	18	829	4	18,721

Table 4.2: MTC-CI-ID-MVL steady-states: The natural steady-states for MTC-CI-MVL model. These are achieved by allowing the model to run over long periods of time.

4.4.2 MTC-CI-ID including a minimum viral load (MTC-CI-ID-MVL)

Incorporating a discrete latent viral term into MTC-CI-ID model produces the following set of equations (MTC-CI-ID-MVL):

MTC-CI-ID-MVL: multiple-target-cell chronic-infection intracellular-delay minimum-viral-load model

$$\frac{dT_p(t)}{dt} = \lambda_p - \delta_p T_p(t) - (1-\epsilon)k_p V(t) T_p(t) \tag{4.11a}$$

$$\frac{dT_s(t)}{dt} = \lambda_s - \delta_s T_s(t) - (1-f\epsilon)k_s V(t) T_s(t) \tag{4.11b}$$

$$\frac{dT_p^*(t)}{dt} = (1-\alpha)(1-\epsilon)k_p V(t-\tau) T_p(t-\tau) e^{-\delta\tau} - \delta T_p^*(t) \tag{4.11c}$$

$$\frac{dT_s^*(t)}{dt} = (1-\alpha)(1-f\epsilon)k_s V(t-\tau) T_s(t-\tau) e^{-\delta\tau} - \delta T_s^*(t) \tag{4.11d}$$

$$\frac{dC_p^*(t)}{dt} = \alpha(1-\epsilon)k_p V(t-\tau) T_p(t-\tau) e^{-\mu\tau} - \mu C_p^*(t) \tag{4.11e}$$

$$\frac{dC_s^*(t)}{dt} = \alpha(1-f\epsilon)k_s V(t-\tau) T_s(t-\tau) e^{-\mu\tau} - \mu C_s^*(t) \tag{4.11f}$$

$$\frac{dV(t)}{dt} = N_T\delta(T_p^*(t) + T_s^*(t)) + N_C\mu(C_p^*(t) + C_s^*(t)) - cV(t) + V_{mvl} \tag{4.11g}$$

Again this changes the viral term (V) by including a minimum viral load V_{mvl}. As can be seen in *Fig. 4.7* the time taken to reach viral set-point is again no longer dependent on the period for which therapy is successful. However, its impact is not as pronounced as for STC models, as MTC-CI models inherently include a low level viral term due to the chronic infected cells.

The steady-states for this model are shown in Table 4.2. The *off-therapy* steady-states are different from those for the STC model (Table 4.1) because the same parameter values are used for both models, but the MTC model includes extra compartments, which change the dynamics of the model, and thus the steady-state. However, viral doubling-time remains similar and it is this aspect that is most relevant to modelling therapy events. Further, the steady-states are not unique to a specific set of parameter values but, for consistency, these are kept constant across the three models discussed here.

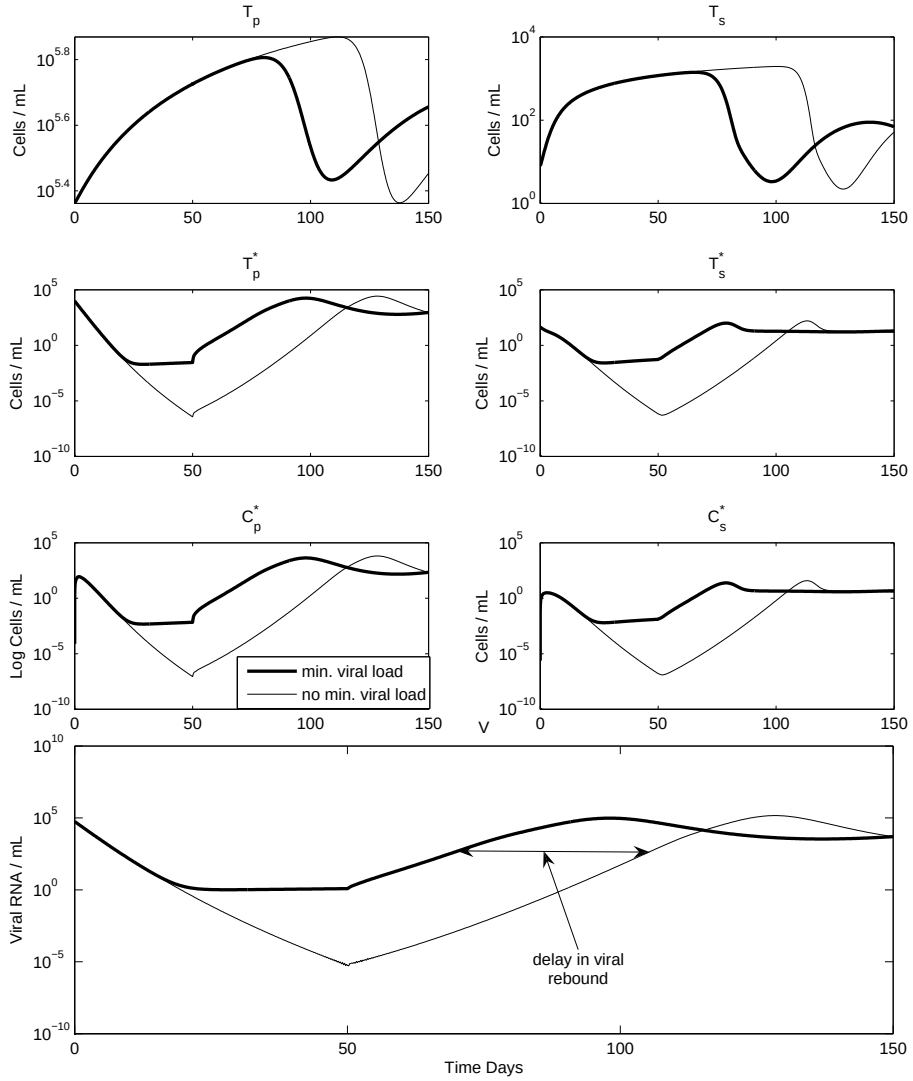

Figure 4.7: Effect of setting a minimum viral load on MTC-CI-ID model: Impact of including a minimum viral load, (MTC-CI-ID-MVL), thus allowing for latency. Shown is the difference between models with and without minimum viral load over two treatment events, 0-50 therapy introduction, 50-150 therapy removal. Highlighted is the delay in reaching viral steady-state when viral load is allowed to drop to unrealistic levels.

Steady-state	$T_p(t)$	$T_s(t)$	$T_p^*(t)$	$T_s^*(t)$	$V(t)$	$E(t)$
On treatment	995,346	2,619	2	4	32	12
Off treatment	233,031	8	7,718	32	41,142	26

Table 4.3: MTC-IR-ID-MVL steady-states: The natural steady-states for MTC-IR-MVL model. These are achieved by allowing the model to run over long periods of time.

4.4.3 MTC-IR-ID including a minimum viral load (MTC-IR-ID-MVL)

The MTC-IR model including a minimum viral load is as follows:

MTC-IR-ID-MVL: multiple-target-cell immune-response intracellular-delay minimum-viral-load model

$$\frac{dT_p(t)}{dt} = \lambda_p - \delta_p T_p(t) - (1-\epsilon)k_p V(t) T_p(t) \tag{4.12a}$$

$$\frac{dT_s(t)}{dt} = \lambda_s - \delta_s T_s(t) - (1-f\epsilon)k_s V(t) T_s(t) \tag{4.12b}$$

$$\frac{dT_p^*(t)}{dt} = (1-\epsilon)k_p V(t-\tau) T_p(t-\tau) e^{-\delta\tau} - \delta T_p^*(t) - m_p E(t) T_p^*(t) \tag{4.12c}$$

$$\frac{dT_s^*(t)}{dt} = (1-f\epsilon)k_s V(t-\tau) T_s(t-\tau) e^{-\delta\tau} - \delta T_s^*(t) - m_s E(t) T_s^*(t) \tag{4.12d}$$

$$\frac{dV(t)}{dt} = N_T \delta (T_p^*(t) + T_s^*(t)) - \tag{4.12e}$$

$$\big[(1-\epsilon)p_p k_p T_p(t) + (1-f\epsilon)p_s k_s T_s(t)\big] V(t) - cV(t) + V_{mvl} \tag{4.12f}$$

$$\frac{dE(t)}{dt} = \lambda_E + \frac{b_E(T_p^*(t) + T_s^*(t))}{(T_p^*(t) + T_s^*(t)) + K_b} E(t) - \tag{4.12g}$$

$$\frac{d_E(T_p^*(t) + T_s^*(t))}{(T_p^*(t) + T_s^*(t)) + K_d} E(t) - \delta_E E(t) \tag{4.12h}$$

Again this is as for the STC and MTC-CI models with a constant viral source included in the viral term. As can be seen in *Fig. 4.8* this produces similar results to before, highlighting its inclusion when modelling therapy introduction events.

The steady-states are given in Table 4.3. As the parameters used across all three models were based on this MTC-IR model they produce the desired viral steady-state of approximately 42,000 HIV RNA $copies/mL$.

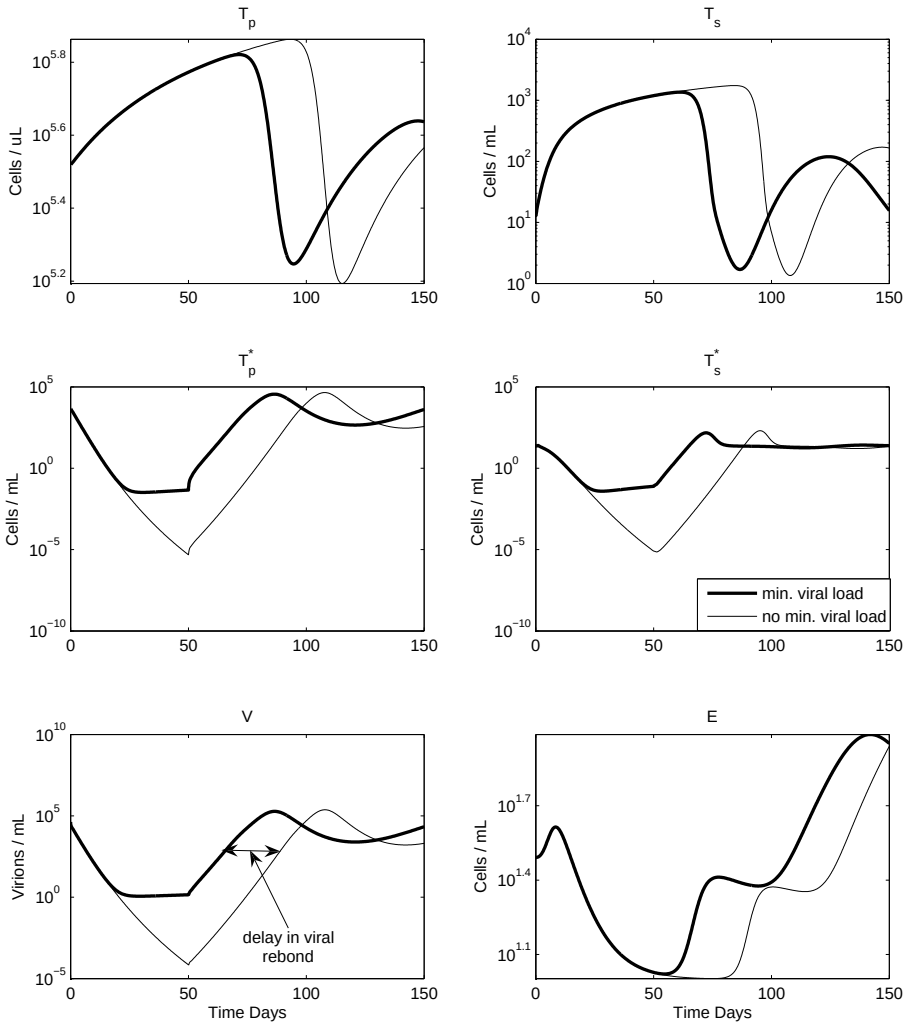

Figure 4.8: Effect of setting a minimum viral load on MTC-IR-ID model: Impact of including a minimum viral load, (MTC-IR-ID-MVL), thus allowing for latency. Shown is the difference between models with and without minimum viral load over two treatment events, 0-50 therapy introduction, 50-100 therapy removal. Highlighted is the delay in reaching viral steady-state when unrealistically low viral load are allowed.

4.5 Summary of inclusion of intracellular delay and latency

This chapter covers the necessary updates to current models such that they can accurately represent both therapy introduction and removal. To achieve this both intracellular delay and viral latency must be accounted for.

4.5.1 Intracellular delay

Inclusion of a discrete intracellular delay, into the three models of Chapter 3, is discussed. This produces a significant increase in viral doubling-time is observed, with a corresponding increase in the time to reach viral set-point, when therapy is removed, summarised in Table 4.4.

The impact of intracellular delay is more far-reaching, however, implying that viral rebound, or viral blips, can not be sustained from low level of virus, even though continuously replicating, and must come from another source, e.g. a stimulation of the immune response which releases latent virus [191, 192]. This is supported by [80] whereby the virus is shown not to mutate, as expected during this replication, but is due to a static viral strain, implying that it comes from latently infected cells, which only produce virus when stimulated. Furthermore, the infection delay models discussed here do not include the latter source, so that when the viral load increases these will also be activated, and will add to the viral pool, further reducing the delay. This additional source offers and explanation of viral rebound behaviour and viral blips. Consequently, the requirement is to to think beyond suppression of the actively-replicating virus and instead to focusing on the influence of the resting virus pool, (e.g. latently infected cells of the immune system).

	doubling-time of virus	
Model	$0hrs$ intracellular delay	$24hrs$ intracellular delay
STC	0.98 day	1.65 day
MTC-CI	1.03 day	1.69 day
MTC-IR	0.96 day	1.67 day

Table 4.4: Model doubling-time: Comparison of doubling-time for the three models discussed

4.5.2 HIV latency

The inclusion of HIV latency is presented here only in simplistic form, through a constant minimum level of virus, which is not affect by therapy. Inclusion of this latency term, nevertheless, is important for viral rebound on therapy removal, as it allows for a residual base line of infection. As can be seen from *Fig. 4.5*, *Fig. 4.7* and *Fig. 4.8* original models allow virus levels to drop to unrealistic levels without the inclusion of latency.

4.5.3 Overall model selection based on viral load doubling-time

Both doubling-time and half-life are important system properties. In this context, the first five days of growth (*Fig. 4.9*), can be seen to be approximately linear, (log plot). Thus, from this initial growth phase the doubling-time of HIV can be calculated for each model, shown in Table 4.4. This is also possible for viral half-life, which is reduced slightly by incorporation of intracellular delay, (from 1.29 to 1.27 days across all models).

In a recent study of primary HIV infection the average doubling-time is given as 0.65 days (0.56- 0.91 days) [193]. If this is compared with our models, 1.00 days without intracellular delay and 1.67 days with intracellular delay, intracellular delay clearly contributes markedly in any model used for therapy removal. Furthermore, the rate given by Ribeiro et al. (2010) is for primary infection, and this increases when the adaptive immune response is also included. Some studies put this doubling-time at approximately 1.6 - 2.0 days when active immune response is taken into account, as is the case when therapy is removal [194, 195, 196, 197]. Thus the significant increase seen with inclusion of intracellular delay is consistent with *in vivo* studies.

Intracellular delay (day)	0.0	0.5	1.0	1.5	2.0
Doubling-time (T_d) (day)	1.03	1.37	1.82	2.26	2.70

Table 4.5: Intracellular delay and doubling-time: The effect of varying intracellular delay on viral doubling-time, selected values from *Fig. 4.10*

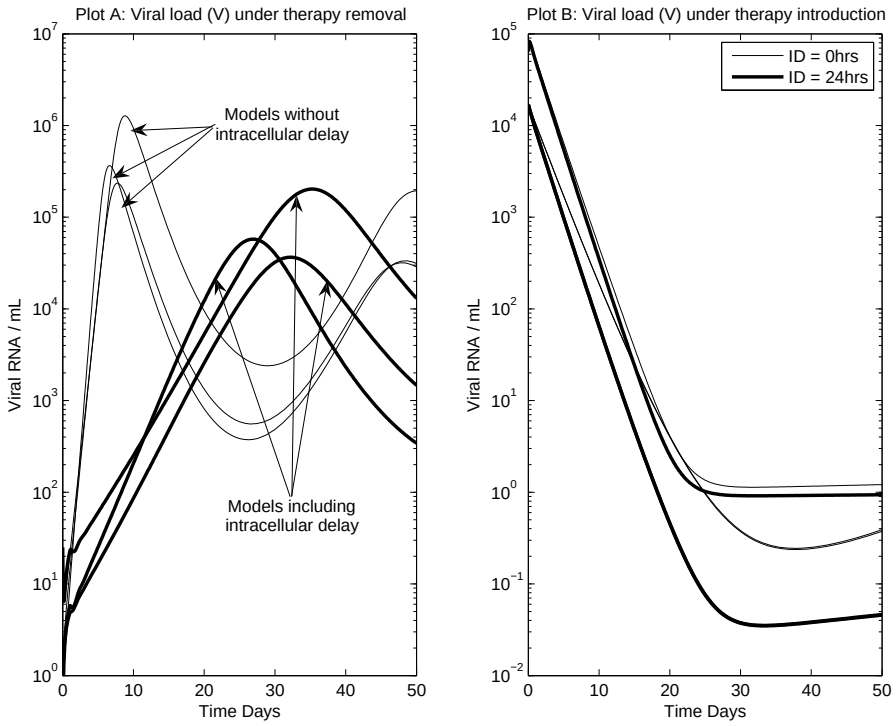

Figure 4.9: Effect of intracellular delay across all models: Comparison of inclusion of intracellular delay across all models, (STC-ID-MVL, MTC-CI-ID-MVL and MTC-IR-ID-MVL). Plot A shows the effect on viral doubling-time for therapy removal. Specifically shown is the difference in viral doubling-time between zero intracellular delay ($ID = 0hrs$, $T_d = 1.00days$) and an intracellular delay of one day ($ID = 24hrs$, $T_d = 1.67days$). Plot B shows there is little change in viral half-life when intracellular delay is accounted for under therapy introduction, (for $ID = 0hrs$ or $ID = 24hrs$, $T_{1/2} = 1.28days$).

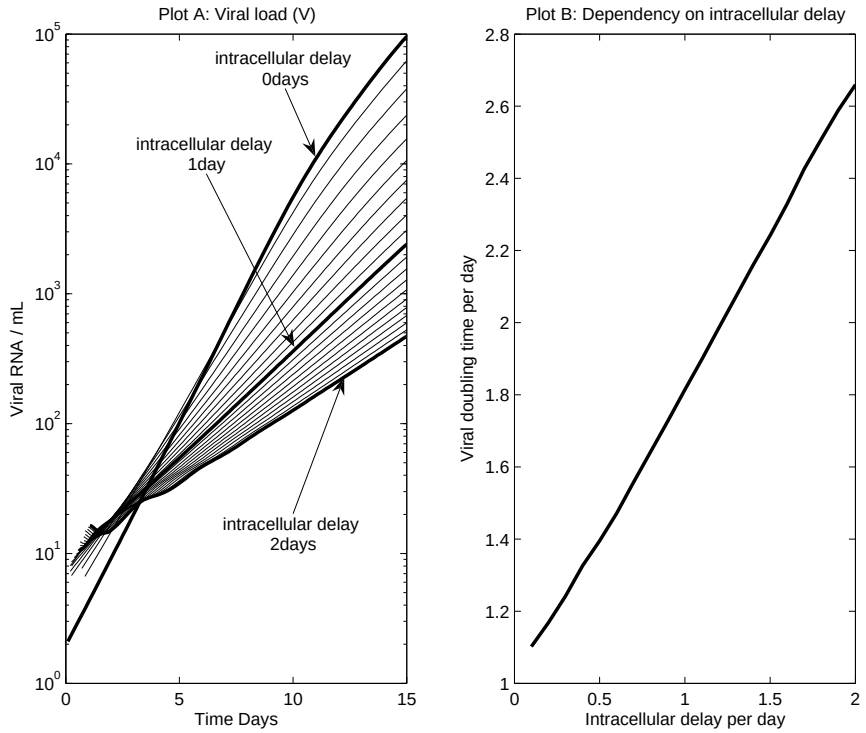

Figure 4.10: MTC-IR-ID delay effect: The effect of inclusion of intracellular delay on viral doubling-time. Plot A shows how doubling-time increases as intracellular delay is varied from 0 to 2 days. Plot B shows this linear relationship between intercellular delay and viral doubling-time, whereby the viral doubling time, (T_d), is given based on intracellular delay.

4.6 Summary

In modelling treatment interruption it is essential to have a set of models which can accurately model both therapy introduction and removal. While original models, discussed in Chapter 3, were adequate for therapy introduction, intracellular delay and HIV latency were introduced to allow for better modelling of therapy removal. Intracellular delay, in a discrete form, was incorporated, increasing viral doubling from 1.00 to 1.67 days, with a corresponding increase in reaching viral set-point. HIV latency was also introduced, in the form of a minimum viral level, to eliminate the unrealistically low viral levels which original models allowed. Thus, this chapter developed a set of models capable of modelling treatment interruption, discussed in Chapter 6. However, additional complexity was necessary to achieve this, which the next chapter strives to reduce.

Chapter 5

Dimensional analysis

The previous chapter demonstrated the importance of intracellular delay and HIV latency when modelling therapy removal. In this chapter, alternative simplified solutions of these models are developed by converting them to a dimensionless system. This conversion allows accurate comparison of parameters and initial conditions. Again viral doubling-time and half-life are used to compare these dimensionless parameters, highlighting those which are key and providing a basis for reduction of model complexity. Identifying these key parameters becomes more important as the models become increasingly more complex, allowing retention of only those which have significant impact on overall model function. Dimensional analysis, (DA), can be used to achieve this reduction of parameter space [198, 153, 154, 199]. To illustrate the viability of this approach the three models developed so far are reformed using dimensionless expressions, the converted dimensionless parameters individually varied and performance indicators, viral doubling-time and half-life, compared. The results of this analysis are summarised here, with full details given in Appendix C.

5.1 Model parameter comparison using dimensional analysis

The aim of DA is to facilitate comparison between each of the parameters used to describe a mathematical model. This comparison allows elimination of unimportant parameters, promoting simplification. To allow for accurate comparison, each parameter is made 'dimensionless' (i.e. scaling each to unity). The process for rendering a model dimensionless also reduces the number of parameters and is described below.

5.1.1 Dimensionless STC-ID-MVL model (STC-ID-MVL-DA)

To convert the STC model, Eqn. (4.10), each variable and parameter is divided by a factor such that their dimensions cancel. The dimension of each variable and parameter is given in Tables A.1 and A.2 respectively, thus, for example, time, (t), has dimension *time* and is made dimensionless ($\bar{t}$) by multiplying it by δ, which has dimension of *time*$^{-1}$. The variables, (T_p, T_p^* and V,), have dimension *length*$^{-3}$, (as these are measured by volume), and can be made dimensionless by dividing by their initial conditions. Continuing this process, using the dimensions and values given in Tables A.1 and A.2, the following dimensionless representation of the STC-ID-MVL can be derived, (STC-ID-MVL-DA):

STC-ID-MVL-DA: single-target-cell intracellular-delay minimum-viral-load dimensional-analysis model

$$\frac{d\bar{T}_p(\bar{t})}{d\bar{t}} = A - B\bar{T}_p(\bar{t}) - C\bar{V}(\bar{t})\bar{T}_p(\bar{t}) \tag{5.1a}$$

$$\frac{d\bar{T}_p^*(\bar{t})}{d\bar{t}} = C\bar{V}(\bar{t}-\bar{\tau})\bar{T}_p(\bar{t}-\bar{\tau})e^{-D} - \bar{T}_p^*(\bar{t}) \tag{5.1b}$$

$$\frac{d\bar{V}(\bar{t})}{d\bar{t}} = E\bar{T}_p^*(\bar{t}) - F\bar{V}(\bar{t}) + G \tag{5.1c}$$

where;

$$\bar{t} = t\delta,\ \bar{\tau} = \tau\delta,\ \bar{T}_p(\bar{t}) = \frac{T_p(t)}{T_{p0}},\ \bar{T}_p^*(\bar{t}) = \frac{T_p^*(t)}{T_{p0}},\ \bar{V}(\bar{t}) = \frac{V(t)}{T_{p0}} \tag{5.2a}$$

$$A = \frac{\lambda_p}{\delta T_{p0}},\ B = \frac{\delta_p}{\delta},\ C = (1-\epsilon)\frac{k_p T_{p0}}{\delta}, \tag{5.2b}$$

$$D = \delta\tau,\ E = N_T,\ F = \frac{c}{\delta},\ G = \frac{V_{lvl}}{T_{p0}} \tag{5.2c}$$

This dimensionless system is based on both parameter values and initial conditions so each dimensionless parameter and variable will change, depending on what therapy event is being modelled. For example, *C* varies from off-therapy steady state to introduction of therapy across on-therapy steady state and therapy removal, as seen in Table 5.1, whereas *D* remains constant across this spectrum. Thus, when comparing dimensionless parameters it is necessary to match initial conditions and therapy events.

Converting a model to its dimensionless representation allows detailed sensitivity analysis of each dimensionless parameter and initial condition. By varying each parameter and its initial condition, these can be compared accurately, (as parameters are scaled to each other). Further, individual variation of each parameter, and initial condition, while holding the remainder constant, makes it possible to determine the impact each has on overall model function. Table 5.2 gives a summary of the key dimensionless parameters and initial

Dimensionless parameters		Off therapy steady-state	Therapy introduction	On Therapy steady-state	Therapy removal
A	$\frac{\lambda_p}{\delta T_{p0}}$	0.0621	0.0621	0.0238	0.0238
B	$\frac{\delta_p}{\delta}$	0.0143	0.0143	0.0143	0.0143
C	$(1-\epsilon)\frac{k_p T_{p0}}{\delta}$	0.2629	0.0263	0.0686	0.6857
D	$\delta\tau$	0.7000	0.7000	0.7000	0.7000
E	N_T	3.4783	3.4783	0.0002	0.0002
F	$\frac{c}{\delta}$	18.5714	18.5714	18.5714	18.5714
G	$\frac{V_{lvl}}{T_{p0}}$	0.0000	0.0000	0.0000	0.0000
Initial conditions					
$\bar{T}_{p0}$	$\frac{T_p}{T_{p0}}$	1.0000	1.0000	1.0000	1.0000
$\bar{T}^*_{p0}$	$\frac{T^*_p}{T_{p0}}$	1.0000	1.0000	1.0000	1.0000
$\bar{V}_0$	$\frac{V}{T_{p0}}$	0.1826	0.1826	0.0000	0.0000

Table 5.1: STC-ID-MVL-DA dimensionless values The values for each of the dimensionless parameters and initial conditions across both therapy events and steady-states.

conditions, the full set is given in Table C.2. As before, for incorporation of intracellular delay, model performance is determined by viral doubling-time and half-life. By relating the dimensionless quantities back to the original model the biological meaning of the key components can be retrieved:

Viral source: $C = (1-\epsilon)\frac{k_p T_{p0}}{\delta}$ Changes in this are expected to impact upon viral doubling-time. As it is significantly reduced by therapy it is less important for viral half-life.

Intracellular delay: $D = \delta\tau$ The impact of intracellular delay has been seen in the previous chapter, and is possibly the most important factor for these models.

Number of virions produced per cell: $E = N_T$ If the number of virions produced per infected cell changes, so too will the viral doubling-time. Again, its importance is decreased due to drug therapy, which blocks most viral production.

Viral clearance rate: $F = \frac{c}{\delta}$ As for production of virus, clearance changes the amount of virus present.

Initial target cell concentration: $\bar{T}_{p0} = \frac{T_p}{T_{p0}}$ Changing the number of cells which HIV targets also changes the amount of virus produced, as there will be more or less of these available.

	Therapy removal				Therapy introduction			
Dim.Less	Initial	doubling-time (day)			Initial	half-life (day)		
par	value	Low	High	% diff	value	Low	High	% diff
C	0.03	2.80	2.02	-27.71 %	0.69	1.23	1.25	1.12 %
D	0.70	1.99	2.74	37.83 %	0.70	1.23	1.25	1.94 %
E	100.00	2.79	2.02	-27.61 %	100.00	1.21	1.27	4.77 %
F	18.57	2.01	2.72	35.37 %	18.57	1.24	1.21	-2.67 %
Initial conditions								
$\bar{T}_{p0} = \frac{T_{p0}}{T_{p0}}$	1.00	2.71	2.06	-23.71 %	1.00	1.21	1.24	1.93 %

Table 5.2: STC-ID-MVL-DA parameter variation effect: Quantification of effect in variation in initial parameter values and initial conditions based on doubling-time and half-life of viral growth. Initial values were varied from 90% to 110% of their initial value, with the resulting change in viral growth shown.

The key components follow the underlying function of this model, i.e. varying either the source or production and clearance rates of virus will change the viral doubling-time. The effect of intracellular delay has already been discussed in the previous chapter, and is clearly shown to have a significant impact. A summary of the effect of variation of the dimensionless parameters and initial conditions is given in *Fig. 5.1*, with outlying values clearly indicated. The full version given in *Fig. C.1* and *Fig. C.2*. As can be seen from any of these figures, therapy removal is more sensitive to model values than therapy introduction. These are important considerations when modelling both therapy events, as seen in Chapter 6.

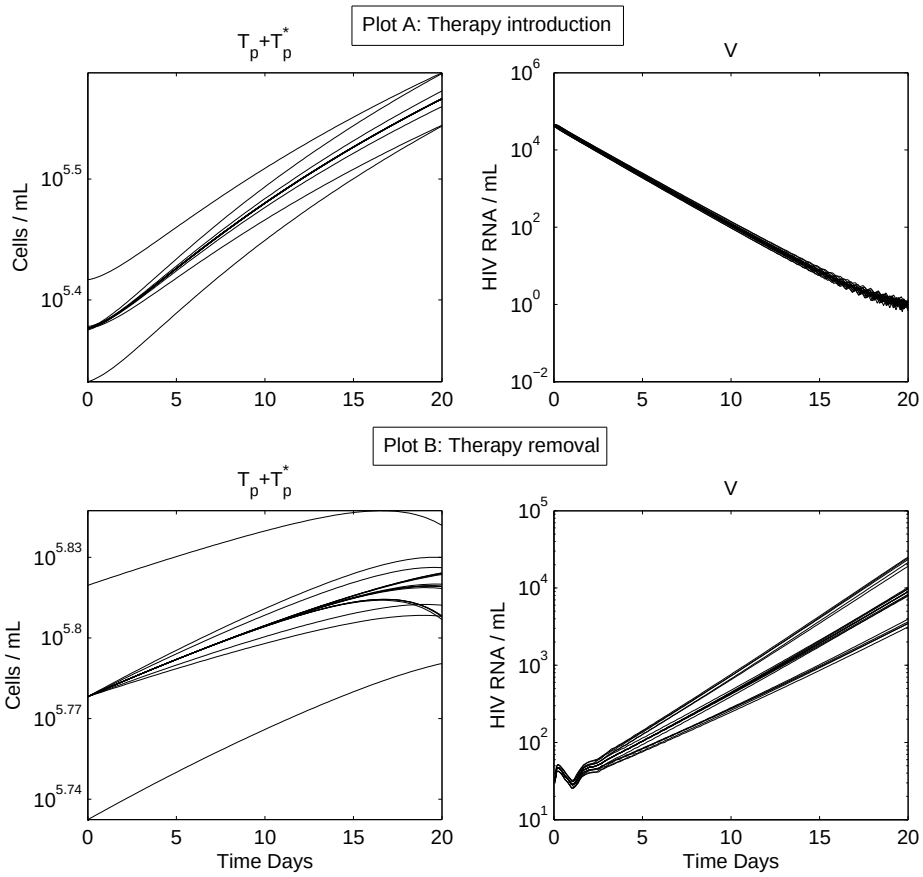

Figure 5.1: STC-ID-MVL-DA parameter variation for therapy introduction: Effect of varying dimensionless parameters and initial conditions for the STC-ID-MVL-DA model for therapy introduction. The specific values are given in Tables 5.2 and C.2

5.1.2 Dimensionless MTC-CI-ID-MVL model (MTC-CI-ID-MVL-DA)

Using the same process for making the STC-ID-MVL model dimensionless, and with variables and parameters given in Tables A.1 and A.2, the following dimensionless representation of the MTC-CI-ID-MVL model (MTC-CI-ID-MVL-DA) is observed:

MTC-CI-ID-MVL-DA: multiple-target-cell chronic-infection intracellular-delay minimum-viral-load dimensional-analysis model

$$\frac{d\bar{T}_p(\bar{t})}{d\bar{t}} = A - B\bar{T}_p(\bar{t}) - C\bar{V}(\bar{t})\bar{T}_p(\bar{t}) \tag{5.3a}$$

$$\frac{d\bar{T}_s(\bar{t})}{d\bar{t}} = D - E\bar{T}_s(\bar{t}) - F\bar{V}(\bar{t})\bar{T}_s(\bar{t}) \tag{5.3b}$$

$$\frac{d\bar{T}^*_p(\bar{t})}{d\bar{t}} = G\bar{V}(\bar{t}-\bar{\tau})\bar{T}_p(\bar{t}-\bar{\tau})e^{-H} - \bar{T}^*_p(\bar{t}) \tag{5.3c}$$

$$\frac{d\bar{T}^*_s(\bar{t})}{d\bar{t}} = I\bar{V}(\bar{t}-\bar{\tau})\bar{T}_s(\bar{t}-\bar{\tau})e^{-H} - \bar{T}^*_s(\bar{t}) \tag{5.3d}$$

$$\frac{d\bar{C}^*_p(\bar{t})}{d\bar{t}} = J\bar{V}(\bar{t}-\bar{\tau})\bar{T}_p(\bar{t}-\bar{\tau})e^{-K} - L\bar{C}^*_p(\bar{t}) \tag{5.3e}$$

$$\frac{d\bar{C}^*_s(\bar{t})}{d\bar{t}} = M\bar{V}(\bar{t}-\bar{\tau})\bar{T}_s(\bar{t}-\bar{\tau})e^{-K} - L\bar{C}^*_s(\bar{t}) \tag{5.3f}$$

$$\frac{d\bar{V}(\bar{t})}{d\bar{t}} = N\bar{T}^*_p(\bar{t}) + O\bar{T}^*_s(\bar{t}) - P\bar{C}^*_p(\bar{t}) - Q\bar{C}^*_s(\bar{t}) - R\bar{V}(\bar{t}) + S \tag{5.3g}$$

where;

$$\bar{t} = \delta t,\ \bar{\tau} = \delta\tau,\ \bar{T}_p = \frac{T_p}{T_{p0}},\ \bar{T}_s = \frac{T_s}{T_{s0}},\ \bar{T}^*_p = \frac{T^*_p}{T_{p0}}, \tag{5.4a}$$

$$\bar{T}^*_s = \frac{T_s}{T_{s0}},\ \bar{C}^*_p = \frac{C^*_p}{T_{p0}},\ \bar{C}^*_s = \frac{C^*_s}{T_{s0}},\ \bar{V} = \frac{V}{T_{p0}} \tag{5.4b}$$

$$A = \frac{\lambda_p}{\delta T_{p0}},\ B = \frac{\delta_p}{\delta},\ C = (1-\epsilon)\frac{k_p T_{p0}}{\delta},\ D = \frac{\lambda_s}{\delta T_{s0}}, \tag{5.4c}$$

$$E = \frac{\delta_s}{\delta},\ F = (1-f\epsilon)\frac{k_s T_{p0}}{\delta},\ G = (1-\alpha)C,\ H = \delta\tau, \tag{5.4d}$$

$$I = (1-\alpha)F,\ J = \alpha C,\ K = \mu\tau,\ L = \frac{\mu}{\delta},\ M = \alpha F,\ N = N_T, \tag{5.4e}$$

$$O = N_T\frac{T_{s0}}{T_{p0}},\ P = N_C\frac{\mu}{\delta},\ Q = N_C\frac{\mu}{\delta}\frac{T_{s0}}{T_{p0}},\ R = \frac{c}{\delta},\ S = \frac{V_{lvl}}{T_{p0}} \tag{5.4f}$$

	Therapy removal				Therapy introduction			
Dim.Less	Initial	doubling-time (days)			Initial	half-life (days)		
par	value	Low	High	% diff	value	Low	High	% diff
G	0.55	4.34	2.90	-33.19 %	0.70	1.14	1.17	2.58 %
H	0.70	2.88	4.14	43.56 %	8.57	1.16	1.15	-0.69 %
N	100.00	4.34	2.90	-33.19 %	18.57	1.14	1.17	2.30 %
R	18.57	2.82	4.21	49.50 %	0.36	1.17	1.14	-2.55 %
Initial conditions								
$\bar{T}_{p0} = \frac{T_p}{T_{p0}}$	1.00	4.61	3.01	-34.67 %	1.00	1.14	1.16	2.09 %

Table 5.3: MTC-CI-ID-MVL-DA parameter variation effect: Quantification of effect in variation in initial parameter values and initial conditions based on doubling-time and half-life of viral growth. Initial values were varied from 90% to 110% of their initial value, with the resulting change in viral growth shown.

As before, different therapy events produce different values for the dimensionless parameters; these are given in Table C.3. Variation in these parameters and initial conditions produce similar results to that for the STC-ID-MVL-DA model above. These again focus on viral production (G and N), number of target cells ($\bar{T}_{p0}$), intracellular delay (H) and viral clearance rate (R). These results are summarised in Table 5.3, with full results given in Table C.4. Again sensitivity is focused on therapy removal, as summarised in *Fig. 5.2* with the full version given in *Fig. C.3* and *Fig. C.4*.

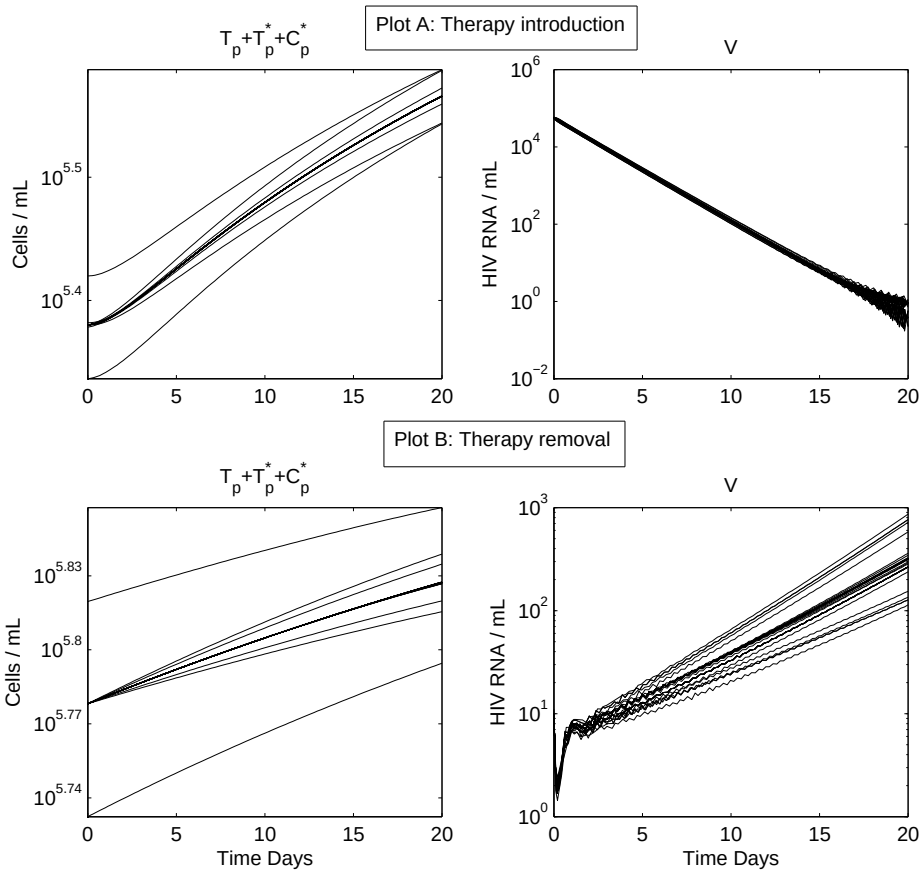

Figure 5.2: MTC-CI-ID-MVL-DA parameter variation for therapy introduction: Effect of varying dimensionless parameters and initial conditions for the MTC-CI-ID-MVL-DA model for therapy introduction. The specific values are given in Tables 5.3 and C.4

5.1.3 Dimensionless MTC-IR-ID-MVL (MTC-IR-ID-MVL-DA)

Again the MTC-IR-ID-MVL model can be made dimensionless, (MTC-IR-ID-MVL-DA), with Tables A.1 and A.2 giving the necessary variables and parameters:

MTC-IR-ID-MVL-DA: multiple-target-cell immune-response intracellular-delay minimum-viral-load dimensional-analysis model

$$\frac{d\bar{T}_p(\bar{t})}{d\bar{t}} = A - B\bar{T}_p(\bar{t}) - C\bar{V}(\bar{t})\bar{T}_p(\bar{t}) \tag{5.5a}$$

$$\frac{d\bar{T}_s(\bar{t})}{d\bar{t}} = D - E\bar{T}_s(\bar{t}) - F\bar{V}(\bar{t})\bar{T}_s(\bar{t}) \tag{5.5b}$$

$$\frac{d\bar{T}^*_p(\bar{t})}{d\bar{t}} = C\bar{V}(\bar{t}-\bar{\tau})\bar{T}_p(\bar{t}-\bar{\tau})e^{-G} - \bar{T}^*_p(\bar{t}) - H\bar{E}(\bar{t})\bar{T}^*_p(\bar{t}) \tag{5.5c}$$

$$\frac{d\bar{T}^*_s(\bar{t})}{d\bar{t}} = F\bar{V}(\bar{t}-\bar{\tau})\bar{T}_s(\bar{t}-\bar{\tau})e^{-G} - \bar{T}^*_s(\bar{t}) - I\bar{E}(\bar{t})\bar{T}^*_s(\bar{t}) \tag{5.5d}$$

$$\frac{d\bar{V}(\bar{t})}{d\bar{t}} = J\bar{T}^*_p(\bar{t}) + K\bar{T}^*_s(\bar{t}) - L\bar{V}(\bar{t})\bar{T}_p(\bar{t}) - M\bar{V}(\bar{t})\bar{T}_p(\bar{t}) - N\bar{V}(\bar{t}) + S \tag{5.5e}$$

$$\frac{d\bar{E}(\bar{t})}{d\bar{t}} = O + P\frac{\bar{T}^*_p(\bar{t}) + \bar{T}^*_s(\bar{t})}{(\bar{T}^*_p(\bar{t}) + \bar{T}^*_s(\bar{t})) + Q}\bar{E}(\bar{t}) - \tag{5.5f}$$

$$R\frac{\bar{T}^*_p(\bar{t}) + \bar{T}^*_s(\bar{t})}{(\bar{T}^*_p(\bar{t}) + \bar{T}^*_s(\bar{t})) + S}\bar{E}(\bar{t}) - T\bar{E}(\bar{t}) + U\bar{E}(\bar{t}) \tag{5.5g}$$

where;

$$\bar{t} = \delta t,\ \bar{\tau} = \delta\tau,\ \bar{T}_p = \frac{T_p}{T_{p0}},\ \bar{T}_s = \frac{T_s}{T_{s0}}, \tag{5.6a}$$

$$\bar{T}^*_p = \frac{T^*_p}{T_{p0}},\ \bar{T}^*_s = \frac{T_s}{T_{s0}},\ \bar{V} = \frac{V}{T_{p0}},\ \bar{E} = \frac{E}{T_{p0}} \tag{5.6b}$$

$$A = \frac{\lambda_p}{\delta T_{p0}},\ B = \frac{\delta_p}{\delta},\ C = (1-\epsilon)\frac{k_p T_{p0}}{\delta},\ D = \frac{\lambda_s}{\delta T_{s0}},\ E = \frac{\delta_s}{\delta}, \tag{5.6c}$$

$$F = (1-f\epsilon)\frac{k_s T_{s0}}{\delta},\ G = \delta\tau,\ H = \frac{m_p T_{p0}}{\delta},\ I = \frac{m_s T_{s0}}{\delta}, \tag{5.6d}$$

$$J = N_T,\ K = \frac{N_T T_{s0}}{T_{p0}},\ L = \frac{(1-\epsilon)p_p k_p T_{p0}}{\delta}, \tag{5.6e}$$

$$M = \frac{(1-f\epsilon)p_s k_s T_{s0}}{\delta},\ N = \frac{c}{\delta},\ O = \frac{\lambda_E}{T_{p0}\delta},\ P =,\ Q = \frac{K_b}{T_{p0}}, \tag{5.6f}$$

$$R = \frac{d_E}{\delta},\ S = \frac{K_d}{T_{p0}},\ T = \frac{\delta_E}{\delta},\ U = \frac{V_{lvl}}{T_{p0}} \tag{5.6g}$$

	Therapy removal				Therapy introduction			
Dim.Less	Initial	doubling-time (days)			Initial	half-life (days)		
par	value	Low	High	% diff	value	Low	High	% diff
C	0.04	2.52	1.97	-22.02 %	0.69	1.25	1.30	3.81 %
G	0.70	1.95	2.51	29.21 %	0.70	1.28	1.27	-0.63 %
J	100.00	2.52	1.97	-22.03 %	100.00	1.25	1.30	3.89 %
N	18.57	1.89	2.57	35.79 %	18.57	1.30	1.26	-2.53 %
Initial conditions								
$\bar{T}_{p0} = \frac{T_{p0}}{T_{p0}}$	1.00	2.46	2.00	-18.96 %	1.00	1.26	1.29	3.11 %

Table 5.4: MTC-IR-ID-MVL-DA parameter variation effect: Quantification of effect in variation in initial parameter values and initial conditions based on doubling-time and half-life of viral growth. Initial values were varied from 90% to 110% of their initial value, with the resulting change in viral growth shown.

The different therapy events, corresponding to the dimensionless parameter values, are given in Table C.5. As before, changing the parameters and initial conditions produce similar results. These follow the same pattern as before focusing on viral production (C and J), number of target cells ($\bar{T}_{p0}$), intracellular delay (G) and viral clearance rate (N). A summary of these results is given in Table 5.3, with full set of results given in Table C.4. Therapy removal is again the main focus, as shown in *Fig. 5.2* with the full version spectrum for therapy introduction, *Fig. C.3*, and therapy removal, *Fig. C.4*, also given.

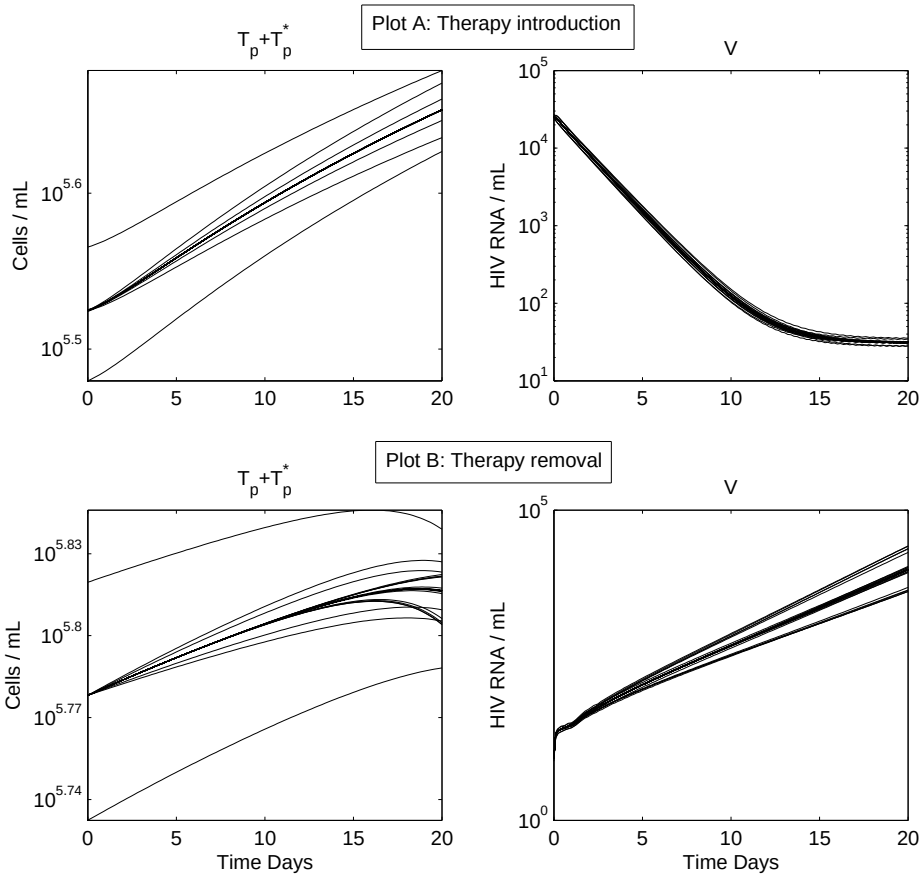

Figure 5.3: MTC-IR-ID-MVL-DA parameter variation for therapy introduction: Effect of varying dimensionless parameters and initial conditions for the MTC-IR-ID-MVL-DA model for therapy introduction. The specific values are given in Tables 5.4 and C.6

5.2 Summary of sensitivity analysis

This chapter took the models developed in Chapter 4 and converted them to their dimensionless version. This allowed the overall impact on model function of each individual dimensionless parameter, and initial condition, to be evaluated. When these results were converted back to their original form, underlying biological function could be evaluated. Thus when compared over all three models (STC-ID-MVL-DA, MTC-CI-ID-MVL-DA and MTC-IR-ID-MVL-DA), clear insight on key parameters could be obtained. These key results can be summarised by identifying that overall model function is determined by:

- Amount of virus produced from target cells
- Amount of target cells available
- Clearance rate of virus

The other contribution to overall model function is intracellular delay, as discussed in Chapter 4. The work of this chapter gives strong indications as to which parameters must be included in any viable model form, and which have less impact. These considerations become increasingly more important as models attempt to incorporate more detailed biological representation. Furthermore, while the additional complexity, by including intracellular delay and minimum viral load, is small, overall model complexity is increasing, e.g. detailed incorporation of immune function can result in doubling of compartments [200].

Chapter 6

Modelling treatment interruptions

Over the course of HIV infection there will generally be some interruption of therapy, either due to therapy failure or administration issues. However, investigations into structured treatment interruptions, (STIs), have also been carried out, with a view to reduce the burden of continual therapy. The results of the majority of these trials have been controversial; the best are inconclusive and the worst indicate increased mortality [112, 113, 56]. Generally, however, the treatment interruptions under investigation were large, (weeks to months), as the primary aim of these trials was to investigate auto-immunity, whereby the immune system alone could control HIV replication, as seen in the case of 'elite-controllers' [101]. Unfortunately, this proved unsuccessful and most patients displayed viral rebound similar to initial infection with a corresponding drop in $CD4^{+}T$ cells counts. As a result of these failures STI trials have not been recommended, specifically since the failure of the large scale SMART trial [112]. Now however, with demand for therapy increasing in resource-limited and remote regions, there will be more instances of unplanned therapy interruptions, as continual access to ART can not be guaranteed, (as seen with TB drugs in developing countries [201]). Furthermore, it may prove necessary to include planned interruptions to therapy, in an effort to maintain cost-effective regimes. Thus, it is necessary to develop a safer method of investigating why STIs have failed in the past and whether successful STI guidelines can be established for the future. This research suggests using mathematical modelling to investigate this, with the aim of proposing treatment strategies which can maintain viral suppression during interruptions. If this approach proves successful, a significant reduction in the cost of therapy, along with improved drug administration schedules, may be possible, particulary in circumstances where resources are limited.

This chapter used the models, developed in Chapter 4, specifically the MTC-IR-ID-MVL model, (Eqn.(4.12)), to investigate STI, using interruption combinations of varying lengths. The MTC-IR-ID-MVL model is selected as it provides the key components necessary to investigate therapy removal, specifically:

multiple target cells to allow bi-phasic viral reduction during therapy introduction

immune response to account for the reduction in viral load due to the immune system combating HIV replication

intracellular delay to increase the viral doubling time, thus slowing viral rebound

latency to allow for a minimum viral load under drug induced viral suppression

Based on this a potential STI regime is suggested which controls replication but provides cost savings.

6.1 Structured treatment interruption

The delay model (MTC-IR-ID-MVL) and original model (MTC-IR) are compared over two existing STI regimes. This demonstrates the impact intracellular delay has on model predictions. A number of contrasting STI regimes are then compared, using only the MTC-IR-ID-MVL model, allowing selection of a potential STI which combines viral control and cost savings. A continual therapy regime is also included to provide a base line comparison. Logically these regimes follow the weekly period, allowing therapy interruption to be consistent across days and weeks. It should be noted that the strategies developed generally do not relate to any specific trials, but are only an indication of potential future trials.

6.1.1 Two-week-on two-week-off strategy (14/14)

A strategy of weeks off-therapy periods is common for STI trials [112, 113, 56]. Demonstrated here is an illustrative 14 day on and 14 day off regime, although these times can be varied and produce similar results. Older STI regimes generally involve even longer periods off therapy, (months), as they strived for auto viral control [101], but as indicated, by the models already discussed, viral load generally rebounds to set-point within weeks.

As can be seen, (*Fig. 6.1*), this typical STI strategy will allow a significant average viral load to develop, ($586 virions/mL$), with peak of $3,371 virions/mL$ being produced. When this is compared with an average viral load of only $33 virions/mL$, for continual therapy, a shorter period off therapy is indicated. The shorter the period for which therapy is removed for then the lower the peak vial load, essential to reducing the potential of drug resistant mutations developing. However, there is a minimum time needed for the body to metabolise specific ART drugs and thus a minimum time for off-therapy follows, suggested as a minimum of 2 days.

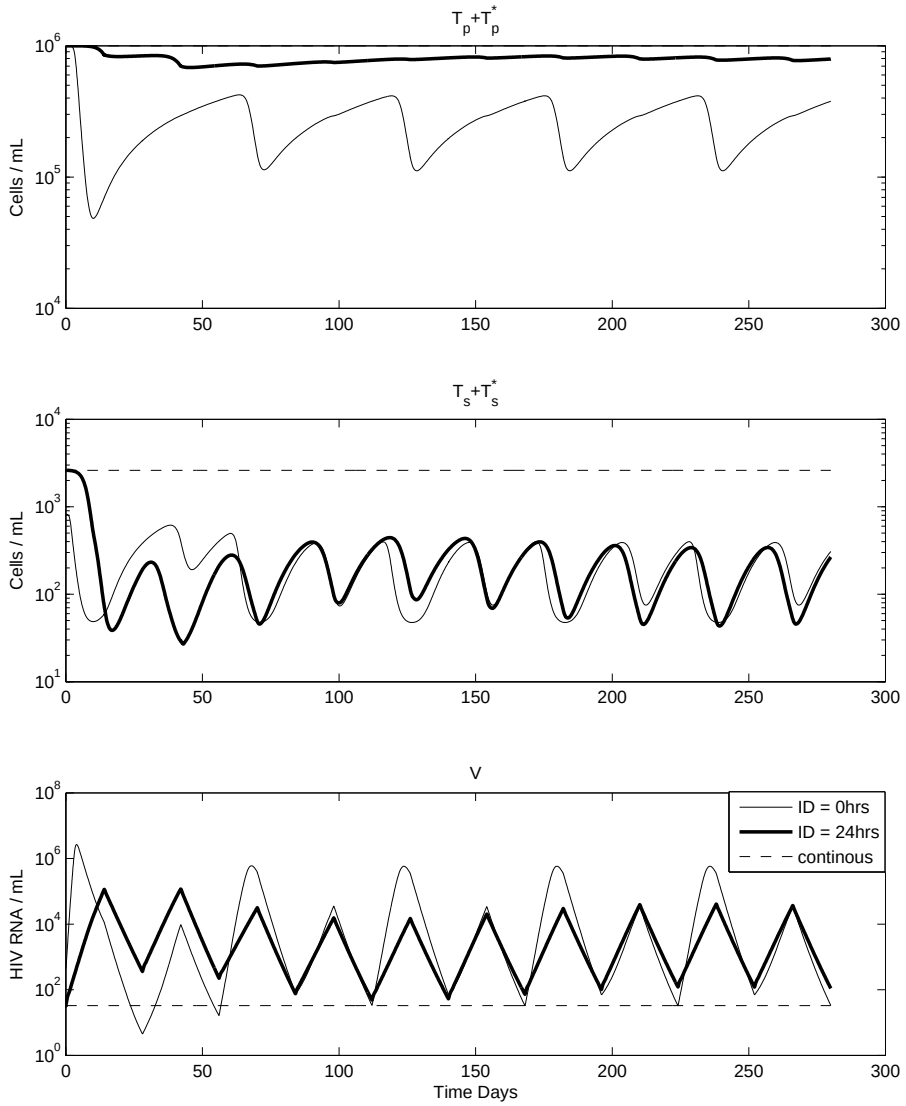

Figure 6.1: STI using MTC-IR-ID-MVL model with 14d on and 14d off: This is an example of an equal on/off therapy STI. This shows an average viral load of $8,446 virions/mL$ with zero delay and $586 virions/mL$ for 24hr delay, compared with $33 virions/mL$ for continuous therapy. The peak viral loads are $58,137 virions/mL$ and $3,371 virions/mL$ respectively.

Also shown is the same STI regime for a non-delay model, (MTC-IR). As can be seen, (*Fig. 6.1*), this produces a higher average viral load ($8,446 virions/mL$) and significantly higher viral peaks ($58,137 virions/mL$). This further emphasis the point made in Chapter 4, that intracellular delay needs to be included in modelling therapy removal. The plot also shows a continual therapy line for reference, this has an average viral load of $33 virions/mL$.

A therapy regime like this allows a 50% cost saving, (i.e. therapy is only required for 50% of the time), while limiting replication and allowing target cells to maintain reasonable levels. However, the relatively high viral peaks, ($3,371 virions/mL$), mean a higher chance of developing drug resistant mutations, (DRMs), increasing the chance of therapy failure. Based on this a shorter cycle regime is suggested.

6.1.2 Five-day-on two-day-off strategy (5/2)

Another trial, shown to suppress viral replication long term, suggests taking treatment Monday to Friday and taking the two weekend days off (Saturday and Sunday), also know as weekend-off strategy [202, 203]. This involves the shortest logical interruption of two days. Furthermore, residual drug levels need to well understood, minimising the chance of mono-therapy events occurring, as these could greatly increase the chance of DRMs occurring. To avoid potential mono-therapy events occurring specific drugs ideally need to be stopped at different stages, to allow for their varying metabolising rates, potentially reducing the off-therapy period.

This shorter STI produces superior viral suppression compared with the 14/14 regime, (*Fig. 6.2*), only $412 virions/mL$ average viral load, with a peak of $712 virions/mL$. Specifically it is the reduction in peak viral load which is important, only 20% of the 14/14 peak, ($3,371 virions/mL$ reduced to $712 virions/mL$). The peak viral load is crucial as this gives a larger viral pool from which to produce mutations.

Based on the 5/2 strategy a cost saving of 29% could be made, when compared with continual therapy, while maintaining relatively low viral loads. As discussed in Chapter 2, this could be a method of reducing cost of HIV therapy, specifically in a resource limited region. Furthermore, this strategy could prove useful if access to therapy is not consistent, i.e. it may prove better to stop therapy for two days than to reduce overall therapy levels for limited drug availability. Also based on continuing trials this regime appears to be reasonable successful producing positive results [202, 203].

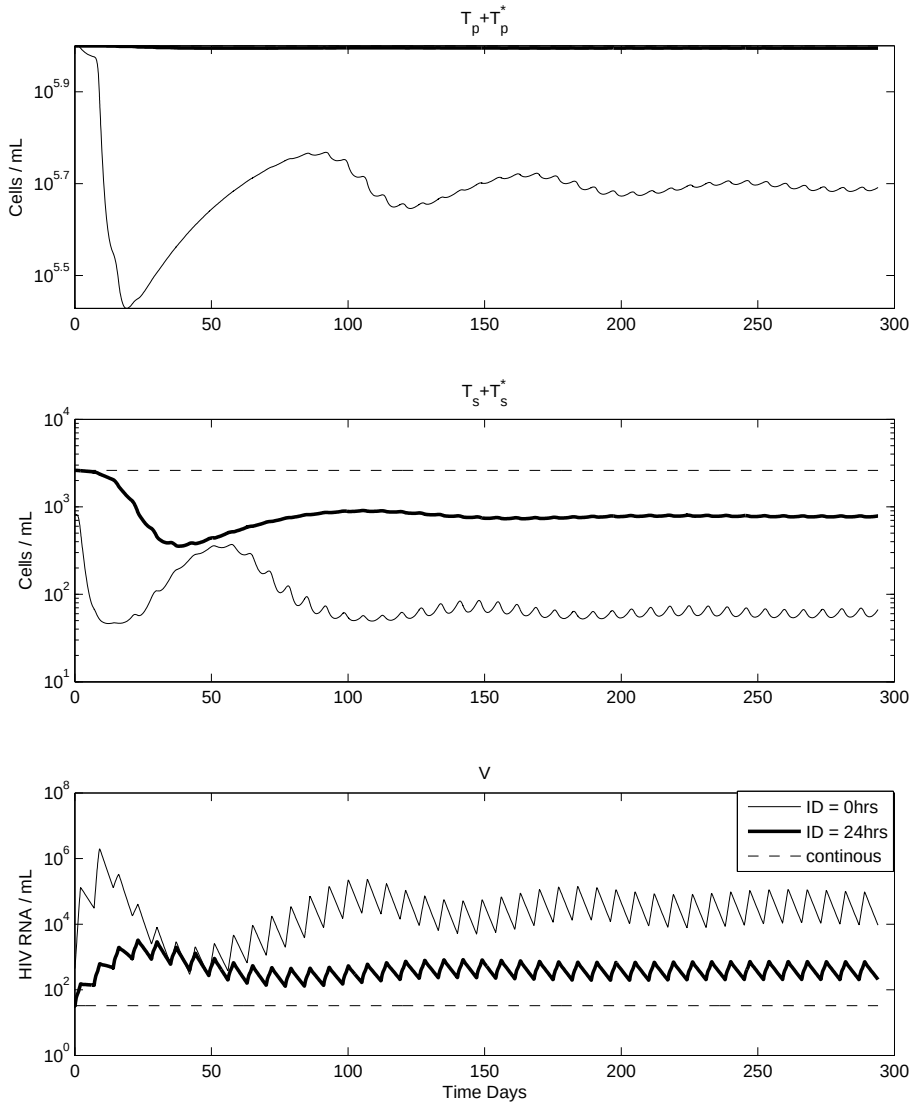

Figure 6.2: STI using MTC-IR-ID-MVL model with 5d on and 2d off: This shorter STI shows an average viral load of $4,951 virions/mL$ with zero delay and $412 virions/mL$ for 24hr delay, compared with $33 virions/mL$ for continuous therapy. Peak viral loads are lower, $10,037 virions/mL$ and $712 virions/mL$ respectively.

6.1.3 Impact of length of varying on/off period

Demonstrated above is the impact that duration of therapy removal has on STI regimes, the longer the period off-therapy the higher the peak in viral load and thus increased potential of mutations developing. However, it is not clear what impact the ratio of on-therapy to off-therapy periods has. Thus three regimes are compared, the 5/2 regime is compared with a scaled up version of this, 20/8 (20 days on and 8 days off), and longer on period of 26/2 (26 days on and 2 days off). Again a continuous therapy period is given for reference.

When these three regimes are compared, (*Fig. 6.3*), it is clear that the shorter the time off therapy the better, as the viral rebound is reduced. Furthermore, the longer the period on-therapy the better, as viral load is reduced. This means that the 26/2 strategy produces the best overall results, but is not a very practical STI regime, as there is little cost saving, only 7%. Also, the 20/8 is shown to have lower average viral load than 5/2, ($352 virions/mL$ compared to $437 virions/mL$), but has a significantly higher viral peak, (over twice, $1,648 virions/mL$ compared to $756 virions/mL$). Based on these results a compromise is needed, whereby therapy is administered for long enough to reduce viral load but contains sufficient treatment interruptions to make the regime practically viable. Thus a number of strategies are compared in the next section.

6.1.4 Overall STI regime comparison

The above investigation demonstrated that there is a clear need to balance on/off periods in order to reduce average and peak viral load while maintaining target cell levels and making meaningful cost savings. Based on this, a number of potential regimes were compared, with the results shown in Table. 6.1. As all regimes follow the weekly cycle, thus days off-therapy are consistent. As can be seen the average viral load remains consistent for like cost savings, but peak viral load increases with increasing time off therapy. Highlighted are two potential regimes which balance the trade off between cost and viral suppression, i.e. the 18/3 and 24/4 regimes.

The 18/3 and 24/4 regimes gives relatively low average viral load, ($120-118 virions/mL$), and relatively low peak load, ($285 - 338 virions/mL$), highlighted in Table. 6.1 and illustrated in *Fig. 6.3*. This allows a 14% reduction in overall cost of therapy while maintaining control of HIV replication. Although only a slightly better result than the similar 12/2 regimes, it allows extra time for ART to be cleared from the body. Furthermore, although average viral load is similar for other regimes, (30/5, 36/6 and 42/7), the increase in off-therapy period results in increasing viral peaks. Thus a 24/4 regime could be argued for, as it follows both a weekly and monthly cycle, while maintaining viral load. This regime also maintains target cell levels, necessary to allow the immune system to fight off opportunistic infections.

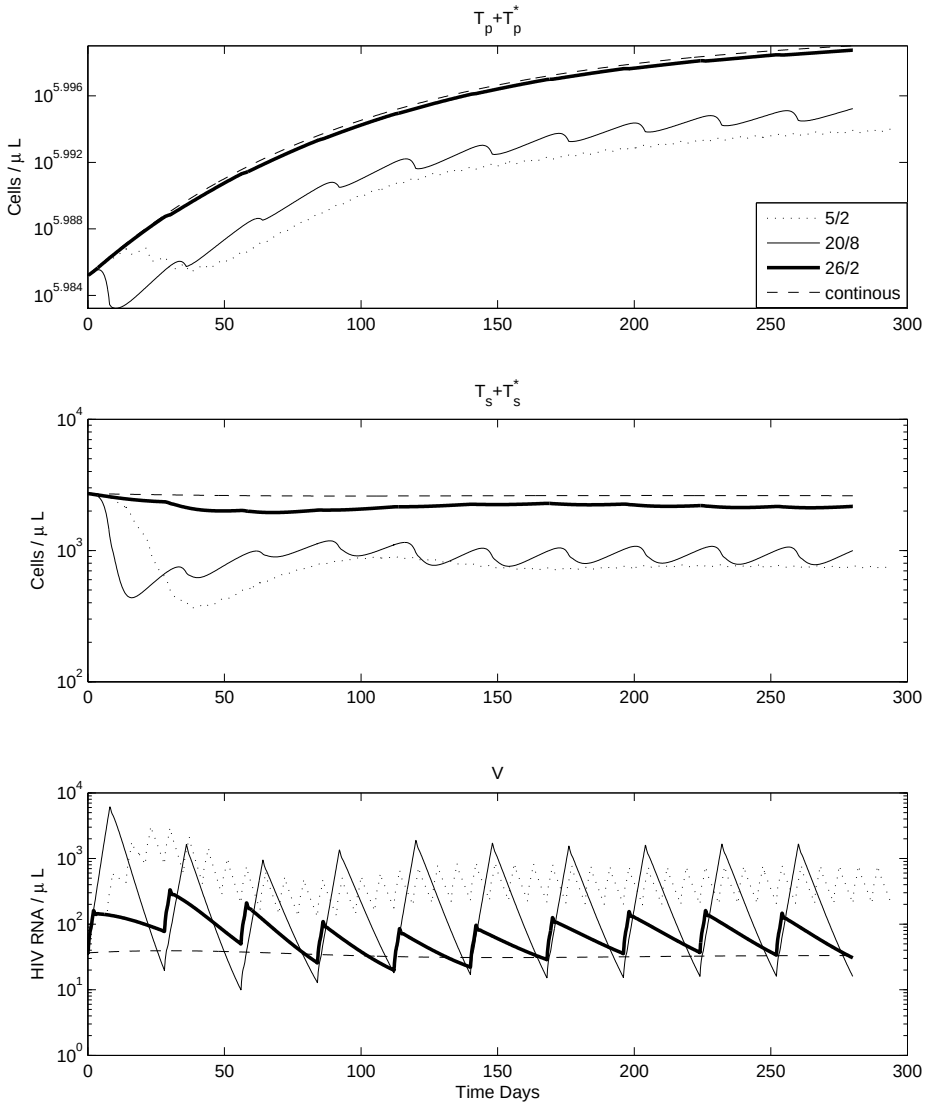

Figure 6.3: Comparison between 5/2, 20/8 and 26/2 STI using MTC-IR-ID-MVL model: This give a comparison between a number of potential STI; 5/2, a scaled up 5/2 to give 20d on and 8d off (20/8), and a 26d on and 2d off (26/2). The average viral loads are $437 virions/mL$, $352 virions/mL$ and $68 virions/mL$ respectively. The peak viral loads are $756 virions/mL$, $1,648 virions/mL$ and $141 virions/mL$ respectively.

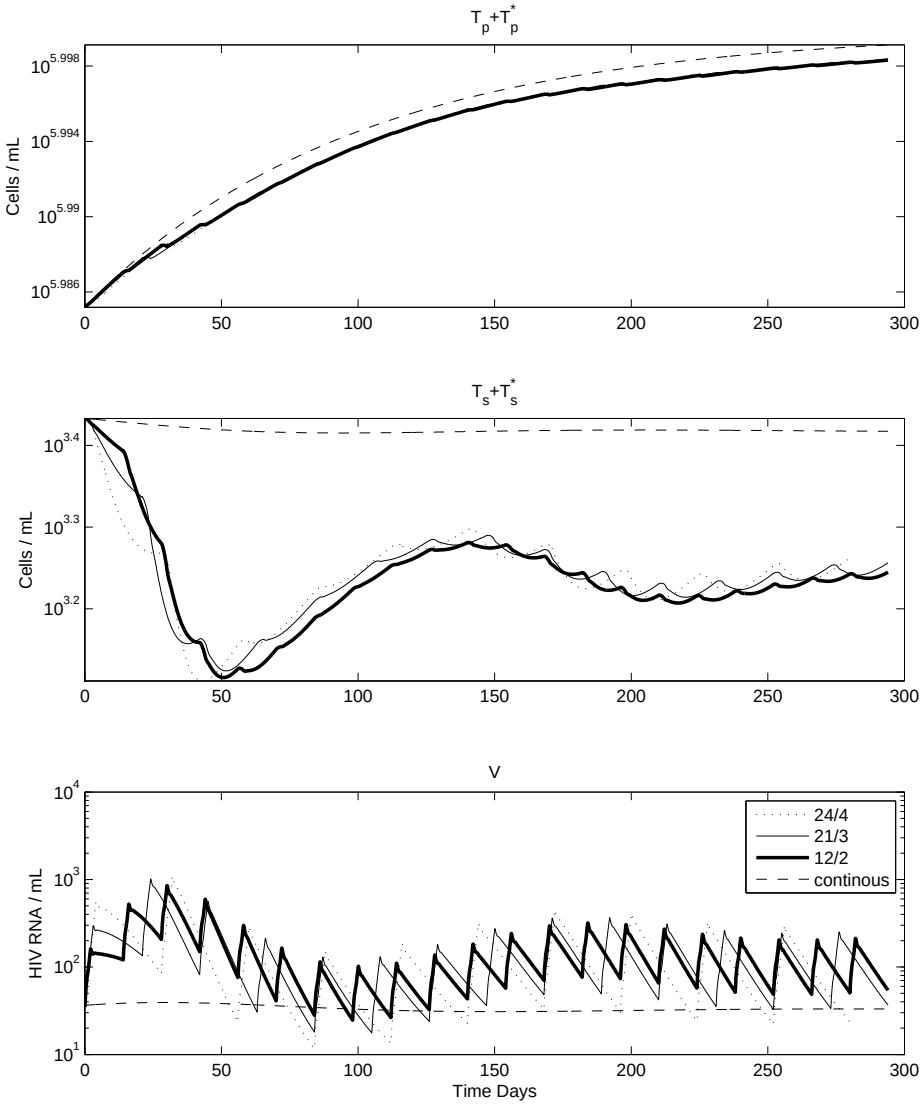

Figure 6.4: Suggested best practice overall STI regime 18/3: This demonstrated a potential best practice regime of 18 days on and 3 days off. The average viral load is $120 virions/mL$ with a peak of $285 virions/mL$. The potential cost savings are 17%.

Strategy on/off (days)	average viral load ($virions/mL$)	peak viral load ($virions/mL$)	% cost savings
5/2	437	756	29
12/2	126	320	14
11/3	209	623	21
19/2	86	171	10
18/3	**120**	**285**	**14**
17/4	168	465	19
16/5	235	751	24
26/2	70	138	7
25/3	92	218	11
24/4	**118**	**338**	**14**
23/5	151	507	18
22/6	201	743	21
21/7	558	1,086	25
30/5	114	408	14
36/6	121	495	14
42/7	117	610	14

Table 6.1: Comparison of STI regimes Potential STI regimes compared based on average viral load, peak viral load and cost savings. Highlighted are potential regimes which provide the best trade off between cost and suppression.

6.2 Summary of structured treatment interruptions

This chapter used the models developed, specifically the MTC-IR-ID-MVL model, to investigate current and potential STIs. It was highlighted how equal period of on/off therapy could not fully control HIV replication, as viral growth is generally faster than viral clearance, specifically from secondary target cells. Furthermore, a 6/1 ratio was suggested as best tradeoff between viral suppression and cost saving, thus for every 1 day off therapy 6 days of therapy was needed to reduce viral rebound. Based on this rationale, a 24/4 regime could be suggested, as it follows a monthly cycle, as a potential cost saving regime for resource limited areas. This 6/1 ratio can also be used where availability of therapy is not consistent, i.e. for every day missed 6 days of therapy should be administered to reduce viral load.

Chapter 7

Conclusions and future direction

This research focused on a set of deterministic models of within-host HIV progression. These include published ODE models, adapted to incorporate a more sophisticated set of disease features, thus producing a set of DDE models, which were then used to investigate STI. The stages in developing the final DDE model used for STI are summarised below. Limitations and potential improvements are then discussed, giving a direction for future research. This is followed by an overall conclusion.

7.1 Summary of findings

This research is based on a set of recognised ODE models, (STC, MTC-CI and MTC-IR), which are set in context and discussed in detail in Chapter 3. As these ODE models assume that once a cell becomes infected it immediately starts producing virions it is necessary to modify them to incorporate intracellular delay, as this is crucial when modelling therapy removal. Incorporating a fixed time of 24hrs between infection and production, the viral doubling-time in increased, from ≈ 1 day to ≈ 1.7 day, thus matching published estimates. It is also shown that viral half-life is relatively unaffected by inclusion of intracellular delay. When the two types of model are compared, (delay against no-delay), viral rebound is shown to be significantly slowed in the former case. This demonstrates that inclusion of intracellular delay is necessary when modelling therapy removal.

Another significant problem of original ODE models is unrealistically low viral load under drug induced viral suppression. Thus, a minimum low viral load is incorporated, (STC-ID-L, MTC-CI-ID-L and MTC-IR-ID-L), which allows for latently infected cells as they are unaffected by conventional therapy. The inclusion of these latent cells is necessary to maintain a consistent viral rebound and time to viral set-point. Combining this feature with intracellular delay produces a DDE models which can be used for both therapy introduction and removal, as is needed for investigation of treatment interruptions.

The complexity of models used to describe HIV progression has increased dramatically, over the last number of years, as additional features are incorporated. In the context of this research the original mid 1990's models, (STC models), have been modified dramatically, (MTC-CI and MTC-IR), leading to further complexity, due to inclusion of intracellular delay and latency. Dimensional analysis is introduced as method of retaining model tractability, under this increased model complexity. By using DA the key parameters of a specific model can be identified, thus reducing the parameter space. This allows potential adaptation of these general models to individual patients, not least for targeted therapy. As modelling of HIV progression develops, DA thus provides a relatively simple method of analysing individual parameters.

The culmination of this research is modelling treatment interruptions, using the DDE models developed in Chapter 4, (STC-ID-L, MTC-CI-ID-L and MTC-IR-ID-L). With increased access to therapy required, this becomes a important issue, as there is a need to better understand the dynamics of therapy removal. Specifically, in resource-limited regions continual access to therapy can not be guaranteed, e.g. due to limited drug availability, (comparable to that seen with TB treatment). A number of alternative potential treatment regimes are compared, using the MTC-IR-ID-L model, suggesting an interruption regime of 24/4, (i.e. 24 days on therapy and 4 days off). This regime could produce a cost saving of 14%, compared with continual therapy, without significantly affecting viral suppression. Furthermore, this suggests that when ART is limited, it is better to stop therapy for a period rather than reducing individual drug levels. This cessation reduces the potential to develop drug-resistant viral mutations, due to increased viral load coupled with selective pressure seen when reducing continual drug levels.

7.2 Future direction

The DDE models developed here are based on ODE models, which have been previously validated. The incorporation of intracellular delay is based on the biological time necessary to start producing virions and produces results consistent with known viral half-life and doubling-time. However, these DDE models need to be compared with individual patient data before the suggested regimes can be implemented. Furthermore, as the specific data needed to fully validate these models is only available under STI trials, which are tested under strict ethical conditions, suggested regimes would need to be modified as necessary. This, coupled with DA tailoring models to individuals could enable development of successful STI regimes in the future.

Outside of regime testing and validation, a number of improvements could be incorporated into these DDE models:

Distributed intracellular delay: Only a fixed intracellular delay has been incorporated to date, based on findings for STC models. However, these findings were mainly based on therapy introduction, which has been shown to be unaffected by intracellular delay, and investigation for a distributed delay should be considered.

Detailed immune response: Viral rebound is limited by the immune response fighting infection; this needs more detailed investigation [200, 204]. For example, the time needed to activate the adaptive immune response should also be accounted for.

Latent virus The level of latent virus needs to be incorporated in more detail, as this forms the basis from which viral rebound grows thus changing the time to reach viral set-point [129, 205].

Once the desired level of model accuracy has been validated a potential next step would be to optimise the treatment regimes proposed. This can be achieved using optimal control theory, which is based on a set of differential equations used to minimise a cost function based on a set of criteria using varying principles [206]. In this case the period on/off therapy is optimised based on the criteria of minimising viral load based on the limited treatment available. Furthermore, some aspects of this have been investigated previously, using different techniques, e.g. feedback control, open-loop control and model predictive control [207, 208, 209, 210, 183]. However, all these models lacked the inclusion of intracellular delay, which has been shown to decrease viral rebound, so their conclusions need to revisited.

7.3 Concluding remarks

In the current climate of limited funding the shortfall between those in need of HIV therapy and those receiving it requires new treatment strategies to be developed. This research investigates structured treatment interruptions as a potential means of achieving treatment cost reductions while maintaining successful care, particularly in resource limited regions. However, the past failures of long-term interruptions has meant new trials are not recommended and another method of analysis was required.

Over the course of the HIV/AIDS pandemic various mathematical models have been utilised to enhance our understanding. These models are generally developed to investigate specific aspects of disease progression, with some modelling techniques proving better suited to particular aspects than others. As such, the popularity of individual model types vary depending on investigation trends. The differential equation models at the core of this research are particulary suited to treatment interruptions, as they focus on cell counts and viral loads. While the widespread use of these ODE models peaked in the late 1990's they have maintained pace with new developments through numerous additions. However, further modifications have proven necessary to allow analysis of treatment interruptions; specifically, the inclusions of intracellular delay, which slows viral rebound, and latency, which provides a low level of viral load which therapy can not reach. Combined with the novel use of dimensional analysis, also presented here, a set of models, which could be used for both treatment events and relatively rapidly adapted to match individuals and situations, were developed.

Analysis of these treatment interruption models developed suggest therapy should only be removed for a period of days, from an initial regime of consistent undetectable viral load. This short interruption period indicates why longer-term interruption regimes have failed in the past and suggests potential future options to test, e.g. a 24 day-on and 4 day-off cycle. The combination of these initial regimes with dimensional analysis provide the potential to design more accurate treatment interruption schedules in the future, based on individual patient data. Furthermore, by utilising control theory techniques, these regimes could be refined further. This refinement is necessary as treatment interruption strategies are likely to grow in popularity, in order to meet increased therapy demand. Thus, it is hoped that ability of the DDE models developed, here to investigate treatment interruptions will provide a stimulus to this area of research.

Bibliography

[1] Centers for Disease Control and Prevention. *Diagnoses of HIV Infection and AIDS in the United States and Dependent Areas, 2009*. www.cdc.gov/hiv/surveillance/resources/reports/2009report/pdf/2009SurveillanceReport.pdf, accessed 24 November 2011, 2009.

[2] Health Service Executive. *HIV & AIDS in Ireland 2010*. www.drugsandalcohol.ie/15223/1/HPSC_HIV_AIDS_2010.pdf, accessed 24 November 2011, 2010.

[3] unicef. *South Africa Statistics*. www.unicef.org/infobycountry/southafrica_statistics.html, accessed 24 November 2011, 2011.

[4] C.W. Dieffenbach and A.S. Fauci. Thirty years of HIV and AIDS: Future challenges and opportunities. *Annals of Internal Medicine*, 154(11):766–771, 2011.

[5] M.S. Cohen, N. Hellmann, J.A. Levy, K. DeCock, and J. Lange. The spread, treatment, and prevention of HIV-1: evolution of a global pandemic. *The Journal of clinical investigation*, 118(4):1244–1254, 2008.

[6] UNAIDS. ***Global report: UNAIDS report on the global AIDS epidemic 2010***. www.unaids.org/globalreport/Global_report.htm, accessed 24 November 2011, 2010.

[7] Henry J. Kaiser Family Foundation. *Fact Sheet: The Global HIV/AIDS Epidemic*. www.kff.org/hivaids/upload/3030-15.pdf, accessed 24 November 2011, 2010.

[8] UNAIDS. *Global report: Fact Sheet: Sub-Saharan Africa*. www.unaids.org/documents/20101123_FS_SSA_em_en.pdf, accessed 24 November 2011, 2010.

[9] R. Hecht, L. Bollinger, J. Stover, W. McGreevey, F. Muhib, C.E. Madavo, and D. de Ferranti. Critical choices in financing the response to the global HIV/AIDS pandemic. *Health Affairs*, 28(6):15911605, 2009.

[10] E.M. Gardner, M.P. McLees, J.F. Steiner, C. del Rio, and W.J. Burman. The spectrum of engagement in HIV care and its relevance to test-and-treat strategies for prevention of HIV infection. *Clinical Infectious Diseases*, 52(6):793–800, 2011.

[11] M. Mahy, J. Stover, K. Stanecki, R. Stoneburner, and J.M. Tassie. Estimating the impact of antiretroviral therapy: regional and global estimates of life-years gained among adults. *Sexually Transmitted Infections*, 86(Suppl 2):ii67, 2010.

[12] UN. *The Millennium Development Goals Report 2010*. www.un.org/millenniumgoals/aids.shtml, accessed 24 November 2011, 2010.

[13] T.C. Quinn. HIV epidemiology and the effects of antiviral therapy on long-term consequences. *AIDS (London, England)*, 22(Suppl 3):S7, 2008.

[14] S. Moir, T.W. Chun, and A.S. Fauci. Pathogenic Mechanisms of HIV Disease. *Annual Review of Pathology: Mechanisms of Disease*, 6:223–248, 2011.

[15] J.B. Nachega, M.J. Mugavero, M. Zeier, M. Vitória, and J.E. Gallant. Treatment simplification in HIV-infected adults as a strategy to prevent toxicity, improve adherence, quality of life and decrease healthcare costs. *Patient Preference and Adherence*, 5:357, 2011.

[16] D.E. Bennett, R.J. Camacho, D. Otelea, D.R. Kuritzkes, H. Fleury, M. Kiuchi, W. Heneine, R. Kantor, M.R. Jordan, J.M. Schapiro, et al. Drug resistance mutations for surveillance of transmitted HIV-1 drug-resistance: 2009 update. *PLoS One*, 4(3):e4724, 2009.

[17] M. Callaghan, N. Ford, and H. Schneider. A systematic review of task-shifting for HIV treatment and care in Africa. *Human Resources for Health*, 8(1):8, 2010.

[18] MMWR. Pneumocystis Pneumonia - Los Angeles. *Morbidity and Mortality Weekly Report*, 5:30, 1981.

[19] Centers for Disease Control and Prevention. *Acquired Immunodeficiency Syndrome (AIDS) Weekly Surveillance Report - United States - 1983*. www.cdc.gov/hiv/topics/surveillance/resources/reports/pdf/surveillance82.pdf, accessed 24 November 2011, 1983.

[20] Henry J. Kaiser Family Foundation. *Fact Sheet: The HIV/AIDS Epidemic in the United States*. www.kff.org/hivaids/upload/3029-12.pdf, accessed 24 November 2011, 2011.

[21] UNAIDS. *Global report: Fact Sheet: North America, Western and Central Europe*. www.unaids.org/documents/20101123_FS_nawe_em_en.pdf, accessed 24 November 2011, 2010.

[22] D. Serwadda, NK Sewankambo, JW Carswell, AC Bayley, RS Tedder, RA Weiss, RD Mugerwa, A. Lwegaba, GB Kirya, RG Downing, et al. Slim disease: a new disease in Uganda and its association with HTLV-III infection. *The Lancet*, 326(8460):849–852, 1985.

[23] World Health Organization, United Nations Childrens Fund and UNAIDS. *Towards universal access: scaling up priority HIV/AIDS interventions in the health sector. Progress report 2010*. www.who.int/hiv/pub/2010progressreport/report/en/index.html, accessed 23 November 2011, 2010.

[24] E. De Clercq. Anti-HIV drugs: 25 compounds approved within 25 years after the discovery of HIV. *International Journal of Antimicrobial Agents*, 33(4):307–320, 2009.

[25] K.B. Hymes, T. Cheung, J.B. Greene, N.S. Prose, A. Marcus, H. Ballard, D.C. William, and L.J. Laubenstein. Kaposi's sarcoma in homosexual men-a report of eight cases. *The Lancet*, 318(8247):598–600, 1981.

[26] F. Barre-Sinoussi, J.C. Chermann, F. Rey, M.T. Nugeyre, S. Chamaret, J. Gruest, C. Dauguet, C. Axler-Blin, F. Vezinet-Brun, C. Rouzioux, et al. Isolation of a T-lymphotropic retrovirus from a patient at risk for acquired immune deficiency syndrome (AIDS). *Science*, 220(4599):868, 1983.

[27] S. Wain-Hobson, P. Sonigo, O. Danos, S. Cole, and M. Alizon. Nucleotide sequence of the AIDS virus, LAV. *Cell*, 40(1):9–17, 1985.

[28] M. Alizon, P. Sonigo, F. Barre-Sinoussi, J.C. Chermann, P. Tiollais, L. Montagnier, and S. Wain-Hobson. Molecular cloning of lymphadenopathy-associated virus. *Nature*, 312(5996):757–760, 1984.

[29] R.C. Gallo and L. Montagnier. The Discovery of HIV as the Cause of AIDS. *The New England Journal of Medicine*, 349(24):2283, 2003.

[30] A. Rambaut, D. Posada, K.A. Crandall, and E.C. Holmes. The causes and consequences of HIV evolution. *Nature Reviews Genetics*, 5(1):52–61, 2004.

[31] B. Korber, M. Muldoon, J. Theiler, F. Gao, R. Gupta, A. Lapedes, BH Hahn, S. Wolinsky, and T. Bhattacharya. Timing the ancestor of the HIV-1 pandemic strains. *Science*, 288(5472):1789–1796, 2000.

[32] T. Zhu, B.T. Korber, A.J. Nahmias, E. Hooper, P.M. Sharp, and D.D. Ho. An African HIV-1 sequence from 1959 and implications for the origin of the epidemic. *Nature*, 391(6667):594–7, 1998.

[33] T.I. de Silva, M. Cotten, and S.L. Rowland-Jones. HIV-2: the forgotten AIDS virus. *Trends in Microbiology*, 16(12):588–595, 2008.

[34] M.F. Schim van der Loeff, S. Jaffar, A.A. Aveika, S. Sabally, T. Corrah, E. Harding, A. Alabi, A. Bayang, K. Ariyoshi, and H.C. Whittle. Mortality of HIV-1, HIV-2 and HIV-1/HIV-2 dually infected patients in a clinic-based cohort in The Gambia. *AIDS*, 16(13):1775, 2002.

[35] G.S. Gottlieb, P.S. Sow, S.E. Hawes, I. Ndoye, M. Redman, A.M. Coll-Seck, M.A. Faye-Niang, A. Diop, J.M. Kuypers, C.W. Critchlow, et al. Equal Plasma Viral Loads Predict a Similar Rate of CD4 T Cell Decline in Human Immunodeficiency Virus (HIV) Type 1-and HIV-2-Infected Individuals from Senegal, West Africa. *Journal of Infectious Diseases*, 185(7):905, 2002.

[36] A.J. Kandathil, S. Ramalingam, R. Kannangai, S. David, and G. Sridharan. Molecular epidemiology of HIV. *Indian Journal of Medical Research*, 121(4):333–344, 2005.

[37] A.P. Galvani and J. Novembre. The evolutionary history of the CCR5-D32 HIV-resistance mutation. *Microbes and Infection*, 7:302–309, 2005.

[38] J.W. Sleasman and M.M. Goodenow. HIV-1 infection. *Journal of Allergy and Clinical Immunology*, 111:582–592, 2003.

[39] P.N. Fultz, H.M. McClure, D.C. Anderson, R.B. Swenson, R. Anand, and A. Srinivasan. Isolation of a T-Lymphotropic Retrovirus from Naturally Infected Sooty Mangabey Monkeys (Cercocebus atys). *Proceedings of the National Academy of Sciences*, 83(14):5286–5290, 1986.

[40] M. Essex and P.J. Kanki. The origins of the AIDS virus. *Scientific America*, 259(4):64–71, 1988.

[41] D.C. Douek, M. Roederer, and R.A. Koup. Emerging concepts in the immunopathogenesis of AIDS. *Annual Review of Medicine*, 60:471, 2009.

[42] HIV Medicine. *HIV Medicine 2007*. `http://hivmedicine.com/textbook.htm`, accessed 23 November 2011, 2007.

[43] A.M. Ortiz and G. Silvestri. Immunopathogenesis of AIDS. *Current Infectious Disease Reports*, 11(3):239–245, 2009.

[44] D.L. Sodora and G. Silvestri. Immune activation and AIDS pathogenesis. *AIDS*, 22(4):439, 2008.

[45] Z. Grossman, M. Meier-Schellersheim, W.E. Paul, and L.J. Picker. Pathogenesis of HIV infection: what the virus spares is as important as what it destroys. *Nature Medicine*, 12(3):289–295, 2006.

[46] P.D. McCormack, J. Thomas, M. Malik, and C.M. Staschen. Cold stress, reverse T3 and lymphocyte function. *Alaska Medicine*, 40(3):55, 1998.

[47] S. Langford, J. Ananworanich, and D. Cooper. Predictors of disease progression in HIV infection: a review. *AIDS Research and Therapy*, 4(1):11, 2007.

[48] S.G. Deeks and A.N. Phillips. Clinical Review: HIV infection, antiretroviral treatment, ageing, and non-AIDS related morbidity. *British Medical Journal*, 338:a3172, 2009.

[49] T.H. Mogensen, J. Melchjorsen, C.S. Larsen, and S.R. Paludan. Innate immune recognition and activation during HIV infection. *Retrovirology*, 7(1):54, 2010.

[50] R. Lachmann. Herpes simplex virus latency. *Expert Reviews in Molecular Medicine*, 5(29):1–14, 2003.

[51] L. Corey, A. Wald, C.L. Celum, and T.C. Quinn. The effects of herpes simplex virus-2 on HIV-1 acquisition and transmission: a review of two overlapping epidemics. *JAIDS Journal of Acquired Immune Deficiency Syndromes*, 35(5):435, 2004.

[52] D.D. Ho, A.U. Neumann, A.S. Perelson, W. Chen, J.M. Leonard, and M. Markowitz. **Rapid turnover of plasma virions and CD4 lymphocytes in HIV-1 infection**. *Nature*, 373:123–126, 1995.

[53] X. Wei, S.K. Ghosh, M.E. Taylor, V.A. Johnson, E.A. Emini, P. Deutsch, J.D. Lifson, S. Bonhoeffer, M.A. Nowak, B.H. Hahn, et al. Viral dynamics in human immunodeficiency virus type 1 infection. *Nature*, 373:117–122, 1995.

[54] R.F. Siliciano and W.C. Greene. HIV Latency. *Cold Spring Harbor Perspectives in Medicine*, 1(1), 2011.

[55] D.M. Margolis. Mechanisms of HIV latency: an emerging picture of complexity. *Current HIV/AIDS Reports*, 7(1):37–43, 2010.

[56] NP Pai, J. Lawrence, AL Reingold, and JP Tulsky. Structured treatment interruptions (sti) in chronic unsuppressed hiv infection in adults (cochrane review). *The Cochrane Database of Systematic Reviews*, 3:CD006148.

[57] S. Attia, M. Egger, M. Müller, M. Zwahlen, and N. Low. Sexual transmission of HIV according to viral load and antiretroviral therapy: systematic review and meta-analysis. *AIDS*, 23(11):1397, 2009.

[58] D.N. Burns, C.W. Dieffenbach, and S.H. Vermund. Rethinking prevention of HIV type 1 infection. *Clinical Infectious Diseases*, 51(6):725, 2010.

[59] K. Buchacz, R.K. Baker, F.J. Palella Jr, J.S. Chmiel, K.A. Lichtenstein, R.M. Novak, K.C. Wood, J.T. Brooks, et al. AIDS-defining opportunistic illnesses in US patients, 1994-2007: a cohort study. *AIDS*, 24(10):1549, 2010.

[60] K.K. Arien, V. Jespers, and G. Vanham. HIV sexual transmission and microbicides. *Reviews in Medical Virology*, 21(2):110–133, 2011.

[61] T.D. Mastro and I. De Vincenzi. Probabilities of sexual HIV-1 transmission. *Aids*, 10:S75, 1996.

[62] A.S. Perelson and P.W. Nelson. **Mathematical analysis of HIV-1 dynamics in vivo**. *SIAM Review*, 41(1):3–44, 1999.

[63] L. Waters, L. John, and M. Nelson. Non-nucleoside reverse transcriptase inhibitors: a review. *International Journal of Clinical Practice*, 61(1):105–118, 2007.

[64] H. Minkoff. Human Immunodeficiency Virus Infection in Pregnancy. *Obstetrics & Gynecology*, 101(4):797–810, 2003.

[65] S. Sierra, B. Kupfer, and R. Kaiser. Basics of the virology of HIV-1 and its replication. *Journal of Clinical Virology*, 34(4):233–244, 2005.

[66] C.M. Coleman and L. Wu. HIV interactions with monocytes and dendritic cells: viral latency and reservoirs. *Retrovirology*, 6(1):51, 2009.

[67] P.J. Norris and E.S. Rosenberg. CD4+ T helper cells and the role they play in viral control. *Journal of Molecular Medicine*, 80(7):397–405, 2002.

[68] Y. Belkaid and B.T. Rouse. Natural regulatory T cells in infectious disease. *Nature immunology*, 6(4):353–360, 2005.

[69] P. Benaroch, E. Billard, R. Gaudin, M. Schindler, and M. Jouve. HIV-1 assembly in macrophages. *Retrovirology*, 7(1):1–10, 2010.

[70] L. Wu and V.N. KewalRamani. Dendritic-cell interactions with HIV: infection and viral dissemination. *Nature Reviews Immunology*, 6(11):859–868, 2006.

[71] E. Hunter and R. Swanstrom. Retrovirus envelope glycoproteins. *Current Topics in Microbiology and Immunology*, 157:187–253, 1990.

[72] H.T. Banks, D.M. Bortz, and S.E. Holte. Incorporation of variability into the modeling of viral delays in HIV infection dynamics. *Mathematical Biosciences*, 183(1):63–91, 2003.

[73] R.V. Culshaw and S. Ruan. A delay-differential equation model of HIV infection of CD4 T-cells. *Mathematical Biosciences*, 165:27–39, 2000.

[74] D.M. Bortz and P.W. Nelson. **Sensitivity analysis of a nonlinear lumped parameter model of HIV infection dynamics**. *Bulletin of Mathematical Biology*, 66(5):1009–1026, 2004.

[75] H.T. Banks and D.M. Bortz. **A parameter sensitivity methodology in the context of HIV delay equation models**. *Journal of Mathematical Biology*, 50(6):607–625, 2005.

[76] J.E. Mittler, B. Sulzer, A.U. Neumann, and A.S. Perelson. **Influence of delayed viral production on viral dynamics in HIV-1 infected patients**. *Mathematical Biosciences*, 152(2):143–163, 1998.

[77] P.W. Nelson and A.S. Perelson. Mathematical analysis of delay differential equation models of HIV-1 infection. *Mathematical Biosciences*, 179(1):73–94, 2002.

[78] P.W. Nelson, J.D. Murray, and A.S. Perelson. A model of HIV-1 pathogenesis that includes an intracellular delay. *Mathematical Biosciences*, 163(2):201–215, 2000.

[79] A. Marcello. Latency: the hidden HIV-1 challenge. *Retrovirology*, 3(1):7, 2006.

[80] M. Coiras, M.R. López-Huertas, M. Pérez-Olmeda, and J. Alcamí. Understanding HIV-1 latency provides clues for the eradication of long-term reservoirs. *Nature Reviews Microbiology*, 7(11):798–812, 2009.

[81] A.S. Perelson, A.U. Neumann, M. Markowitz, J.M. Leonard, and D.D. Ho. **HIV-1 dynamics in vivo: virion clearance rate, infected cell life-span, and viral generation time**. *Science*, 271(5255):1582–6, 1996.

[82] J. Komano, Y. Futahashi, E. Urano, K. Miyauchi, T. Murakami, Z. Matsuda, and N. Yamamoto. The interaction of HIV-1 with the host factors. *Japanese journal of Infectious Diseases*, 58(3):125, 2005.

[83] P.A. Chan and R. Kantor. Transmitted drug resistance in nonsubtype B HIV-1 infection. *HIV Therapy*, 3(5):447–465, 2009.

[84] SM Blower, AN Aschenbach, HB Gershengorn, and JO Kahn. Predicting the unpredictable: Transmission of drug-resistant HIV. *Nature Medicine*, 7(9):1016–1020, 2001.

[85] B. Taiwo, R.L. Murphy, and C. Katlama. Novel antiretroviral combinations in treatment-experienced patients with HIV infection: rationale and results. *Drugs*, 70(13):1629–1642, 2010.

[86] S.M. Hammer, J.J. Eron, P. Reiss, R.T. Schooley, M.A. Thompson, S. Walmsley, P. Cahn, M.A. Fischl, J.M. Gatell, M.S. Hirsch, et al. Antiretroviral treatment of adult HIV infection. *JAMA: the journal of the American Medical Association*, 300(5):555, 2008.

[87] Centers for Disease Control and Prevention. Revised surveillance case definitions for HIV infection among adults, adolescents, and children aged< 18 months and for HIV infection and AIDS among children aged 18 months to< 13 years-United States, 2008. *MMWR Recommendations and Reports*, 57(RR-10):1–12, 2008.

[88] World Health Organization. *WHO case definitions of HIV for surveillance and revised clinical staging and immunological classification of HIV-related disease in adults and children*. `www.who.int/hiv/pub/guidelines/hivstaging/en/index.html`, accessed 24 November 2011, 2007.

[89] Y. Pommier, A.A. Johnson, and C. Marchand. Integrase inhibitors to treat HIV/AIDS. *Nature Reviews Drug Discovery*, 4(3):236–248, 2005.

[90] Y. El Safadi, V. Vivet-Boudou, and R. Marquet. HIV-1 reverse transcriptase inhibitors. *Applied Microbiology and Biotechnology*, 75(4):723–737, 2007.

[91] T. Cihlar and A.S. Ray. Nucleoside and nucleotide HIV reverse transcriptase inhibitors: 25 years after zidovudine. *Antiviral Research*, 85(1):39–58, 2010.

[92] M.P. de Béthune. Non-nucleoside reverse transcriptase inhibitors (NNRTIs), their discovery, development, and use in the treatment of HIV-1 infection: a review of the last 20 years (1989-2009). *Antiviral Research*, 85(1):75–90, 2010.

[93] J.J. Eron. HIV-1 protease inhibitors. *Clinical Infectious Diseases*, 30(Supplement 2):S160, 2000.

[94] Concorde Coordinating Committee. Concorde: MRC/ANRS randomised double-blind controlled trial of immediate and deferred zidovudine in symptom-free HIV infection. *Lancet*, 343:871–81, 1994.

[95] L.M. Mofenson. Protecting the next generationeliminating perinatal HIV-1 infection. *New England Journal of Medicine*, 362(24):2316–2318, 2010.

[96] P.A. Volberding, S.W. Lagakos, MA Koch, C. Pettinelli, MW Myers, DK Booth, HH Balfour Jr, RC Reichman, JA Bartlett, and MS Hirsch. Zidovudine in asymptomatic human immunodeficiency virus infection. A controlled trial in persons with fewer than 500 CD4-positive cells per cubic millimeter. The AIDS Clinical Trials

Group of the National Institute of Allergy and Infectious Diseases. *The New England Journal of Medicine*, 322(14):941, 1990.

[97] M.A. Fischl, C.B. Parker, C. Pettinelli, M. Wulfsohn, M.S. Hirsch, A.C. Collier, D. Antoniskis, M. Ho, D.D. Richman, and E. Fuchs. A randomized controlled trial of a reduced daily dose of zidovudine in patients with the acquired immunodeficiency syndrome. The AIDS Clinical Trials Group. *The New England Journal of Medicine*, 323(15):1009, 1990.

[98] O. Kirk, A. Mocroft, T.L. Katzenstein, A. Lazzarin, F. Antunes, P. Francioli, R.P. Brettle, J.M. Parkin, J. Gonzales-Lahoz, and J.D. Lundgren. Changes in use of antiretroviral therapy in regions of Europe over time. *AIDS*, 12(15):2031, 1998.

[99] A. Mocroft, C. Katlama, AM Johnson, C. Pradier, F. Antunes, F. Mulcahy, A. Chiesi, A.N. Phillips, O. Kirk, J.D. Lundgren, et al. AIDS across Europe, 1994-98: the EuroSIDA study. *The Lancet*, 356(9226):291–296, 2000.

[100] R. Luo, M.J. Piovoso, J. Martinez-Picado, and R. Zurakowski. Optimal Antiviral Switching to Minimize Resistance Risk in HIV Therapy. *PLoS ONE*, 6(11):e27047, 2011.

[101] BM Baker, BL Block, AC Rothchild, and BD Walker. Elite control of HIV infection: implications for vaccine design. *Expert Opinion on Biological Therapy*, 9(1):55, 2009.

[102] S. Broder and R.C. Gallo. A pathogenic retrovirus (HTLV-III) linked to AIDS. *The New England Journal of Medicine*, 311(20):1292, 1984.

[103] R.C. Gallo, S.Z. Salahuddin, M. Popovic, G.M. Shearer, M. Kaplan, B.F. Haynes, T.J. Palker, R. Redfield, J. Oleske, B. Safai, et al. Frequent detection and isolation of cytopathic retroviruses (HTLV-III) from patients with AIDS and at risk for AIDS. *Science*, 224(4648):500, 1984.

[104] E. Benfenati, G. Gini, S. Hoffmann, and R. Luttik. Comparing in vivo, in vitro and in silico methods and integrated strategies for chemical assessment: problems and prospects. *ATLA*, 38:153–66, 2010.

[105] V. Isham. Mathematical modelling of the transmission dynamics of HIV infection and AIDS: a review. *Journal of the Royal Statistical Society. Series A (Statistics in Society)*, pages 5–49, 1988.

[106] D. Kirschner. Using Mathematics to Understand HIV Immune Dynamics. *AMS Notices*, 43(2):191–202, 1996.

[107] A.S. Perelson. Modelling viral and immune system dynamics. *Nature Reviews Immunology*, 2(1):28–36, 2002.

[108] D. Wodarz and M.A. Nowak. Mathematical models of HIV pathogenesis and treatment. *BioEssays*, 24(12):1178–1187, 2002.

[109] R.V. Culshaw. Review of HIV models: The role of the natural immune response and implications for treatment. *Journal of Biological Systems*, 12(2):123–136, 2004.

[110] C.A. Stoddart and R.A. Reyes. Models of HIV-1 disease: A review of current status. *Drug Discovery Today: Disease Models*, 3(1):113–119, 2006.

[111] D.D. Richman, D.M. Margolis, M. Delaney, W.C. Greene, D. Hazuda, and R.J. Pomerantz. The challenge of finding a cure for HIV infection. *Science*, 323(5919):1304, 2009.

[112] WM El-Sadr, J.D. Lundgren, JD Neaton, F. Gordin, D. Abrams, RC Arduino, A. Babiker, W. Burman, N. Clumeck, CJ Cohen, et al. **CD4+ count-guided interruption of antiretroviral treatment**. *New England journal of Medicine*, 355(22):2283–2296, 2006.

[113] M. Holodniy, S.T. Brown, D.W. Cameron, T.C. Kyriakides, B. Angus, A. Babiker, J. Singer, D.K. Owens, A. Anis, R. Goodall, et al. Results of Antiretroviral Treatment Interruption and Intensification in Advanced Multi-Drug Resistant HIV Infection from the OPTIMA Trial. *PloS one*, 6(3):e14764, 2011.

[114] J.N. Krieger. Male circumcision and HIV infection risk. *World Journal of Urology*, pages 1–11, 2011.

[115] H.A. Weiss, S.L. Thomas, S.K. Munabi, and R.J. Hayes. Male circumcision and risk of syphilis, chancroid, and genital herpes: a systematic review and meta-analysis. *Sexually transmitted infections*, 82(2):101, 2006.

[116] R.A. Brooks, M. Etzel, L.E. Klosinski, A.A. Leibowitz, S. Sawires, G. Szekeres, M. Weston, and T.J. Coates. Male circumcision and HIV prevention: looking to the future. *AIDS and Behavior*, 14(5):1203–1206, 2010.

[117] N.L. Letvin. Progress Toward An HIV Vaccine. *Annual Review of Medicine*, 56(1):213–223, 2005.

[118] M.P. Girard, S. Osmanov, O.M. Assossou, and M.P. Kieny. Human immunodeficiency virus(HIV) immunopathogenesis and vaccine development: A review. *Vaccine*, 29(37):6191–6218, 2011.

[119] D.M. Brainard, E. Seung, N. Frahm, A. Cariappa, C.C. Bailey, W.K. Hart, H.S. Shin, S.F. Brooks, H.L. Knight, Q. Eichbaum, et al. Induction of robust cellular and humoral virus-specific adaptive immune responses in human immunodeficiency virus-infected humanized BLT mice. *Journal of Virology*, 83(14):7305, 2009.

[120] C. Münk, J. Zielonka, H. Constabel, B.P. Kloke, B. Rengstl, M. Battenberg, F. Bonci, M. Pistello, M. Löchelt, and K. Cichutek. Multiple restrictions of human immunodeficiency virus type 1 in feline cells. *Journal of Virology*, 81(13):7048–7060, 2007.

[121] S.P. O'Neil, F.J. Novembre, A.B. Hill, C. Suwyn, C.E. Hart, T. Evans-Strickfaden, D.C. Anderson, J. deRosayro, J.G. Herndon, M. Saucier, et al. Progressive Infection in a Subset of HIV-1Positive Chimpanzees. *Journal of Infectious Diseases*, 182(4):1051, 2000.

[122] A.R. Rodriguez, B.P. Arulanandam, V.L. Hodara, H.M. McClure, E.K. Cobb, M.T. Salas, R. White, and K.K. Murthy. Influence of interleukin-15 on CD8+ natural killer cells in human immunodeficiency virus type 1-infected chimpanzees. *Journal of general virology*, 88(2):641, 2007.

[123] A. Marini, J.M. Harper, and F. Romerio. An in vitro system to model the establishment and reactivation of HIV-1 latency. *The Journal of Immunology*, 181(11):7713, 2008.

[124] N. Bellomo, C. Bianca, and M. Delitala. Complexity analysis and mathematical tools towards the modelling of living systems. *Physics of Life Reviews*, 6(3):144–175, 2009.

[125] J.D. Murray. *Mathematical Biology I*. Springer, 2002.

[126] F.J. Bruggeman and H.V. Westerhoff. The nature of systems biology. *Trends in Microbiology*, 15(1):45–50, 2007.

[127] C.J. Tomlin and J.D. Axelrod. Biology by numbers: mathematical modelling in developmental biology. *Nature Reviews Genetics*, 8(5):331–340, 2007.

[128] B.M. Adams, H.T. Banks, M. Davidian, H.D. Kwon, H.T. Tran, S.N. Wynne, and E.S. Rosenberg. **HIV dynamics: Modeling, data analysis, and optimal treatment protocols**. *Journal of Computational and Applied Mathematics*, 184(1):10–49, 2005.

[129] D.S. Callaway and A.S. Perelson. **HIV-1 infection and low steady state viral loads**. *Bulletin of Mathematical Biology*, 64(1):29–4, 2002.

[130] D. Perrin, H.J. Ruskin, J. Burns, and M. Crane. An agent-based approach to immune modelling. *Computational Science and Its Applications-ICCSA 2006*, pages 612–621, 2006.

[131] B. Larder, D. Wang, A. Revell, J. Montaner, R. Harrigan, F. De Wolf, J. Lange, S. Wegner, L. Ruiz, M.J. Pérez-Elías, et al. The development of artificial neural networks to predict virological response to combination HIV therapy. *Antiviral Therapy*, 12(1):15, 2007.

[132] H. Miao, X. Xia, A.S. Perelson, and H. Wu. On identifiability of nonlinear ODE models and applications in viral dynamics. *SIAM review. Society for Industrial and Applied Mathematics*, 53(1):3, 2011.

[133] R.M. Merrill. *Introduction to epidemiology*. Jones & Bartlett Learning, 2009.

[134] R.V. Culshaw. Mathematical modeling of AIDS progression: limitations, expectations, and future directions. *Journal of American Physicians and Surgeons*, 11(4):101, 2006.

[135] R.M. Anderson. The Epidemiology of HIV Infection: Variable Incubation Plus Infectious Periods and Heterogeneity in Sexual Activity. *Journal of the Royal Statistical Society. Series A (Statistics in Society)*, 151(1):66–98, 1988.

[136] R.M. Anderson and R.M.C. May. *Infectious Diseases of Humans: Dynamics and Control*. Oxford University Press, 1991.

[137] O. Diekmann and J. Heesterbeek. *Mathematical Epidemiology of Infectious Diseases: model building, analysis and interpretation*. John Wiley & Son, 2000.

[138] H. Inaba. Mathematical analysis of an age-structured SIR epidemic model with vertical transmission. *Discrete and Continuous Dynamical Systems-Series B (DCDS-B)*, 6:69–96, 2006.

[139] R. Naresh, A. Tripathi, and S. Omar. Modelling the spread of AIDS epidemic with vertical transmission. *Applied mathematics and computation*, 178(2):262–272, 2006.

[140] M.J. Keeling and K.T.D. Eames. Review. Networks and epidemic models. *Journal of The Royal Society Interface*, 2(4):295–307, 2005.

[141] T. Brown, L. Bao, A.E. Raftery, J.A. Salomon, R.F. Baggaley, J. Stover, and P. Gerland. Modelling HIV epidemics in the antiretroviral era: the UNAIDS estimation and projection package 2009. *Sexually Transmitted Infections*, 86(Suppl 2):ii3, 2010.

[142] UNAIDS. *Epidemiological software and tools*. `www.unaids.org/en/dataanalysis/tools/`, accessed 24 November 2011, 2011.

[143] R.M. Zorzenon dos Santos and S. Coutinho. Dynamics of HIV Infection: A Cellular Automata Approach. *Physical Review Letters*, 87(16):168102, 2001.

[144] W.Y. Tan and H. Wu. Stochastic modeling of the dynamics of CD4+ T-cell infection by HIV and some Monte Carlo studies. *Mathematical Biosciences*, 147(2):173–205, 1998.

[145] H.C. Tuckwell and E. Le Corfec. A stochastic model for early HIV-1 population dynamics. *Journal of Theoretical Biology*, 195:450, 1998.

[146] R.B. Pandey, R. Mannion, and H.J. Ruskin. Effect of cellular mobility on immune response. *Physica A: Statistical Mechanics and its Applications*, 283(3-4):447–450, 2000.

[147] M. Bernaschi and F. Castiglione. Design and implementation of an immune system simulator. *Computers in Biology and Medicine*, 31(5):303–331, 2001.

[148] H.J. Ruskin, R.B. Pandey, and Y. Liu. Viral load and stochastic mutation in a Monte Carlo simulation of HIV. *Physica A: Statistical Mechanics and its Applications*, 311(1-2):213–220, 2002.

[149] M. Bernaschi and F. Castiglione. Selection of escape mutants from immune recognition during HIV infection. *Immunology and Cell Biology*, 80:307–313, 2002.

[150] D. Hecquet, H.J. Ruskin, and M. Crane. Optimisation and parallelisation strategies for Monte Carlo simulation of HIV infection. *Computers in Biology and Medicine*, 37(5):691–699, 2007.

[151] A. Kemper. Modeling network growth with network theory and cellular automata. *Journal of Modelling in Management*, 1(1):75–84, 2006.

[152] BM Adams, HT Banks, M. Davidian, and ES Rosenberg. Estimation and prediction with HIV-treatment interruption data. *Bulletin of Mathematical Biology*, 69(2):563–584, 2007.

[153] P.W. Bridgman. ***Dimensional Analysis***. Yale University Press, 1922.

[154] G. Astarita. Dimensional analysis, scaling, and orders of magnitude. *Chemical Engineering Science*, 52(24):4681–4698, 1997.

[155] A.S. Perelson, P. Essunger, Y. Cao, M. Vesanen, A. Hurley, K. Saksela, M. Markowitz, and D.D. Ho. Decay characteristics of HIV-1-infected compartments during combination therapy. *Nature*, 387(6629):188–191, 1997.

[156] A.V.M. Herz, S. Bonhoeffer, R.M. Anderson, R.M. May, and M.A. Nowak. Viral dynamics in vivo: Limitations on estimates of intracellular delay and virus decay. *Proceedings of the National Academy of Sciences*, 93(14):7247–7251, 1996.

[157] M.G. Pellegrino, G. Li, M.J. Potash, and D.J. Volsky. Contribution of multiple rounds of viral entry and reverse transcription to expression of human immunodeficiency virus type 1. A quantitative kinetic study. *Journal of Biological Chemistry*, 266(3):1783–1788, 1991.

[158] G. Pantaleo, C. Graziosi, L. Butini, P.A. Pizzo, S.M. Schnittman, D.P. Kotler, and A.S. Fauci. Lymphoid Organs Function as Major Reservoirs for Human Immunodeficiency Virus. *Proceedings of the National Academy of Sciences*, 88(21):9838–9842, 1991.

[159] D.S. Dimitrov, R.L. Willey, H. Sato, L.J. Chang, R. Blumenthal, and M.A. Martin. Quantitation of human immunodeficiency virus type 1 infection kinetics. *Journal of Virology*, 67(4):2182–2190, 1993.

[160] G. Reibnegger, D. Fuchs, A. Hausen, E.R. Werner, M.P. Dierich, and H. Wachter. Theoretical Implications of Cellular Immune Reactions against Helper Lymphocytes Infected by an Immune System Retrovirus. *Proceedings of the National Academy of Sciences*, 84(20):7270–7274, 1987.

[161] A.S. Perelson, D.E. Kirschner, and R. De Boer. Dynamics of HIV infection of CD4+ T cells. *Mathematical Biosciences*, 114(1):81–125, 1993.

[162] P. Essunger and A.S. Perelson. Modeling HIV infection of CD4+ T-cell subpopulations. *Journal of Theoretical Biology*, 170(4):367–91, 1994.

[163] M.A. Nowak, R.M. May, and R.M. Anderson. The evolutionary dynamics of HIV-1 quasispecies and the development of immunodeficiency disease. *AIDS*, 4(11):1095–103, 1990.

[164] M.A. Nowak, R.M. Anderson, A.R. McLean, T.F. Wolfs, J. Goudsmit, and R.M. May. Antigenic diversity thresholds and the development of AIDS. *Science*, 254(5034):963, 1991.

[165] M. Nowak. The evolution of viruses. Competition between horizontal and vertical transmission of mobile genes. *Journal of Theoretical Biology*, 150(3):339–47, 1991.

[166] M.A. Nowak and R.M. May. Mathematical biology of HIV infections: Antigenic variation and diversity threshold. *Mathematical Bioscience*, 106(1):1–21, 1991.

[167] M.A. Nowak, R.M. May, R.E. Phillips, S. Rowland-Jones, D.G. Lalloo, S. McAdam, P. Klenerman, B. Koeppe, K. Sigmund, and C.R.M. Bangham. Antigenic oscillations and shifting immunodominance in HIV-1 infections. *Nature*, 375(6532):606–611, 1995.

[168] M.A. Nowak. AIDS pathogenesis: from models to viral dynamics in patients. *Journal of Acquired Immune Deficiency Syndromes and Human Retrovirology*, 10(1):S1–5, 1995.

[169] R.M. Berry and M.A. Nowak. Defective escape mutants of HIV. *Journal of Theoretical Biology*, 171(4):387–95, 1994.

[170] M. Piatak Jr, M.S. Saag, L.C. Yang, S.J. Clark, J.C. Kappes, K.C. Luk, B.H. Hahn, G.M. Shaw, and J.D. Lifson. High levels of HIV-1 in plasma during all stages of infection determined by competitive PCR. *Science*, 259(5102):1749–1754, 1993.

[171] J. Mulder, N. McKinney, C. Christopherson, J. Sninsky, L. Greenfield, and S. Kwok. Rapid and simple PCR assay for quantitation of human immunodeficiency virus type 1 RNA in plasma: application to acute retroviral infection. *Journal of Clinical Microbiology*, 32(2):292–300, 1994.

[172] J.M. Coffin et al. HIV population dynamics in vivo: implications for genetic variation, pathogenesis, and therapy. *Science*, 267(5197):483–489, 1995.

[173] M.A. Nowak, R.M. Anderson, M.C. Boerlijst, S. Bonhoeffer, R.M. May, and A.J. McMichael. HIV-1 evolution and disease progression. *Science*, 274(5289):1008–11, 1996.

[174] M.A. Nowak, S. Bonhoeffer, G.M. Shaw, and R.M. May. Anti-viral drug treatment: dynamics of resistance in free virus and infected cell populations. *Journal of Theoretical Biology*, 184:203–217, 1997.

[175] S. Bonhoeffer, J.M. Coffin, and M.A. Nowak. Human immunodeficiency virus drug therapy and virus load. *Journal of Virology*, 71(4):3275–3278, 1997.

[176] S. Bonhoeffer, R.M. May, G.M. Shaw, and M.A. Nowak. Virus dynamics and drug therapy. *Proceedings of the National Academy of Sciences*, 94(13):6971–6976, 1997.

[177] P.J.R. Goulder, R.E. Phillips, R.A. Colbert, S. McAdam, G. Ogg, M.A. Nowak, P. Giangrande, G. Luzzi, B. Morgana, and A. Edwards. Late escape from an immunodominant cytotoxic T-lymphocyte response associated with progression to AIDS. *Nature Medicine*, 3(2):212–217, 1997.

[178] L.M. Wein, S.A. Zenios, and M.A. Nowak. Dynamic multidrug therapies for HIV: A control theoretic approach. *Journal of Theoretical Biology*, 185(1):15–29, 1997.

[179] L. Wang and M.Y. Li. Mathematical analysis of the global dynamics of a model for HIV infection of CD4 T cells. *Mathematical Biosciences*, 200(1):44–57, 2006.

[180] N.I. Stilianakis and D. Schenzle. On the intra-host dynamics of HIV-1 infections. *Mathematical biosciences*, 199(1):1–25, 2006.

[181] L. Rong, Z. Feng, and A.S. Perelson. Mathematical Analysis of Age-Structured HIV-1 Dynamics with Combination Antiretroviral Therapy. *SIAM Journal on Applied Mathematics*, 67:731, 2007.

[182] S. Bonhoeffer, M. Rembiszewski, G.M. Ortiz, and D.F. Nixon. Risks and benefits of structured antiretroviral drug therapy interruptions in HIV-1 infection. *AIDS*, 14(15):2313, 2000.

[183] B.M. Adams, H.T. Banks, H.D. Kwon, and H.T. Tran. Dynamic multidrug therapies for HIV: Optimal and STI control approaches. *Mathematical Biosciences and Engineering: MBE*, 1(2):223–241, 2004.

[184] MathWorks. *Documentation for ode23, ode45, ode113, ode15s, ode23s, ode23t, ode23tb*. `http://www.mathworks.co.uk/help/techdoc/ref/ode45.html`, accessed 23 November 2011, 2011.

[185] MathWorks. *Documentation for dde23*. `http://www.mathworks.co.uk/help/techdoc/ref/dde23.html`, accessed 23 November 2011, 2011.

[186] K.S. Keedy and D.M. Margolis. Therapy for persistent HIV. *Trends in Pharmacological Sciences*, 31(5):206–211, 2010.

[187] T.W. Chun, J.S. Justement, D. Murray, C.W. Hallahan, J. Maenza, A.C. Collier, P.M. Sheth, R. Kaul, M. Ostrowski, S. Moir, et al. Rebound of plasma viremia following cessation of antiretroviral therapy despite profoundly low levels of HIV reservoir: implications for eradication. *AIDS (London, England)*, 24(18):2803, 2010.

[188] L. Rong and A.S. Perelson. Modeling HIV persistence, the latent reservoir, and viral blips. *Journal of Theoretical Biology*, 260(2):308–331, 2009.

[189] M.A. Capistran and F.J. Solis. On the modeling of long-term HIV-1 infection dynamics. *Mathematical and Computer Modelling*, 50(5):777–782, 2009.

[190] L. Rong and A.S. Perelson. Asymmetric division of activated latently infected cells may explain the decay kinetics of the HIV-1 latent reservoir and intermittent viral blips. *Mathematical biosciences*, 217(1):77–87, 2009.

[191] L.E. Jones and A.S. Perelson. Opportunistic infection as a cause of transient viremia in chronically infected HIV patients under treatment with HAART. *Bulletin of Mathematical Biology*, 67(6):1227–1251, 2005.

[192] G.K. Sahu, D. Paar, S.D.W. Frost, M.M. Smith, S. Weaver, and M.W. Cloyd. Low-level plasma HIVs in patients on prolonged suppressive highly active antiretroviral therapy are produced mostly by cells other than CD4 T-cells. *Journal of Medical Virology*, 81(1):9–15, 2009.

[193] R.M. Ribeiro, L. Qin, L.L. Chavez, D. Li, S.G. Self, and A.S. Perelson. Estimation of the initial viral growth rate and basic reproductive number during acute HIV-1 infection. *Journal of Virology*, 84(12):6096, 2010.

[194] F. García, M. Plana, C. Vidal, A. Cruceta, et al. Dynamics of viral load rebound and immunological changes after stopping effective antiretroviral therapy. *Aids*, 13(11):F79, 1999.

[195] R.T. Davey, N. Bhat, C. Yoder, T.W. Chun, J.A. Metcalf, R. Dewar, V. Natarajan, R.A. Lempicki, J.W. Adelsberger, K.D. Miller, et al. HIV-1 and T cell dynamics after interruption of highly active antiretroviral therapy (HAART) in patients with a history of sustained viral suppression. *Proceedings of the National Academy of Sciences of the United States of America*, 96(26):15109, 1999.

[196] P.R. Harrigana, M. Whaley, and J.S.G. Montaner. Rate of HIV-1 RNA rebound upon stopping antiretroviral therapy. *Aids*, 13(8):F59, 1999.

[197] T.W. Chun, R.T. Davey, M. Ostrowski, J.S. Justement, D. Engel, J.I. Mullins, and A.S. Fauci. Relationship between pre-existing viral reservoirs and the re-emergence of plasma viremia after discontinuation of highly active anti-retroviral therapy. *Nature Medicine*, 6(7):757–761, 2000.

[198] E. Buckingham. On physically similar systems; illustrations of the use of dimensional equations. *Physical Review*, 4(4):345–376, 1914.

[199] Y.T. Cheng and C.M. Cheng. Scaling, dimensional analysis, and indentation measurements. *Materials Science and Engineering: R: Reports*, 44(4-5):91–149, 2004.

[200] F. Wasserstein-Robbins. A mathematical model of HIV infection: simulating T4, T8, macrophages, antibody, and virus via specific anti-HIV response in the presence of adaptation and tropism. *Bulletin of Mathematical Biology*, 72(5):1208–1253, 2010.

[201] WHO. *Global tuberculosis control 2011*. `http://www.who.int/entity/tb/publications/global_report/2011/gtbr11_full.pdf`, accessed 25 January 2012, 2011.

[202] C.J. Cohen, A.E. Colson, A.G. Sheble-Hall, K.A. McLaughlin, and G.D. Morse. Pilot study of a novel short-cycle antiretroviral treatment interruption strategy: 48-week results of the five-days-on, two-days-off (FOTO) study. *HIV Clinical Trials*, 8(1):19–23, 2007.

[203] B.J. Rudy, J. Sleasman, B. Kapogiannis, C.M. Wilson, J. Bethel, L. Serchuck, S. Ahmad, and C.K. Cunningham. Short-cycle therapy in adolescents after continuous therapy with established viral suppression: the impact on viral load suppression. *AIDS Research and Human Retroviruses*, 25(6):555–561, 2009.

[204] HT Banks, M. Davidian, S. Hu, G.M. Kepler, and ES Rosenberg. Modelling HIV immune response and validation with clinical data. *Journal of Biological Dynamics*, 2(4):357–385, 2008.

[205] M. Di Mascio, R.M. Ribeiro, M. Markowitz, D.D. Ho, and A.S. Perelson. Modeling the long-term control of viremia in HIV-1 infected patients treated with antiretroviral therapy. *Mathematical Biosciences*, 188(1-2):47–62, 2004.

[206] A. Bensoussan, G. Da Prato, M.C. Delfour, and S.K. Mitter. *Representation and control of infinite dimensional systems*. Birkhauser Boston, 2007.

[207] G. Pannocchia, M. Laurino, and A. Landi. A model predictive control strategy toward optimal structured treatment interruptions in anti-HIV therapy. *IEEE Transactions on Biomedical Engineering*, 57(5):1040–1050, 2010.

[208] J. David, H.T. Tran, and H.T. Banks. HIV model analysis and estimation implementation under optimal control based treatment strategies. *International Journal of Pure and Applied Mathematics*, 57(3):357–392, 2009.

[209] H.T. Banks, H.D. Kwon, J.A. Toivanen, and H.T. Tran. A state-dependent Riccati equation-based estimator approach for HIV feedback control. *Optimal Control Applications and Methods*, 27(2):93–121, 2006.

[210] M. Joly and J.M. Pinto. Role of mathematical modeling on the optimal control of HIV-1 pathogenesis. *AIChE journal*, 52(3):856–884, 2006.

Appendix A

Variables and parameter values

This section gives the state variables, parameter definitions and estimates for each model. The tables are divided by dependency on variables and parameters specific to each model, e.g. T_p, T_p^* and V are common to all models but E is only relevant to MTC-IR models. These tables are a summary of those given in Chapter 3, i.e. Tables 3.1, 3.2, 3.3, 3.4, 3.5 and 3.6.

Variable	Units	Description
T_p	$\frac{cells}{\mu L}$	Primary target cells (i.e. CD4^+T cells)
T_p^*	$\frac{cells}{\mu L}$	Primary target acutely infected cells
V	$\frac{virions}{\mu L}$	Infectious virus concentration
T_s	$\frac{cells}{\mu L}$	Secondary target cells (e.g. macrophages)
T_s^*	$\frac{cells}{\mu L}$	Secondary target acutely infected cells
C_p^*	$\frac{cells}{\mu L}$	Primary target chronic infected cells
C_s^*	$\frac{cells}{\mu L}$	Secondary target chronic infected cells
E	$\frac{cells}{\mu L}$	Effector cells

Table A.1: All model variables: Dependent variables for all models discussed

Para.	Units	Value	Description
λ_p	$\frac{cells}{\mu L\ day}$	$10,000$	Production source of primary target cells
δ_p	$\frac{1}{day}$	0.01	Death rate of primary target cells
ϵ	$-$	$0.9 \in [0,1]$	Efficiency of RTI in primary target population
k_p	$\frac{\mu L}{virions\ day}$	8×10^{-7}	Infection rate for primary population
N_T	$\frac{virions}{cell}$	100	No. of virions produced per infected cell
c	$\frac{1}{day}$	13	Clearance rate of virions
δ	$\frac{1}{day}$	0.7	Clearance rate of infected cells
λ_s	$\frac{cells}{\mu L\ day}$	32	Production source of secondary target cells
δ_s	$\frac{1}{day}$	0.01	Death rate of secondary target cells
f	-	$0.34 \in [0,1]$	Reduction in efficiency of treatment in secondary population
k_s	$\frac{\mu L}{virions\ day}$	8×10^{-7}	Infection rate for secondary population
N_c	$\frac{virions}{cell}$	4.11	No. of virions produced per chronically infected cell
α	$\frac{virions}{cell}$	0.195	Ratio of acute to chronic cells
μ	$\frac{1}{day}$	0.7	Clearance rate of chronically infected cells
m_p	$\frac{\mu L}{cells\ day}$	1×10^{-5}	Immune induced clearance rate in primary target
m_s	$\frac{\mu L}{cells\ day}$	1×10^{-5}	Immune induced clearance rate in secondary target
p_p	$\frac{virions}{cell}$	1	Average number of virions produced per primary target infection
p_s	$\frac{virions}{cell}$	1	Average number of virions produced per secondary target infection
λ_E	$\frac{cells}{\mu L\ day}$	1	Production rate of immune effectors
b_E	$\frac{1}{day}$	0.3	Max. birth rate of immune effectors
K_b	$\frac{cells}{\mu l}$	100	Saturation birth for immune effector
d_E	$\frac{1}{day}$	0.25	Max. death rate for immune effectors
K_d	$\frac{cells}{\mu L}$	500	Saturation death for immune effectors
δ_E	$\frac{1}{day}$	0.1	Natural death rate for immune effectors
τ	day	1	Intracellular delay

Table A.2: All parameters: Parameters for all models discussed

Appendix B

Publications / Conferences

2010 3rd International Workshop on Systems Biology (IWSB), *Effect of cell infection delay on treatment interruption models of within-host HIV progression*, poster presentation. *Hamilton Institute, National University Ireland Maynooth, Ireland. August 15-18 2010*

2009 7th IFAC Symposium on Modelling and Control in Biomedical Systems (MCBMS), *Increasing biological accuracy in models of HIV progress while minimising complexity*, contributed paper presentation. *Aalborg, Denmark. 12-14 August 2009*

2008 2nd International Workshop on Systems Biology (IWSB), *Increasing physical realism in models of HIV progress using novel techniques*, poster presentation. *Hamilton Institute, National University Ireland Maynooth, Ireland. August 17-20 2008*

2006 IRCSET Symposium, *The untapped potential of the frequency domain to bring physical realism to HIV models*, poster presentation.

Appendix C

Full dimensional analysis

Chapter 5 converts the models developed in Chapter 4 into their dimensionless representation. The key results of the analysis of these dimensionless models are discussed in Chapter 5, but the full tables of results are given here, together with graphical representations of each of the therapy events.

C.1 STC-ID-L-DA full dimensional analysis

This section gives the full steady states for each therapy event Table C.1. Also given is the full set of parameters for which sensitivity analysis was performed, with their corresponding results, Table C.2. These sensitivity results are also representated in graphical form in *Fig. C.1* and *Fig. C.2*.

Dimensionless parameters		Off therapy SS	Therapy introduction	On Therapy SS	Therapy removal
A	$\frac{\lambda_p}{\delta T_{p0}}$	0.0621	0.0621	0.0238	0.0238
B	$\frac{\delta_p}{\delta}$	0.0143	0.0143	0.0143	0.0143
C	$(1-\epsilon)\frac{k_p T_{p0}}{\delta}$	0.2629	0.0263	0.0686	0.6857
D	$\delta\tau$	0.7000	0.7000	0.7000	0.7000
E	N_T	3.4783	3.4783	0.0002	0.0002
F	$\frac{c}{\delta}$	18.5714	18.5714	18.5714	18.5714
G	$\frac{V_{lvl}}{T_{p0}}$	0.0000	0.0000	0.0000	0.0000
Initial conditions					
$\bar{T}_{p0}$	$\frac{T_p}{T_{p0}}$	1.0000	1.0000	1.0000	1.0000
$\bar{T}^*_{p0}$	$\frac{T^*_p}{T_{p0}}$	1.0000	1.0000	1.0000	1.0000
$\bar{V}_0$	$\frac{V}{T_{p0}}$	0.1826	0.1826	0.0000	0.0000

Table C.1: STC-ID-L-DA dimensionless values The values for each of the dimensionless parameters and initial conditions across both therapy events and steady states (SS).

	Therapy removal				Therapy introduction			
Dim.Less	Initial	Doubling time (day)			Initial	Half life (day)		
par	value	Low	High	% diff	value	Low	High	% diff
A	0.06	2.39	2.27	-5.17 %	0.02	1.25	1.26	1.12 %
B	0.01	2.29	2.37	3.40 %	0.01	1.25	1.25	-0.31 %
C	0.03	2.80	2.02	-27.71 %	0.69	1.23	1.25	1.12 %
D	0.70	1.99	2.74	37.83 %	0.70	1.23	1.25	1.94 %
E	100.00	2.79	2.02	-27.61 %	100.00	1.21	1.27	4.77 %
F	18.57	2.01	2.72	35.37 %	18.57	1.24	1.21	-2.67 %
G	0.00	2.33	2.33	-0.05 %	0.00	1.25	1.26	0.55 %
Initial conditions								
$\bar{T}_{p0} = \frac{T_{p0}}{T_{p0}}$	1.00	2.71	2.06	-23.71 %	1.00	1.21	1.24	1.93 %
$\bar{T}^*_{p0} = \frac{T^*_{p0}}{T_{p0}}$	0.03	2.33	2.33	0.05 %	0.00	1.23	1.25	1.99 %
$\bar{V}_0 = \frac{V_0}{T_{p0}}$	0.16	2.33	2.33	0.00 %	0.00	1.26	1.26	-0.04 %

Table C.2: STC-ID-L-DA parameter variation effect: Quantification of effect in variation in initial parameter values and initial conditions based on doubling time and half life of viral growth. Initial values were varied from 90% to 110% of their initial value, with the resulting change in viral growth shown.

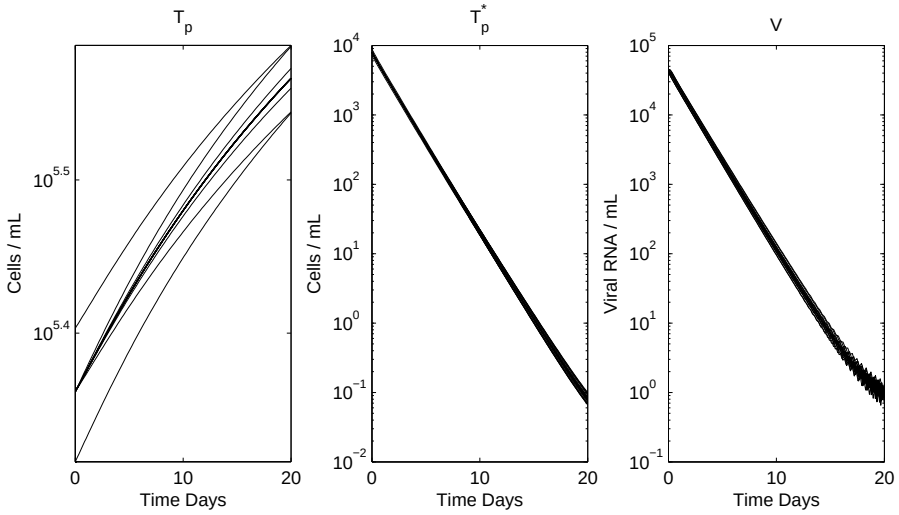

Figure C.1: STC-ID-L-DA parameter variation for therapy introduction: Effect of varying dimensionless parameters and initial conditions for the STC-ID-L-DA model for therapy introduction. The specific values are given in Table C.2

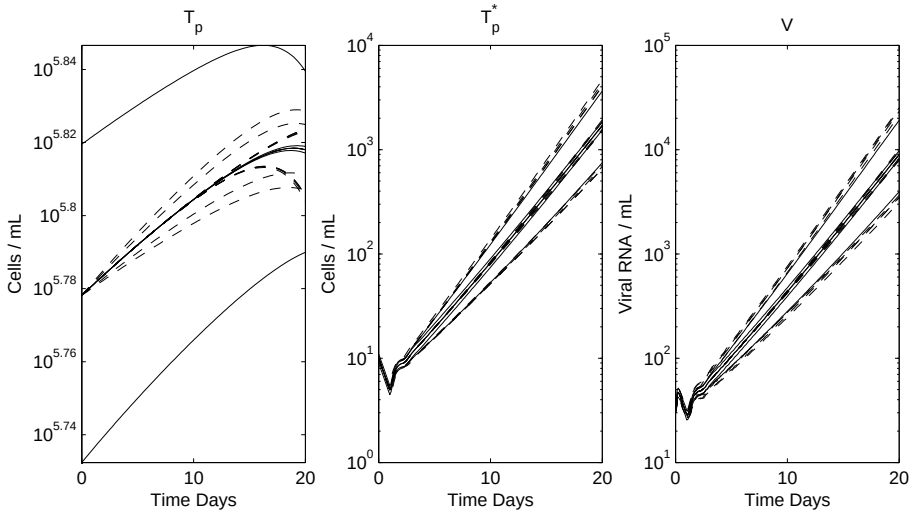

Figure C.2: STC-ID-L-DA parameter variation for therapy removal: Effect of varying dimensionless parameters and initial conditions for the STC-ID-L-DA model for therapy removal. The specific values are given in Table C.2

C.2 MTC-CI-ID-L-DA full dimensional analysis

This section gives the full steady states for each therapy event, Table C.3. Also given is the full set of parameter for which sensitivity analysis was performed, with their corresponding results, Table C.4. These sensitivity results are also represented in graphical form in *Fig. C.3* and *Fig. C.4*.

Dimensionless parameters		Off therapy SS	Therapy introduction	On Therapy SS	Therapy removal
A	$\frac{\lambda_p}{\delta T_{p0}}$	0.0621	0.0621	0.0238	0.0238
B	$\frac{\delta_p}{\delta}$	0.0143	0.0143	0.0143	0.0143
C	$(1-\epsilon)\frac{k_p T_{p0}}{\delta}$	0.2629	0.0263	0.0686	0.6857
D	$\frac{\lambda_s}{\delta T_{s0}}$	5.7143	5.7143	0.0229	0.0229
E	$\frac{\delta_s}{\delta}$	0.0143	0.0143	0.0143	0.0143
F	$(1-f\epsilon)\frac{k_s T_{p0}}{\delta}$	32.8571	22.8029	59.4857	85.7143
G	$(1-\alpha)C$	0.2116	0.2116	0.2116	0.2116
H	$\delta\tau$	0.7000	0.7000	0.7000	0.7000
I	$(1-\alpha)F$	26.4500	18.3563	47.8860	69.0000
J	αC	0.0513	0.0051	0.0134	0.1337
K	$\mu\tau$	0.7000	0.7000	0.7000	0.7000
L	$\frac{\mu}{\delta}$	1.0000	1.0000	1.0000	1.0000
M	αF	6.4071	4.4466	11.5997	16.7143
N	N_T	100.0000	100.0000	100.0000	100.0000
O	$N_T\frac{T_{s0}}{T_{p0}}$	0.0035	0.0035	0.3333	0.3333
P	$N_C\frac{\mu}{\delta}$	4.1100	4.1100	4.1100	4.1100
Q	$N_C\frac{\mu}{\delta}\frac{T_{s0}}{T_{p0}}$	0.0001	0.0001	0.0137	0.0137
R	$\frac{c}{\delta}$	18.5714	18.5714	18.5714	18.5714
S	$\frac{V_{lvl}}{T_{p0}}$	0.0000	0.0000	0.0000	0.0000
Initial conditions					
$\bar{T}_{p0}=\frac{T_p}{T_{p0}}$	$\frac{T_p}{T_{p0}}$	1.0000	1.0000	1.0000	1.0000
$\bar{T}_{s0}=\frac{T_s}{T_{s0}}$	$\frac{T_s}{T_{s0}}$	1.0000	1.0000	1.0000	1.0000
$\bar{T}^*_{p0}=\frac{T^*_p}{T_{p0}}$	$\frac{T^*_p}{T_{p0}}$	0.0435	0.0435	0.0000	0.0000
$\bar{T}^*_{s0}=\frac{T^*_s}{T_{s0}}$	$\frac{T^*_s}{T_{s0}}$	5.6250	5.6250	0.0000	0.0000
$\bar{C}^*_{p0}=\frac{C^*_p}{T_{p0}}$	$\frac{C^*_p}{T_{p0}}$	0.0000	0.0000	0.0000	0.0000
$\bar{C}^*_{s0}=\frac{C^*_s}{T_{s0}}$	$\frac{C^*_s}{T_{s0}}$	0.0000	0.0000	0.0000	0.0000
$\bar{V}_0=\frac{V}{T_{p0}}$	$\frac{V}{T_{p0}}$	0.2391	0.2391	0.0000	0.0000

Table C.3: MTC-CI-ID-L dimensionless values The values for each of the dimensionless parameters and initial conditions across both therapy events and steady states (SS).

	Therapy removal				Therapy introduction			
Dim.Less	Initial	Doubling time (days)			Initial	Half life (days)		
par	value	Low	High	% diff	value	Low	High	% diff
A	0.02	3.51	3.32	-5.53 %	0.02	1.15	1.16	0.81 %
B	0.01	3.35	3.47	3.58 %	0.01	1.15	1.15	-0.21 %
C	0.69	3.41	3.41	0.00 %	0.69	1.15	1.15	-0.02 %
D	0.02	3.41	3.41	-0.01 %	0.04	1.15	1.16	0.42 %
E	0.01	3.41	3.41	0.00 %	0.01	1.15	1.15	0.00 %
F	0.29	3.41	3.41	0.00 %	0.17	1.15	1.15	0.00 %
G	0.55	4.34	2.90	-33.19 %	0.70	1.14	1.17	2.58 %
H	0.70	2.88	4.14	43.56 %	8.57	1.16	1.15	-0.69 %
I	0.23	3.41	3.41	-0.06 %	0.02	1.15	1.15	0.00 %
J	0.13	3.42	3.41	-0.41 %	100.00	1.15	1.15	0.03 %
K	0.70	3.41	3.42	0.29 %	0.20	1.15	1.15	-0.02 %
L	1.00	3.41	3.42	0.32 %	0.69	1.15	1.15	-0.12 %
M	0.06	3.41	3.41	0.00 %	0.17	1.15	1.15	0.00 %
N	100.00	4.34	2.90	-33.19 %	18.57	1.14	1.17	2.30 %
O	0.33	3.41	3.41	-0.06 %	0.00	1.16	1.16	-0.09 %
P	4.11	3.42	3.41	-0.41 %	0.43	1.15	1.15	0.03 %
Q	0.01	3.41	3.41	0.00 %	0.00	1.15	1.15	0.00 %
R	18.57	2.82	4.21	49.50 %	0.36	1.17	1.14	-2.55 %
S	0.00	3.42	3.51	2.65 %	0.00	1.15	1.15	0.11 %
Initial conditions								
$\bar{T}_{p0} = \frac{T_p}{T_{p0}}$	1.00	4.61	3.01	-34.67 %	1.00	1.14	1.16	2.09 %
$\bar{T}_{s0} = \frac{T_s}{T_{s0}}$	1.00	3.55	3.55	-0.08 %	1.00	1.15	1.15	-0.43 %
$\bar{T}^*_{p0} = \frac{T^*_p}{T_{p0}}$	0.00	3.55	3.55	0.00 %	0.00	1.15	1.15	-0.29 %
$\bar{T}^*_{s0} = \frac{T^*_s}{T_{s0}}$	0.00	3.55	3.55	0.00 %	0.00	1.15	1.15	-0.46 %
$\bar{C}^*_{p0} = \frac{C^*_p}{T_{p0}}$	0.00	3.55	3.55	0.00 %	0.00	1.15	1.15	0.00 %
$\bar{C}^*_{s0} = \frac{C^*_s}{T_{s0}}$	0.00	3.55	3.55	0.00 %	0.00	1.15	1.15	0.00 %
$\bar{V}_0 = \frac{V}{T_{p0}}$	0.00	3.61	3.52	-2.67 %	0.00	1.15	1.15	0.07 %

Table C.4: MTC-CI-ID-L-DA parameter variation effect: Quantification of effect in variation in initial parameter values and initial conditions based on doubling time and half life of viral growth. Initial values were varied from 90% to 110% of their initial value, with the resulting change in viral growth shown.

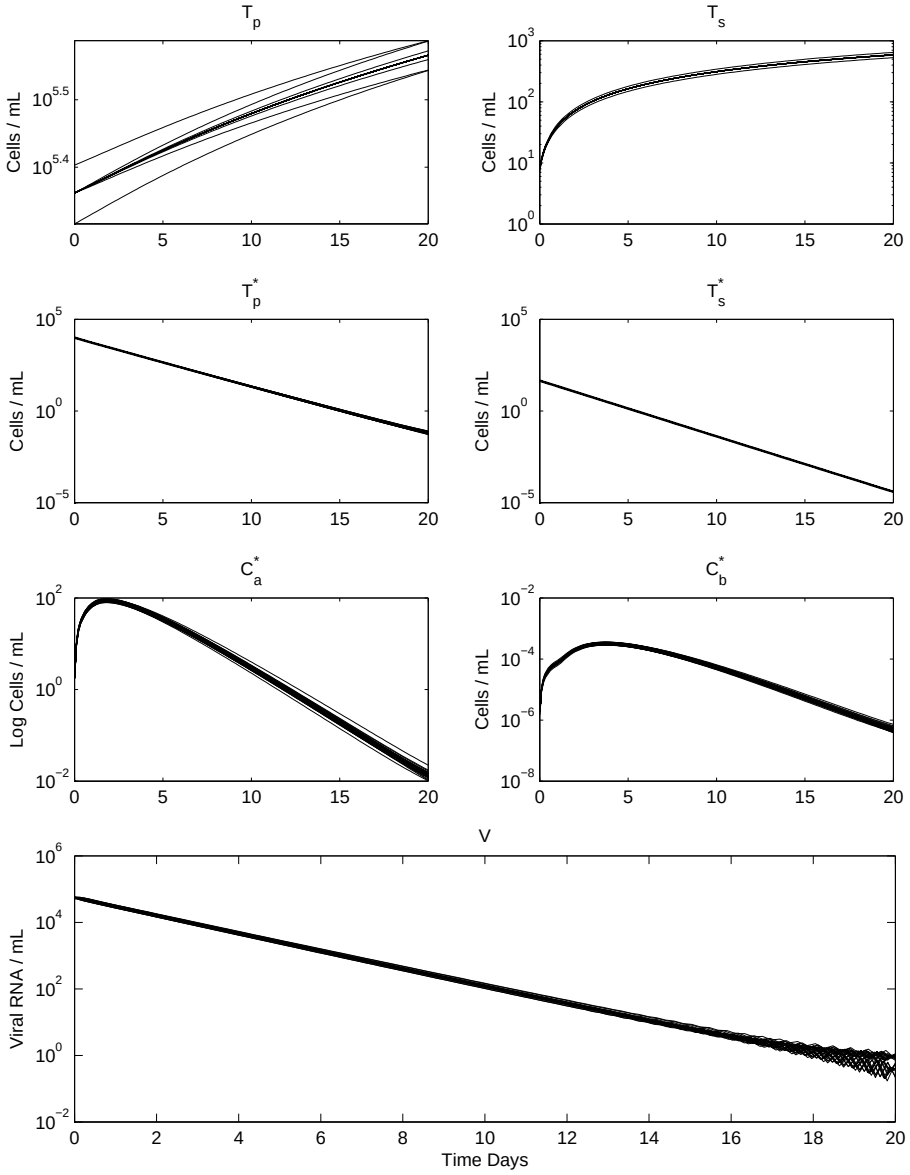

Figure C.3: MTC-CI-ID-L-DA parameter variation for therapy introduction: Effect of varying dimensionless parameters and initial conditions for the STC-ID-L-DA model for therapy introduction. The specific values are given in Table C.4

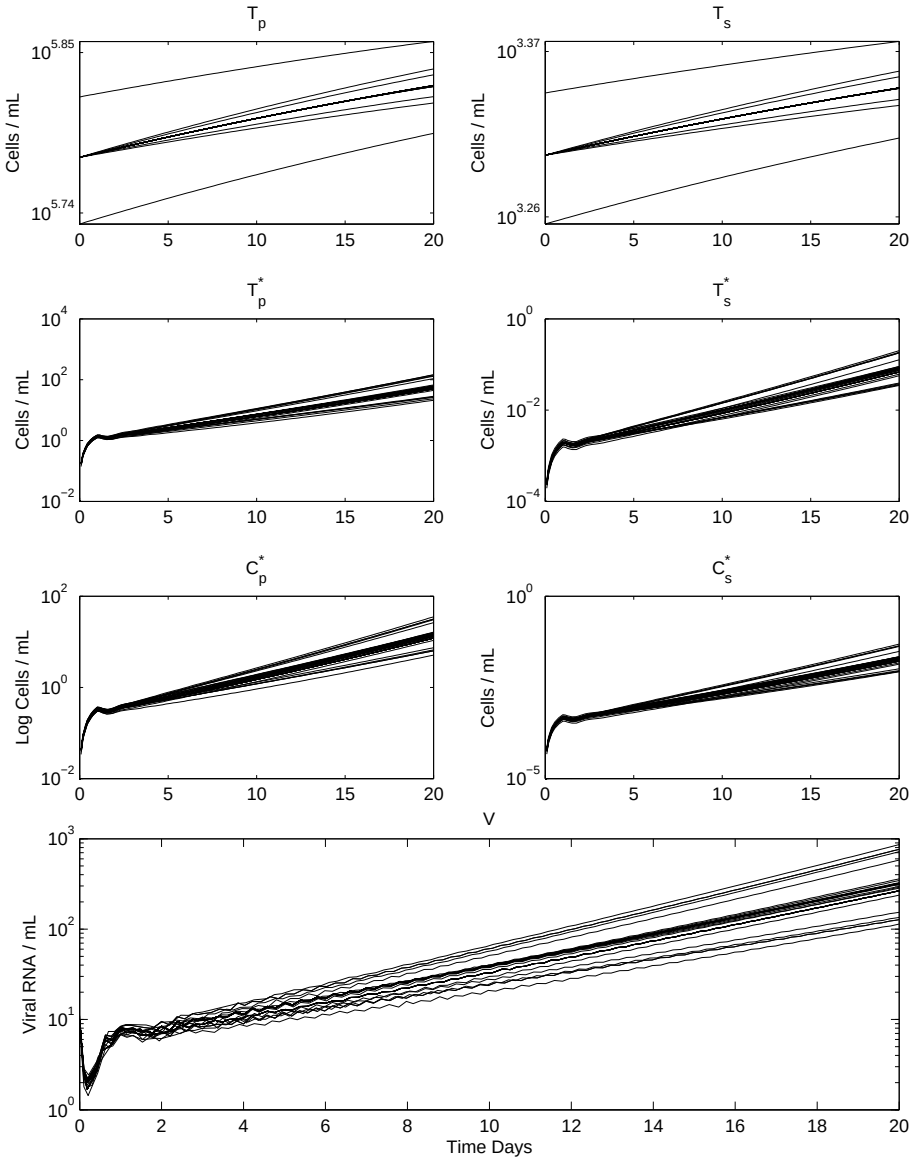

Figure C.4: MTC-CI-ID-L-DA parameter variation for therapy removal: Effect of varying dimensionless parameters and initial conditions for the STC-ID-L-DA model for therapy removal. The specific values are given in Table C.4

C.3 MTC-IR-ID-L-DA full dimensional analysis

This gives the full steady states for each therapy event, Table C.5, and the full set of sensitivity analysis, Table C.6, and a graphical representation, *Fig. C.5* and *Fig. C.6*.

Dimensionless parameters		Off therapy SS	Therapy introduction	On Therapy SS	Therapy removal
A	$\frac{\lambda_p}{\delta T_{p0}}$	0.0433	0.0433	0.0238	0.0238
B	$\frac{\delta_p}{\delta}$	0.0143	0.0143	0.0143	0.0143
C	$(1-\epsilon)\frac{k_p T_{p0}}{\delta}$	0.3771	0.0377	0.0686	0.6857
D	$\frac{\lambda_s}{\delta T_{s0}}$	3.5165	3.5165	0.0381	0.0381
E	$\frac{\delta_s}{\delta}$	0.0143	0.0143	0.0143	0.0143
F	$(1-f\epsilon)\frac{k_s T_{s0}}{\delta}$	0.0019	0.0013	0.1190	0.1714
G	$\delta\tau$	0.7000	0.7000	0.7000	0.7000
H	$\frac{m_p T_{p0}}{\delta}$	4.7143	4.7143	8.5714	8.5714
I	$\frac{m_s T_{s0}}{\delta}$	0.0002	0.0002	0.0171	0.0171
J	N_T	100.0000	100.0000	100.0000	100.0000
K	$\frac{N_T T_{s0}}{T_{p0}}$	0.0039	0.0039	0.2000	0.2000
L	$\frac{(1-\epsilon)p_p k_p T_{p0}}{\delta}$	0.3771	0.0377	0.0686	0.6857
M	$\frac{(1-f\epsilon)p_s k_s T_{s0}}{\delta}$	0.0019	0.0013	0.1190	0.1714
N	$\frac{c}{\delta}$	18.5714	18.5714	18.5714	18.5714
O	$\frac{\lambda_E}{T_{p0}\delta}$	0.0000	0.0000	0.0000	0.0000
P	$\frac{b_E}{\delta}$	0.4286	0.4286	0.4286	0.4286
Q	$\frac{K_b}{T_{p0}}$	0.0003	0.0003	0.0002	0.0002
R	$\frac{d_E}{\delta}$	0.3571	0.3571	0.3571	0.3571
S	$\frac{K_d}{T_{p0}}$	0.0015	0.0015	0.0008	0.0008
T	$\frac{\delta_E}{\delta}$	0.1429	0.1429	0.1429	0.1429
U	$\frac{V_{lvl}}{T_{p0}}$	0.0000	0.0000	0.0000	0.0000
Initial conditions					
$\bar{T}_{p0} = \frac{T_{p0}}{T_{p0}}$	$\frac{T_{p0}}{T_{p0}}$	1.0000	1.0000	1.0000	1.0000
$\bar{T}_{s0} = \frac{T_{s0}}{T_{s0}}$	$\frac{T_{s0}}{T_{s0}}$	1.0000	1.0000	1.0000	1.0000
$\bar{T}^*_{p0} = \frac{T^*_{p0}}{T_{p0}}$	$\frac{T^*_{p0}}{T_{p0}}$	0.0142	0.0142	0.0000	0.0000
$\bar{T}^*_{s0} = \frac{T^*_{s0}}{T_{s0}}$	$\frac{T^*_{s0}}{T_{s0}}$	1.7692	1.7692	0.0000	0.0000
$\bar{V}_0 = \frac{V_0}{T_{p0}}$	$\frac{V_0}{T_{p0}}$	0.0758	0.0758	0.0000	0.0000
$\bar{E}_0 = \frac{E_0}{T_{p0}}$	$\frac{E_0}{T_{p0}}$	0.0001	0.0001	0.0000	0.0000

Table C.5: MTC-IR-ID-L dimensionless values The values for each of the dimensionless parameters and initial conditions across both therapy events and steady states (SS).

	Therapy removal				Therapy introduction			
Dim.Less	Initial	Doubling time (days)			Initial	Half life (days)		
par	value	Low	High	% diff	value	Low	High	% diff
A	0.04	2.24	2.20	-1.75 %	0.02	1.27	1.28	0.48 %
B	0.01	2.21	2.23	1.09 %	0.01	1.28	1.28	-0.15 %
C	0.04	2.52	1.97	-22.02 %	0.69	1.25	1.30	3.81 %
D	3.52	2.22	2.22	0.05 %	0.04	1.27	1.28	0.34 %
E	0.01	2.22	2.22	-0.02 %	0.01	1.28	1.28	-0.16 %
F	0.00	2.22	2.22	-0.01 %	0.17	1.28	1.28	-0.01 %
G	0.70	1.95	2.51	29.21 %	0.70	1.28	1.27	-0.63 %
H	4.71	2.22	2.22	0.00 %	8.57	1.28	1.28	0.00 %
I	0.00	2.22	2.22	0.00 %	0.02	1.28	1.28	0.00 %
J	100.00	2.52	1.97	-22.03 %	100.00	1.25	1.30	3.89 %
K	0.00	2.22	2.22	-0.01 %	0.20	1.28	1.27	-0.29 %
L	0.04	2.21	2.20	-0.24 %	0.69	1.28	1.27	-0.24 %
M	0.00	2.18	2.21	1.25 %	0.17	1.28	1.28	0.10 %
N	18.57	1.89	2.57	35.79 %	18.57	1.30	1.26	-2.53 %
O	0.00	2.22	2.22	0.00 %	0.00	1.28	1.28	0.00 %
P	0.43	2.22	2.22	0.00 %	0.43	1.28	1.28	0.00 %
Q	0.00	2.22	2.22	0.00 %	0.00	1.28	1.28	0.00 %
R	0.36	2.22	2.22	0.00 %	0.36	1.28	1.28	0.00 %
S	0.00	2.19	2.20	0.19 %	0.00	1.27	1.28	0.86 %
T	0.14	2.22	2.22	0.00 %	0.14	1.28	1.28	0.00 %
U	0.00	2.22	2.22	0.00 %	0.00	1.28	1.28	0.00 %
Initial conditions								
$\bar{T}_{p0} = \frac{T_{p0}}{T_{p0}}$	1.00	2.46	2.00	-18.96 %	1.00	1.26	1.29	3.11 %
$\bar{T}_{s0} = \frac{T_{s0}}{T_{s0}}$	1.00	2.18	2.21	1.20 %	1.00	1.28	1.28	-0.33 %
$\bar{T}^*_{p0} = \frac{T^*_{p0}}{T_{p0}}$	0.00	2.22	2.22	0.00 %	0.00	1.28	1.27	-0.63 %
$\bar{T}^*_{s0} = \frac{T^*_{s0}}{T_{s0}}$	0.00	2.22	2.22	0.00 %	0.00	1.28	1.27	-0.29 %
$\bar{V}_0 = \frac{V_0}{T_{p0}}$	0.00	2.16	2.21	2.60 %	0.00	1.28	1.28	0.13 %
$\bar{E}_0 = \frac{E_0}{T_{p0}}$	0.00	2.22	2.22	0.00 %	0.00	1.28	1.28	0.00 %

Table C.6: MTC-IR-ID-L-DA parameter variation effect: Quantification of effect in variation in initial parameter values and initial conditions based on doubling time and half life of viral growth. Initial values were varied from 90% to 110% of their initial value, with the resulting change in viral growth shown.

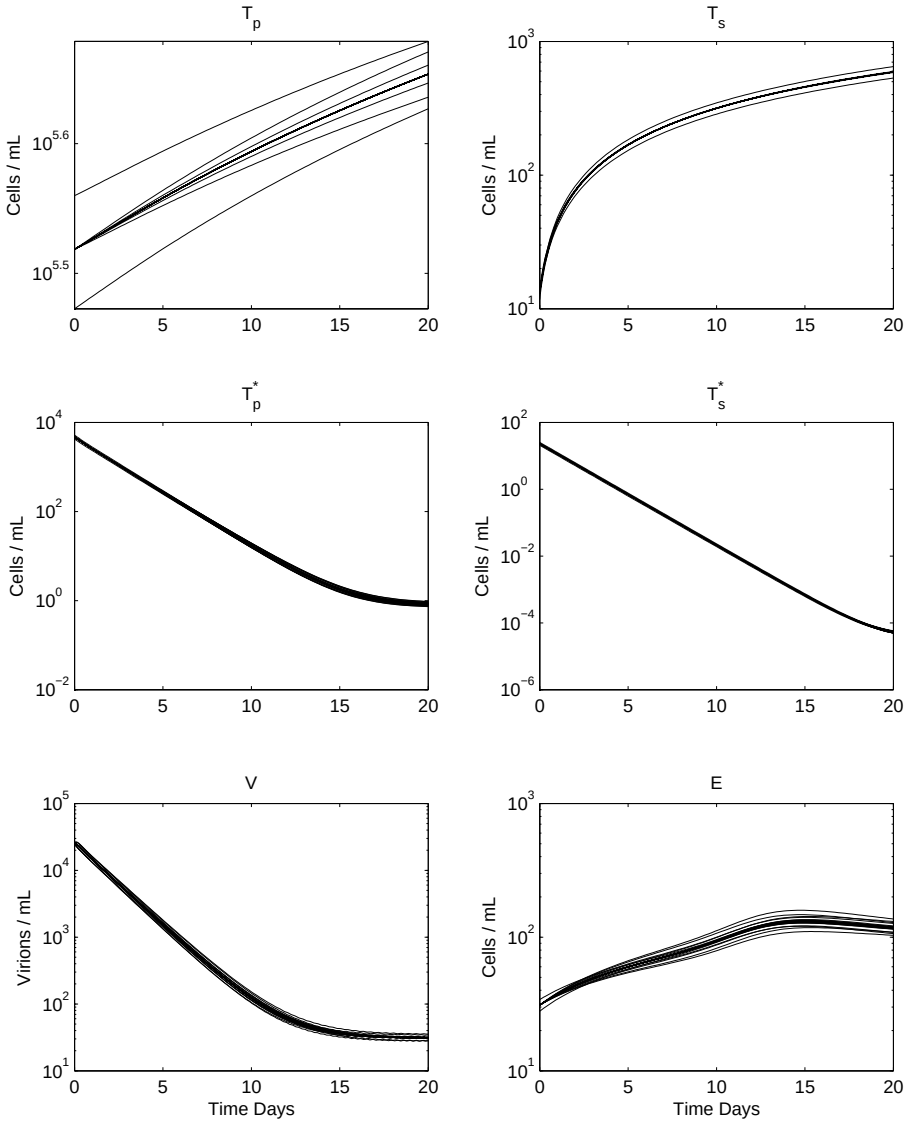

Figure C.5: MTC-IR-ID-L-DA parameter variation for therapy introduction: Effect of varying dimensionless parameters and initial conditions for the STC-ID-L-DA model for therapy introduction. The specific values are given in Table C.6

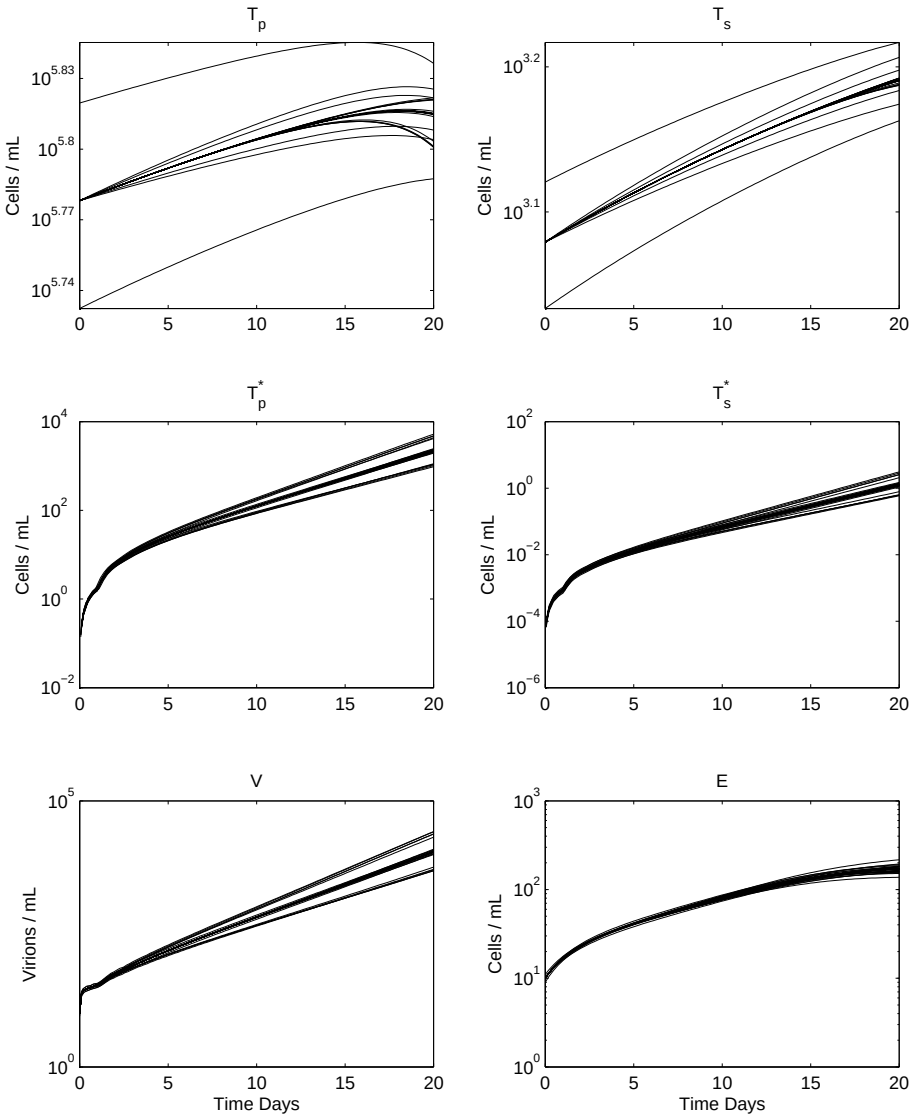

Figure C.6: MTC-IR-ID-L-DA parameter variation for therapy removal: Effect of varying dimensionless parameters and initial conditions for the STC-ID-L-DA model for therapy removal. The specific values are given in Table C.6

Glossary

Acquired immune deficiency syndrome (AIDS)

AIDS, final stage of HIV progression when a patient is at risk of opportunistic infection

Antibody

A protein produced by the body's immune system that recognises and fights infectious organisms and other foreign substances that enter the body. Each antibody is specific to a particular piece of an infectious organism or other foreign substance

B cell

Infection-fighting white blood cells that develop in the bone marrow and spleen. B lymphocytes produce antibodies. In people with HIV, the ability of B lymphocytes to do their job may be damaged

CD4^+ T cell

Also know as T helper-cells. They are a subset of white blood cells which express the CD4 receptors. These play a vital role in orchestrating the body's immune system

Co-infection

Infection with more than one virus, bacterium, or other micro-organism at a given time. For example, an HIV-infected individual may be co-infected with hepatitis C virus (HCV) or tuberculosis (TB)

Delayed differential equation (DDE)

DDEs are a deterministic way of mathematically describing a system which inherently includes some form of delay

Dendritic cells

A type of antigen-presenting cell that picks up foreign substances from the bloodstream and 'presents' them to other parts of the immune system, activating an immune response against the foreign invader

Deoxyribonucleic acid (DNA)

DNA is a chemical structure that contains the genetic instructions for reproduction and protein synthesis for all cells and for many viruses

Dimensional analysis (DA)

DA is used to create a dimensionless system such that each parameter's overall impact on model function can be accurately accessed

Doubling-time (T_d)

Is the time necessary for a population, or quantity, to double in size

Drug resistant mutations (DRM)

DRM are mutations in HIV viral strain which allow it to evade specific drug types

Elite controllers

Patients who have the ability to control HIV replication at a relatively low level despite the absence of therapy

Enzyme

A protein that helps a chemical reaction happen by decreasing the energy needed for the reaction to occur

Glycoprotein

A substance composed of both a protein and a carbohydrate (a sugar molecule) joined together by a chemical linkage

Half-life ($T_{1/2}$)

Is the time necessary for a population, or quantity, to halve in size

Human immunodeficiency virus (HIV)

HIV is a retrovirus which is the underlying cause of AIDS

Intracellular delay (ID)

The time taken between a cell becoming infected by HIV and starting to produce virions

Lymphoid tissue

Very small organs of the immune system that are located throughout the body. Lymph fluid that bathes body tissues is filtered through lymph nodes as it carries white blood cells to and from the blood

Macrophages

A type of disease-fighting white blood cell that destroys foreign invaders and stimulates other immune system cells to fight infection

Ordinary differential equation (ODE)

ODEs are a deterministic way of mathematically describing a system

Proteins

Highly complex biological molecules consisting of specific combinations of amino acids linked together by chemical bonds. Proteins are required for the structure, function, and regulation of the body's cells, tissues, and organs, and each protein has unique functions

Provirus

A DNA version of HIV's genetic material that has been integrated into the host cells own DNA

Retrovirus

A type of virus that stores its genetic information in a single-stranded RNA molecule, then constructs a double-stranded DNA version of its genes using a special enzyme called reverse transcriptase. The DNA copy is then integrated into the host cells own genetic material. HIV is an example of a retrovirus

Ribonucleic acid

RNA is a chemical structure that carries genetic instructions for protein synthesis. Although DNA is the primary genetic material of cells, RNA is the core genetic material for some viruses

Set-point

The level at which viral load stabilises after acute HIV infection. This is also close to the point which viral load will return after therapy failure of cessation

Structured treatment interruption (STI)

STIs are intentional interruptions to ART. These aim to reduce the drug burden experienced by some patients.

T cell

A type of lymphocyte (disease-fighting white blood cell). The 'T' stands for the thymus, where T cells mature. T cells include CD4 cells and CD8 cells, which are both critical components of the body's immune system

Transmission rate

The rate at which an infectious agent is spread between individuals

Viral blips

Intermittent episodes of increased viral activity during ART, specifically these are short-lived peaks which soon return to undetectable viral load

Viral load

Measurement of the amount of viral RNA in the blood system

Virion

A mature virus particle existing freely outside a host cell